UNIVERSIDADE D
COIMBRA

Giuseppe Cammarata

Neurodevelopment effects of valproic acid exposure in human brain organoids

Tese no âmbito do Doutoramento em Biologia Experimental e Biomedicina - especialização em Neurosciências e Doença, orientada pelo Professor Doutor João Miguel Peça Lima Novo Silvestre e co-orientada pelo Professor Doutor Jorge Manuel Castelo Branco de Albuquerque Almeida e co-orientada pela Doutora Catarina Morais Seabra e apresentada ao Instituto de Investigação Interdisciplinar da Universidade de Coimbra.

Julho de 2023

UNIVERSIDADE D
COIMBRA

Giuseppe Cammarata

EFEITOS DA EXPOSIÇÃO AO ÁCIDO VALPRÓICO NO NEURODESENVOLVIMENTO EM ORGANÓIDES CEREBRAIS HUMANOS

Tese no âmbito do Doutoramento em Biologia Experimental e Biomedicina - especialização em Neurosciências e Doença, orientada pelo Professor Doutor João Miguel Peça Lima Novo Silvestre e co-orientada pelo Professor Doutor Jorge Manuel Castelo Branco de Albuquerque Almeida e co-orientada pela Doutora Catarina Morais Seabra e apresentada ao Instituto de Investigação Interdisciplinar da Universidade de Coimbra.

Julho de 2023

This work was performed at the Center for Neuroscience and Cell Biology (CNC), University of Coimbra (with secondment at the University of Edinburgh) and was supported by European Union Horizon 2020 Research and Innovation Programme – SYN2PSY –under grant agreement 813986; by the European Regional Development Fund (ERDF), through the Centro 2020 and through the COMPETE 2020 - Operational Programme for Competitiveness and Internationalisation and Portuguese national funds via FCT – Fundação para a Ciência e a Tecnologia, under project UIDB/04539/2020. This work was further supported by ERA-NET Neuron (FCT/NEURON/0002/2021), the 2019 Pfizer Prize in Basic Sciences and a 2020 IBRO Early Career Award.

Innovative Training Network

To Ponte San Pietro

To Federica Cinelli

ACKNOWLEDGMENT

Around four years ago, I embarked on a journey that took me away from my home, leaving behind my family, and my friends. Little did I know then how stunning and transformative this journey would be. I am incredibly grateful for the unique experiences I've had, and I would like to express my heartfelt appreciation to all those who have been part of this remarkable adventure.

First and foremost, I would like to extend my deepest gratitude to my supervisor, João Peça, for his unwavering support, continuous guidance, and constructive criticism throughout the practical and correction phases of this dissertation. His patience and provision of essential resources and contacts have been instrumental in the success of my research. From the very beginning, he encouraged my independence and allowed me the freedom to explore diverse ideas with minimal objections. I aspire to be as skilled as him in crafting passionate scientific narratives, just as he has done for projects like mine.

To my co-supervisor, Catarina Seabra, I am thankful for her support, enriching discussions, and valuable suggestions. Her emphasis on maintaining a healthy work-life balance and her insights into career management will always serve as a role model for me.

I would also like to express my heartfelt appreciation to Professor Jorge Manuel Castelo Branco de Albuquerque Almeida for his guidance and support in establishing the network analysis.

I consider myself extremely fortunate to have had a supervisor and co-supervisors who genuinely cared about my work and provided the necessary encouragement and guidance along the way.

Completing this work would have been virtually impossible without the unwavering support of all the members of the JP lab. Therefore, I extend my special thanks to Mariana Laranjo, Marta Pereira, and Tiago Reis for their presence and camaraderie in the lab. Your contributions have not only alleviated the low points of my PhD journey but have also amplified its most rewarding aspects. In particular, I thank I would like to express my gratitude to Mariana for being a reliable reference point in the lab, Tiago ever-ready supply of jokes that lightened the atmosphere and Marta for keeping me updated on the latest news and trends in Porto and Coimbra's culinary scene.

It is my immense pleasure to show my best appreciations for Rafaela Oliveira who performed all the electrophysiological experiment in this study and helped me with the analysis. Your invaluable input is much appreciated, and it was a pleasure working and sharing with you our lab duties. Thanks also to Pedro for introducing me into the world of coding and computer hygiene. Finally, I would like to thank the rest of JP lab new and old members for their support in every other aspect of my project.

I would like to thank Luisa Cortes for the indispensable help and expert technical support in microscopy. I want to thank the people with whom I shared the lab over the years and who contributed to the accomplishment of this work: Tatiana, Dominique, Luis, Joana Ferreira, the funniest student Mariana Martins, Miranda Mele and Rui Costa, Débora, and the best pool apprentice Marina.

My PhD was funded by an innovative training network coordinated by Ana Luisa Carvalho. I would like to thank here as first for her incredible achievement and for her willingness in searching for continuous feedback. I would like to thank Doctor Frederico Duque for sharing with me the clinical view on our research in neurodevelopmental disorders. A thank goes also to Peter Kind for hosting my secondment in Edinburgh. A special thank goes to Manuela Rizzi and Owen Dando for helping me in setting the RNA analysis. Lastly, I would like to thank all the principal investigators, industries and the passionate early-stage researchers that participated in this consortium. I hope that this collaboration may only grow in the future.

Beside growing as a scientist, this PhD journey has also played a significant role in my personal growth. I attribute this growth not only to the time spent in the lab but also to the cherished moments shared with friends outside of our academic pursuits. It is with immense gratitude that I express my deepest appreciation to my dear friends Elisa Corti, Gianluca Masella, and yes, Emanuel Tahiri too. Spending time together, whether it was traveling, work launches, riding the waves while surfing, or engaging in game sessions, provided a much-needed respite and kept me grounded throughout this life-changing experience. Your unwavering support and companionship have left an indelible mark on my life during my stay in Portugal.

Finally, this thesis is dedicated to my family, old and new, which endless support and love is unmatched. Grazie mamma e papà, senza il vostro supporto tutto questo non sarebbe stato possibile. Alla mia amata sorella, Concetta, per avermi sempre trasmesso la sua grinta.

To my beloved Federica your constant support and encouragement have meant the world to me, and I am grateful for your presence throughout this journey. Your love and understanding have been a constant source of strength, even when we were physically apart. Thank you for sharing in the challenges and triumphs of my PhD and for being my rock. I am truly lucky to have you by my side.

To all those mentioned above and countless others who have supported me in various ways, both seen and unseen, I am sincerely grateful. Your belief in me, your encouragement, and your contributions have played an integral role in shaping my academic path and accomplishments.

Table of Contents

ABBREVIATIONS

2D	Two-dimensional
3D	Three-dimensional
5-HT	Hydroxy tryptamine
ACSF	Artificial cerebral spinal fluid
AED	Antiepileptic drug
AMPA	α-amino-3-hydroxy-5-methyl-4-isoxazolepropionic acid
AMPAR	α-amino-3-hydroxy-5-methyl-4-isoxazolepropionic acid receptor
ANOVA	Analysis of variance
AP	Action potential
AP-1	Activator protein-1
ASD	Autism spectrum disorder
BDNF	Brain-derived neurotrophic factor
BSA	Bovine serum albumin
BSN	Basson gene
CBZ	Carbamazepine
CD-1	Cluster differentiation-1
CHD8	Chromodomain-helicase-DNA-binding protein 8
CNQX	Cyanquixaline
CREB	cAMP response element-binding protein
CNTNAP	Contactin-associated protein-like 2
CTR	Control
D2R	Dopamine receptor D2
DA	Dopamine
DEG	Differentially expressed gene
DMSO	Dimethyl sulfoxide
DNA	Deoxyribonucleic acid
E/I	Excitatory/inhibitory
EB	Embryoid body
EMA	European medicine agency
ERK	Extracellular signal-regulated protein kinase
FDA	Food and drug administration
FDR	False discovery rate
fEPSC	Field excitatory postsynaptic currend
FMRP	Fragile X mental retardation

FOXG1	Forkhead box protein G1
FVSD	Foetal valproate spectrum disorder
GABA	Gamma amino butyric acid
GABA-A	GABA receptor type A
GABA-B	GABA receptor type B
GABAR	Gamma amino butyric acid receptor
GAD-67	Glutamic acid decarboxylase 67
GDNF	Glial cell neurotrophic factor
GFAP	Glial fibrillary acidic protein
GO	Gene ontology
GSEA	Gene set enrichment analysis
H3	Histone 3
HDAC	Histone deacetylase enzyme
HEPES	N-(2-hydroxyethyl)-1-piperazine-N'-(2-ethanesulfonic acid)
hESC	Human embryotic stem cell
hiPSC	Human induced pluripotent stem cell
HSP	Heat shock protein
IHC	Immunohistochemistry
IQ	Intelligence quotient
KCl	Potassium chloride
LFC	Logarithmic fold change
LTG	Lamotrigine
LTP	Long term potentiation
MAO-A	Monoamine oxidases type A
MAP	Microtubule-associated protein
MCA	Major congenital anomalies
mCO	Mouse cortical organoid
MECP2	Methyl-CpG binding protein 2
mEPSC	Miniature excitatory postsynaptic current
mESC	Mouse embryonic stem cell
miPSC	Miniature inhibitory postsynaptic current
MMP-9	Metalloproteinases-9
mPFC	Medial prefrontal cortex
NEAD	Neurodevelopmental effects of antiepileptic drug
NEUN	Neuronal nuclear marker
NLGN3	Neuroligin 3

NMDA	N-methyl-D-aspartate
NMDAR	N-methyl-D-aspartate receptor
NMDG	N-methyl-d-glucamine
NSC	Neural stem cell
NPC	Neural progenitor cell
NR2A	2A subunit of NMDAR
NR2B	2B subunit of NMDAR
OCT	Optimal cutting temperature
OR	Odd ratio
Par	Prostate apoptosis response
PFA	Paraformaldehyde
PB	Phenobarbital
PBS	Phosphate-buffered saline
PCA	Principal component analysis
RMP	Resting membrane potential
RNA	Ribonucleic acid
RT	Room temperature
RTT	Rett syndrome
SATB2	Special AT-rich sequence-binding protein 2
SERT	Serotonin transporter
SHANK3	SH3 and multiple ankyrin repeat domains protein 3
SMC	Structural maintenance chromatin
SOX2	sex determining region Y- box 2
TBR1	T-box brain transcription factor 1
TNF-α	Tumour necrosis factor α
TrkB	Tyrosine kinase tropomyosin-related kinase
TTX	Tetrodotoxin
USV	Ultrasonic vocalization
vGLUT1	N-methyl-D-aspartate
VPA	Valproic acid
VPALD	Low dose of valproic acid condition
VPAHD	High dose of valproic acid condition
VZ	Ventricular-like zone

KEYWORDS

Autism spectrum disorder
Human neural organoid
Neurodevelopment
Valproic acid

PALAVRAS-CHAVE

Neurodesenvolvimento
Organóide cerebral humano
Perturbação espectro autismo
Ácido valpróico

RESUMO

Compreender as consequências da exposição ao ácido valpróico (VPA) durante o desenvolvimento cerebral humano tem sido um desafio. O VPA é um anticonvulsivo amplamente prescrito e conhecido pelos seus efeitos inibitórios na degradação do ácido gama-aminobutírico, modulação de canais iônicos e inibição de histona desacetilases. O uso de VPA durante a gravidez, por mulheres que sofrem de epilepsia, tem levantado preocupações devido ao maior risco de síndrome fetal por valproato (SFV). O SVF é caracterizado por anomalias congênitas graves (ACGs), problemas cognitivos, e transtorno do espectro do autismo (TEA).
Apesar das restrições atuais ao uso de VPA durante a gravidez, pesquisas com modelos animais e celulares continuam a explorar os mecanismos subjacentes pelos quais o VPA afeta o neurodesenvolvimento e contribuem para o desenvolvimento de TEA.
Embora os modelos *in vivo* de exposição a VPA tenham fornecido informação valiosa sobre os distúrbios do neurodesenvolvimento induzidos por este composto, estes apresentam várias limitações. Primeiro, o protocolo de administração em roedores não reproduz com precisão a exposição fetal humana ao VPA. Segundo, o neurodesenvolvimento humano e de roedores apresenta diferenças críticas. Terceiro, o modelo animal de VPA não consegue capturar totalmente todas vias moleculares, alterações estruturais e mudanças celulares observadas no TEA humano. Estudos que utilizam modelos celulares humanos em culturas tridimensionais (3D) estão ainda em fases iniciais de exploração e no estudo do impacto de VPA sobre o desenvolvimento do cérebro humano.
Este trabalho teve como objetivo preencher esta lacuna de conhecimento, empregando para tal uma abordagem multimodal, incluindo análise imunohistoquímica, sequenciamento de RNA, eletrofisiologia e imagem de cálcio. Foram estudados os efeitos a longo prazo da exposição crônica ao VPA na fisiologia neural e no desenvolvimento de redes neuronais.
De forma consistente com estudos anteriores, observámos uma maior diferenciação neural e um aumento na formação de sinapses glutamatérgicas. Em particular, um aumento na subpopulação de neurônios da camada superficial em organoides expostos ao VPA. Em conformidade com estudos anteriores, também encontramos uma associação significativa com genes associados ao TEA.

Neste estudo, contribuímos para elucidar os mecanismos pelos quais o VPA afeta o desenvolvimento do cérebro humano em desenvolvimento e como essas alterações podem contribuir para distúrbios do neurodesenvolvimento, incluindo o TEA.

ABSTRACT

Understanding the consequences of valproic acid (VPA) exposure during human brain development has been challenging. VPA is a widely prescribed anticonvulsant known for its inhibitory effects on gamma-aminobutyric acid degradation, modulation of ion channels, and inhibition of histone deacetylases. The use of VPA by epileptic women during pregnancy raises concerns due to the heightened risk of Fetal Valproate Spectrum Disorder (FVSD). FVSD is characterized by major congenital anomalies (MCAs) and cognitive impairments, including autism spectrum disorders (ASD).

Despite current restrictions on VPA use in pregnant women, research using animal and culture models continue to explore the underlying mechanisms by which VPA affects neurodevelopment and contributes to the development of ASD.

While *in vivo* VPA models have provided valuable insights into VPA-induced neurodevelopmental disorders, these present several limitations. First, the administration protocol in rodents does not accurately mimic human fetal exposure to VPA. Second, human and rodent neurodevelopment exhibit critical differences. Third, the VPA animal model cannot fully capture all the molecular pathways, structural alterations, and cellular changes observed in human ASD.

Our work aims to fill in this knowledge gap by employing a multimodal approach, including immunohistochemistry analysis, bulk RNA sequencing, electrophysiology, and calcium imaging. We investigated the long-term effects of chronic VPA exposure on neuronal physiology and neuronal network development

Consistent with earlier studies, we observed enhanced neural differentiation and an increase in the formation of glutamatergic synapses. In particular, an increase in superficial layer neuron subpopulation in VPA-exposed organoids. In regard to synaptic formation, we observed that glutamatergic synapses were increased in VPA-exposed organoids at multiple time points. However, there was a distinct pattern concerning inhibitory synapses and gene-related GABAergic transmission. Initially, there was an increase in inhibitory synapses and gene expression associated with GABAergic transmission. As the VPA-exposed organoids matured, these aspects gradually decreased. In keeping with previous research, we also found a significant association with genes associated with ASD.

In this word, we contributed to elucidating the mechanisms through which VPA affects the developing human brain and how these alterations may contribute to neurodevelopmental disorders, including ASD.

CHAPTER 1 | INTRODUCTION

1.1. Valproic acid

Valproic acid (VPA) is a short-chain fatty acid naturally synthesized by *Valeriana Officinalis* (Chateauvieux et al., 2010). Renowned for its broad anticonvulsant action and mood stabilization effect, VPA directly influences the production and degradation of the GABA neurotransmitter and inhibits voltage-gated channels. Consequently, it has emerged as an effective drug for regulating synaptic potentials and treating conditions such as epileptic seizures, bipolar disorder, and has even shown promise as a potential anti-tumour agent (Cerrizuela et al., 2020; Gurvich & Klein, 2002; Péraudeau et al., 2018). Moreover, VPA exerts an inhibitory effect on histone deacetylase enzymes (HDACs), which modulates gene expression (Ghodke-Puranik et al., 2013; Romoli et al., 2019; Terbach & Williams, 2009).

1.2. VPA's impact on Foetal valproate spectrum disorder and Major Congenital Anomalies

The use of VPA by epileptic women during pregnancy has sparked significant concerns due to the heightened risk of a condition known as Fetal Valproate Spectrum Disorder (FVSD) in their children. Several clinical studies have consistently demonstrated that the use of VPA during pregnancy is associated with an increased risk of developing FVSD, showing a higher incidence of major congenital anomalies (MCAs), particularly impacting the cardiac and laryngeal systems, but they also face an increased risk of neurodevelopmental disorders, including autism spectrum disorder (ASD) and speech impairment (Ornoy, 2009; Rasalam et al., 2005; Romoli et al., 2019). In fact, VPA has been identified as the most teratogenic antiepileptic drug (AED) currently available on the market (Koch et al., 1996; Meador, 2008). Recognizing the potential teratogenic effects of AEDs, numerous large-scale pregnancy registries were established to monitor the use and impact of AEDs on pregnancy outcomes. The Quebec pregnancy registry, for instance, reported that among 349 patients with epilepsy, 79.6% were administered AED monotherapy, with 19.9% exposed to VPA monotherapy and 1.6% receiving polytherapy including VPA (Kulaga et al., 2011). Similarly, the Australian Pregnancy Register documented that among epileptic patients, 55% received AED monotherapy, with 17.9% of monotherapy patients being prescribed VPA and 28.9% receiving polytherapy including VPA (Vajda et al., 2012). These reports indicate widespread use of VPA during pregnancy across various regions.

VPA can cause a variety of congenital abnormalities due to its ability to cross the blood placenta barrier. The great majority of MCAs in children exposed to VPA during pregnancy has been shown to be related to the teratogenic effects of VPA rather than to the epileptic disorder

affecting the mother (Genton et al., 2006). VPA and, more generally, AEDs have been linked to neural tube closure impairment and congenital anomalies affecting alimentary, dermatologic, genital, cardiovascular, urinary, pulmonary, and striatal muscular system (Meador, 2008). More precisely, the risk of these defects increased with the frequently performed polytherapy to treat pregnant women affected by epilepsy (Meador, 2008). In subsequent cohort studies, MCAs were found to be considerably increased in VPA monotherapy during the first trimester of pregnancy when compared to other AEDs (Jentink et al., 2010). This study included MCAs like spina bifida, atrial septal defect, cleft palate, hypospadias, polydactyly, and craniosynostosis under VPA monotherapy (Jentink et al., 2010). Additionally, there is extensive clinical literature that reports the risks associated with the in-utero exposition to VPA. To give some examples, the US Federal Drug Administration (FDA) advised the health care professional to inform female patients about the risks of VPA treatment during pregnancy. The collateral effects of this drug listed by this alert were neural tube defects and congenital malformation (Peckman, 2010). Additionally, concentration and period of administration of the drug differ across studies. For reference, VPA ranges of administration have been shown to a minimum of 200 mg to a maximum of 3600 mg per day and risks to the fetus development are directly proportional to the dose used (Mawhinney et al., 2012; Nadebaum et al., 2011a, 2011b; Tomson & Battino, 2011, 2012; Vajda et al., 2012).

Research has focused on patients exposed to monotherapy and aimed to determine the importance of the type of AED, dose, and timing of exposure. For example, Tomson and colleagues used the EURAP pregnancy registry data to study MCA for up to 1 year of age in children exposed to different doses of four frequently used AEDs: carbamazepine, lamotrigine, phenobarbital, and VPA, demonstrating that the risk of birth MCAs can arise in a dose-dependent fashion for all the AEDs (Tomson et al., 2011) **(see Figure 1)**. For VPA, when compared to lamotrigine treatment with a daily dose of 300 mg/day (treatment having the lowest rate of congenital anomalies), the risk of MCAs was increased for daily VPA dose of less than 700 mg/day (Odds Ratio [OR], 2.8), 700 to 1500 mg/day (OR, 5.8), and more than 1500 mg/day (OR, 16.1) (Tomson & Battino, 2012). Similarly, a UK Epilepsy and Pregnancy Register report, with a focus on VPA monotherapy, has shown that high dose of VPA (more than 1000 mg/day) has significantly risen the risk of anomalies compared to a lower daily VPA dose (less than 1000 mg/day) (Mawhinney et al., 2012). Later on, further studies performed by Tomson and colleagues specifically on VPA treatments confirmed that the risk of MCAs was higher when high concentrations of VPA were administered to pregnant women affected by epilepsy (Tomson, Battino, et al., 2015; Tomson, Marson, et al., 2015). Additionally, when monotherapy of VPA was compared to polytherapy of VPA with other AEDs; the polytherapy was observed to have a slightly higher risk of MCAs when compared to monotherapy of VPA (Tomson, Battino,

et al., 2015). Tomson and colleagues investigated the teratogenic risk of eight different AEDs (Tomson et al., 2018). From this study, it was confirmed the relationship between the dose of VPA administered and the increased risk of congenital malformations at 1 year after birth. In addition to that, the research also allowed a comparison between different AEDs and the different dose regimens. The results of this comparison have shown that low dosage of VPA (less or equal than 650 mg/day) carried a risk of MCAs similar to high-dose carbamazepine (more than 700 mg/day) and lamotrigine (more than 325 mg/day) (Tomson et al., 2018). In summary, monotherapy with a low concentration of levetiracetam or lamotrigine appears to be the most appropriate solution to date in women of childbearing potential as well as in pregnancy. Apart from the increasing awareness about the risk of VPA treatment in women of childbearing potential or in pregnancy, a focus should be given also to off-label VPA. Therefore, the use of VPA has diffused also outside of the typical indications, with possible minor surveillance on the potential risk on both short and long-term (Virta et al., 2018).

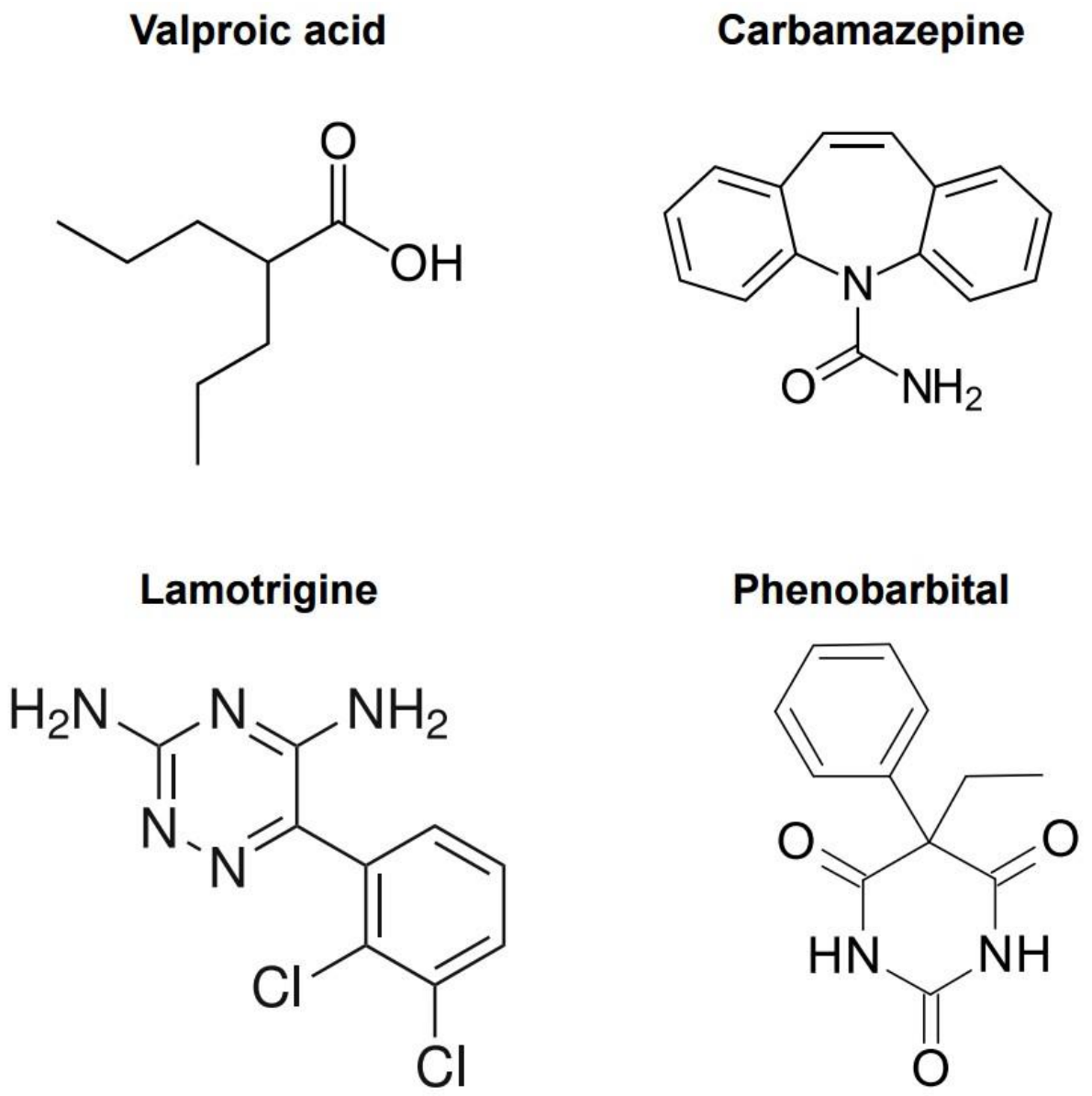

Figure 1: Structural formulae of antiepileptic drugs: Valproic acid, Carbamazepine and Lamotrigine and Phenobarbital: *Valproic acid (upper left) (VPA), Carbamazepine (upper right) (CBZ), Lamotrigine (bottom left) (LTG) Phenobarbital (bottom right) (PB) are antiepileptic drugs that have been associated with congenital malformations of the unborn child when taken during pregnancy. CBZ and LTG are thought to exert their antiepileptic function by inhibition of sodium channels that decreases neuronal excitability. PB exerts their antiepileptic function by acting on GABA-A receptor. CBZ and LTG are associated with a favourable cognitive and behavioural outcome upon in-utero exposure. A link to ASD has been reported for VPA only.*

1.3. VPA impact on Cognitive impairments - autism spectrum disorder

VPA use during pregnancy has also been demonstrated to be involved in the alterations of cognitive functions through its epigenetic effects, some of which were characterized by increased prevalence on the insurgence of ASD and intellectual disability (ID) in the offspring. More precisely, the cognitive impairment was also addressed by clinical investigations on

children exposed in utero to VPA, where prospective studies frequently documented that VPA can be related to an increased probability of cognitive deficit (Cunningham et al., 2003; Thomas et al., 2007, 2008; Tomson, Battino, et al., 2015; Tomson et al., 2018; Tomson, Marson, et al., 2015). The Neurodevelopmental Effects of Antiepileptic Drugs (NEAD) study documented the impact of fetal VPA exposure on children's cognitive functions. The study administered numerous cognitive tests to children whose mothers were treated with VPA monotherapy; and observed that VPA can affect executive functions, IQ, memory, verbal and non-verbal abilities (Meador et al., 2013). Comparable results were also obtained by other investigations on IQ capabilities of children exposed to VPA in utero (Baker et al., 2015). This study confirmed VPA as the central factor affecting children's IQ, even more than the alterations reported in mothers (Baker et al., 2015). Another similar study has observed the cognitive and behavioural impact of AEDs and found that, at lower doses than those required to elicit MCAs, only VPA exposed children had the highest risk to provoke cognitive impairments (Meador et al., 2009). Other investigations contributed to provide pieces of evidence for VPA-induced cognitive and behavioural (Meador et al., 2011; Nadebaum et al., 2011b; Roullet et al., 2013; Shallcross et al., 2011). Additionally, several clinical investigations have associated VPA exposure during the first trimester of pregnancy with an increased risk of ASD in the offspring. Originally, the first associations were made due to an increase of autistic features in children diagnosed with FVSD (Christianson et al., 1994; G. Williams et al., 2001; P. G. Williams & Hersh, 1997). In a study that analysed the effects of prenatal exposition to AEDs have shown that VPA stands out as the most associated with ASD, where 8,9% analysed children exposed to VPA fulfilled the DSM-IV criteria either for autism or Asperger syndrome (Rasalam et al., 2005). A similar conclusion was reached by another study performed by Bromley and colleagues where exposition to VPA resulted in a seven-fold greater incidence of ASD or key symptoms related to ASD including language impairment, reduced attention, social difficulties, and restricted interests (Bromley et al., 2008). Considering the strong impact of VPA exposure on the cognitive functions and neurodevelopment observed by retrospective and prospective studies, the drug has been heavily restricted (Tomson, Battino, et al., 2015; Tomson et al., 2016; Tomson, Marson, et al., 2015). Therefore, the European Medicines Agency (EMA) already revised the indication of VPA treatment, especially in female patients and pregnant women (*Valproate-Related-Substances-Article-31-Referral-Prac-Assessment-Report_en.Pdf*, 2014). Furthermore, EMA's restrictions on the use of VPA led to a significant decreasing trend in the number of prescriptions (Tomson et al., 2019). During the period analysed by this study, the monotherapy administration of VPA declined considerably from 25.9% in 2000 to 6.7% in 2013. Additionally, the polytherapy administration of VPA with other AEDs also greatly decreased during the same period - from 56% in 2000 to 28.8% in 2013 - (Tomson et al., 2019). Even though the prescription of VPA in pregnancy has been markedly reduced, the known impact of VPA on cognitive functions and

increased risk of ASD provided the impetus to better understand the VPA mechanisms of action that we are going to further elucidate.

1.4. Direct effects of VPA

VPA is used as a treatment of epileptic seizures because of its wide spectrum of targets **(see Figure 2)**. Additionally, VPA is known to have mood-stabilizer and neuroprotective properties. One of the main mechanisms that VPA can manipulate is the GABAergic system. More precisely, VPA increases the presence of gamma-aminobutyric acid (GABA) in the pre-synapsis through inhibition of ABAT and ALDH5A1, both of which are involved in the GABA degradation pathway. The increased availability of GABA also facilitates GABA mediated response at the postsynaptic level (C. U. Johannessen & Johannessen, 2003; Rogawski & Löscher, 2004). Apart from the increased production of GABA, VPA also directly interacts with GABA-A and GABA-B receptors and enhances their stimulus-induced response (Cunningham et al., 2003). Specifically, VPA interacts directly with the regulatory regions of GABA receptors, specifically the benzodiazepine-binding sites. This interaction leads to a delay in the extinction of the postsynaptic inhibitory potential, which is mediated by the activation of GABA-A receptors. Additionally, VPA facilitates the binding of baclofen to GABA-B receptors. (Löscher, 1993, 1999; Löscher & Schmidt, 1980). The broad spectrum of actions that VPA imprints on GABA availability may explain why an increased concentration of this neurotransmitter is observed during VPA treatments (C. U. Johannessen, 2000; Löscher, 2011). VPA not only influences the inhibitory GABAergic system, but it also regulates the activity of excitatory glutamatergic system. Indeed, the administration of VPA in rats has been shown to reduce N-methyl-D-aspartate (NMDA) and kainate-induced excitatory activity in the medial prefrontal cortex (Gobbi & Janiri, 2006). Interestingly, VPA promotes neural cortex neuroplasticity through the enhanced expression of NR2A and NR2B subunits of the NMDA receptor (NMDAR). Due to the modulation of NR2A/2B expression, there is also an implication in Ras-ERK pathway signalling and glutamate receptor trafficking (A. J. Kim et al., 2005; Rinaldi et al., 2007). In an *in vivo* study on mice with a genetic mutation at the Bassoon gene (Bsn), which is a mouse line characterized by irregular neuronal activity and spontaneous persistent cortical seizures associated with altered NR2A/2B ratio in NMDAR, administration of VPA led to a rebalancing of the NR2A/2B ratio, rescue of the striatal synaptic plasticity, and a reduction of seizures and mortality (Ghiglieri et al., 2009). Additionally, when VPA was administered chronically, a reduction in surface expression and synaptic localization of GluR1/2 was reported (Du et al., 2008).

Beyond the glutamatergic and GABAergic systems, VPA promotes also the availability of serotonin (5-HT) and dopamine (DA) in the hippocampus and striatum. However, regulation appears to be disconnected to the antiepileptic effects of VPA (Biggs et al., 1992; Ichikawa & Meltzer, 1999). Due to this, VPA is considered an effective antipsychotic. In a study on rats exposed to VPA, an increase of DA-release in the medial prefrontal cortex was observed. Interestingly, the increase of DA in this region was abolished by selective obstruction of the 5-HT1A receptor activity (Ichikawa & Meltzer, 1999; Löscher, 1999, 2002). Another investigation on *in vivo* models of depression has documented the antidepressant action of VPA which promoted 5-HT transporter while inhibiting the monoamine oxidases type A (MAOA), an enzyme involved in the metabolism of 5-HT (Qiu et al., 2014).

VPA appears to have an effect also on the ionic channels which regulate neuronal activity in the brain. In an *in vitro* study using cultured neurons, VPA has been observed to negatively affect neuronal high-frequency repetitive firing at a lower concentration than the one required to depress a normal neuronal activity (McLean & Macdonald, 1986). More precisely, the administration of VPA affects sodium, calcium and potassium ion currents. The inward sodium current is reduced through the blockage of both persistent and fast sodium currents (Taverna et al., 1998; Van den Berg et al., 1993). In large part, VPA anti-seizure properties may come from negative modulation of persistent sodium current (Van den Berg et al., 1993). In addition to the modulation of sodium channels, it has been shown that VPA affects the activity of low threshold T-type calcium channels in peripheral ganglion neurons both at the pre- and post-synaptic levels (Kelly et al., 1990). At higher concentrations, VPA enhances the late potassium outward current amplitude. It has been shown that this action can lead to an increase in the threshold for epileptiform activity (Walden et al., 1993). Additionally, VPA regulation of the ion channel activities may also mediate neuroprotection against ischemic damage *in vitro* (Costa et al., 2006) and in models of epilepsy (Wilson et al., 2007). However, the main effects of VPA effects may unrelated to the downregulation of presynaptic sodium and calcium currents, as shown by recent experimental investigations, addressing membrane permeability performed on an animal-derived hippocampal epilepsy model (Sitges et al., 2016). On the other hand, VPA seems to modulate neuron resting membrane potential by lowering the threshold of voltage-gated M-channels. Therefore, the restoration of the neuron resting potential through the M-channels regulation has been suggested as a possibility for future therapeutic solutions for AEDs like VPA (Kay et al., 2015).

1.5. Indirect effects of VPA - histone deacetylase inhibition

It has been shown that VPA is also capable of exerting effects on gene expression via two main mechanisms: regulation of transcriptional factors, and epigenetic modulation of gene expression via inhibition of HDACs **(see Figure 2)** (Monti et al., 2009). Both mechanisms may take significant time to manifest, even with discontinuous administration of VPA (Monti et al., 2009). “Epigenetic” refers to modifications that do not alter the DNA sequence directly, but that modulates the expression of that sequence through alterations of DNA “accessory data”, such as methylation or histone acetylation status (Feinberg, 2007; Kobow & Blümcke, 2011). The impact of VPA on epigenetics appears to be relevant to its anticonvulsant activity, neuroprotective effects, and ability to modulate neurogenesis (Ghiglieri et al., 2009). Additionally, epigenetic modifications in neuropathologic conditions and epileptic seizures are gaining more attention and have even been proposed as target for new AEDs treatments (Kobow & Blümcke, 2011). Due to the VPA-induced epigenetic alterations, the modulated expression of several signalling molecules, regulation and transcription of synaptic receptors can have an impact on the excitotoxicity and neuroprotective pathways (Monti et al., 2009; Nalivaeva et al., 2009). The VPA epigenetic effect is characterized by its inhibition of HDACs and regulation of brain-derived neurotrophic factor (BDNF) (Ghiglieri et al., 2010). Through the negative interaction between VPA and HDAC, this drug modifies the histone acetylation and DNA methylation balance which consequently alters chromatin and nucleosome status (Cervoni et al., 2002; Cervoni & Szyf, 2001; Tan et al., 2017). Indeed, it has been shown that VPA regulates proteins that control chromatin decondensation and the structural maintenance of chromatin (SMC), SMC-associated proteins and DNA methyltransferases. By modulating these processes, VPA alters the sensitivity of DNA to nuclease activity (Monti et al., 2009). VPA selectively interacts with class I and class II HDACs. By inhibiting the de-acetylation of the histone tails, VPA regulates gene expression by facilitating the access to the transcription sites (Chateauvieux et al., 2010).

On the other hand, VPA can also lead to changes in histone methylation. The induction of mono-, di- and tri-methylation of H3 by the administration of VPA can facilitate transcription activity (Milutinovic et al., 2007). In addition to that, VPA is involved in the interaction between transcription factors, including c-Fos and c-Jun, and the activator protein 1 (AP-1), As a consequence of these interactions, VPA facilitates the expression of AP-1 controlled genes (Chen et al., 1999; Fukuchi et al., 2009). In particular, the interaction between VPA and AP-1, which follows a time- and dose-dependent modality, promotes the transcription of AP-1 dependent genes like GAP-43, 5-HT2A and Bcl-2 (Chen et al., 1997; Sullivan et al., 2004). Other transcription factors modulated by the administration of VPA are CAMP response

element-binding protein (CREB), which is involved in the phosphorylation in neuronal development, migration, memory and synaptic plasticity (Lonze & Ginty, 2002; Monti et al., 2009); and the nuclear factor kappa-light-chain-enhancer of activated B cells (NF-kB), which brings to the regulation of the immune response via the decrease of TNF-alpha and IL-6 (Ichiyama et al., 2000). Even though some investigations on *in vivo* models have shown VPA decreasing NF-kB activity in the frontal cortex (Chen et al., 1999), other studies have demonstrated increasing NF-kB activity in the hippocampus and cortex (Monti et al., 2009). Additionally, this increase seems to be mediated by the ERK pathway which also increases the presence of BDNF (Monti et al., 2009).

BDNF is a brain-specific molecule that can elicit different effects in cells, such as the maintenance of neuronal phenotypes, regulation of synaptic plasticity, survival, growth and migration (Chao, 2003). This molecule appears to be crucial for neurodevelopment, since BDNF expression varies within the different brain development stages (Baquet et al., 2004; Bath & Pimentel, 2017). However, the effects of VPA on BDNF expression have reached contrasting conclusions. To give some examples, an *in vivo* study showed an increase of BDNF mRNA transcription in the neural tube after prenatal VPA administration in rats (Fukuchi et al., 2009). On the other hand, an *in vitro* experiment has shown that cultured cortical neurons were transcribing lower levels of BDNF mRNA when exposed to the drug (Bath & Pimentel, 2017; Bittigau et al., 2003; Shi et al., 2010). Only with the advent of the ELISA technology, it has been possible to observe BDNF protein levels in *in vivo* models. In these recent investigations, VPA has been shown to decrease BDNF protein levels by nearly 50% after early postnatal exposure. A decrease in BDNF expression has also been shown in the cerebellum, while leaving unaffected the BDNF protein levels in the hippocampus (Bath & Pimentel, 2017). Another transcription factor affected by the presence of VPA is glial cell line-derived neurotrophic factor (GDNF), a molecule mainly involved in neuroprotection and cognitive-enhancement (Monti et al., 2009; Wu et al., 2008). The neuroprotective properties of VPA come from the regulation of numerous neuron-specific genes. More precisely, VPA can promote NeuroD, a transcription factor that increases the expression of genes involved in neuron survival like Bad and Bcl-2. The effect of this modulation further promotes GABAergic transmission (Laeng et al., 2004; Monti et al., 2009).

In addition to that, VPA down-regulates apoptotic transcription factors, such as Bax gene, and pro-inflammatory signals including IL-6, Fas-L and metalloproteinases (Sinn et al., 2007). The anticonvulsant property of VPA does not come only from its short-term effects, but also from the epigenetic mechanisms that the drug modulates. As reported in an investigation on human brain post-mortem tissues, VPA modulates the transcription of SCN3A, a gene for the α-isoform of

the voltage-gated sodium channel III. Usually, this isoform is expressed exclusively during childhood (Whitaker et al., 2001), but it has been shown to be overexpressed in adult patients affected by epilepsy and in seizure models (Guo et al., 2008; Tan et al., 2017). Since the presence of SCN3A highly increases excitability in neurons, this isoform appears to be involved in the development of epilepsy. Due to this, it has been suggested as a target for treatment possibly through down-regulation. In further investigation on *in vivo* models exposed to VPA, it has been observed a decrease in SCN3A expression and a reduction in the methylation level of the SCN3A gene promoter. This could explain how VPA-induced epigenetic alterations can also exert anticonvulsant effects through the downregulation of SCN3A transcription (Tan et al., 2017). Other AEDs, such as carbamazine (CBZ) or lamotrigine (LTG), did not exert the same effect on SCN3A expression, therefore, this property is considered limited to VPA (Tan et al., 2017).

Even though AEDs have all anticonvulsant properties, all of them differ in respect of efficacy and cellular pathways affected by the administration of a particular AED or a combination of AEDs if under a polytherapy treatment (Löscher & Schmidt, 2006; Sitges et al., 2016). Additionally, AEDs vary in terms of duration of the treatment. Older AEDs, to give an example, can become less effective in prolonged treatment due to metabolic tolerance developed by the patient or seizure animal model exposed to this AED. Phenobarbital (PB) is part of this old group of AEDs, in which the tolerance arises from the adaptive remodelling of the enzymes involved in the metabolism or elimination of the drug (Löscher, 2011; Löscher & Schmidt, 2006). On the other hand, other AEDs can become more effective when used for prolonged periods of time. To give an example, patients treated with primidone showed an accumulation of PB in their tissues which greatly improved the efficacy of the treatment (Löscher, 2011). For VPA, instead, it has been reported that the epigenetic mechanisms triggered by the inhibitory regulation of HDAC can prevent the seizure-induced neurogenesis (Ghiglieri et al., 2010). More precisely, the VPA impact on BDNF expression seems to have a central role in seizure control (Ghiglieri et al., 2010; Jankowsky & Patterson, 2001; Wyneken et al., 2001, 2003). What has been observed in foci of seizures both in *in vivo* models and patients is an upregulation of BDNF transcription (Jankowsky & Patterson, 2001; M. Takahashi et al., 1999). In addition to the increase of BDNF transcription, also the tyrosine kinase tropomyosin-related kinase B (TrkB), the intracellular receptor binding BDNF, is up-regulated for a long period of time. These two mechanisms together lead to a facilitation of synaptic plasticity and an increase in the neurite growth (Ghiglieri et al., 2010; C.-H. Kim & Lisman, 1999; Wyneken et al., 2001, 2003; Zuccato & Cattaneo, 2009). Therefore, the anticonvulsant property of VPA also comes from its impact on the modulation of the BDNF/TrkB pathway. The role of the upregulation of this pathway during epilepsy has been shown in an *in vivo* model of epilepsy, Bsn mutated mice. The

BDNF/TrkB pathway modulated the striatal plasticity after repeated epileptic seizures in order to change the plasticity pattern of neurons and facilitate feedforward inhibition in the striatal circuitry (Ghiglieri et al., 2010). In this investigation, the Bsn mutant line was characterized by increased TrkB transcription and erroneous distribution of BDNF among fast-spiking interneurons and spiny neurons which altered the striatal synaptic organization. With the administration of VPA for a prolonged period of time, the exposition led to a reduction in the seizures, a correct distribution of BDNF and a return to more physiological TrkB expression (Ghiglieri et al., 2010). This finding elucidates the profound influence of VPA on synaptic plasticity, attributed to its anticonvulsant properties as well as its ability to modulate epigenetic mechanisms.

Despite all the above, however, the precise mechanisms underlying the development of ASD in individuals following *in utero* exposure to this antiepileptic drug remain poorly understood.

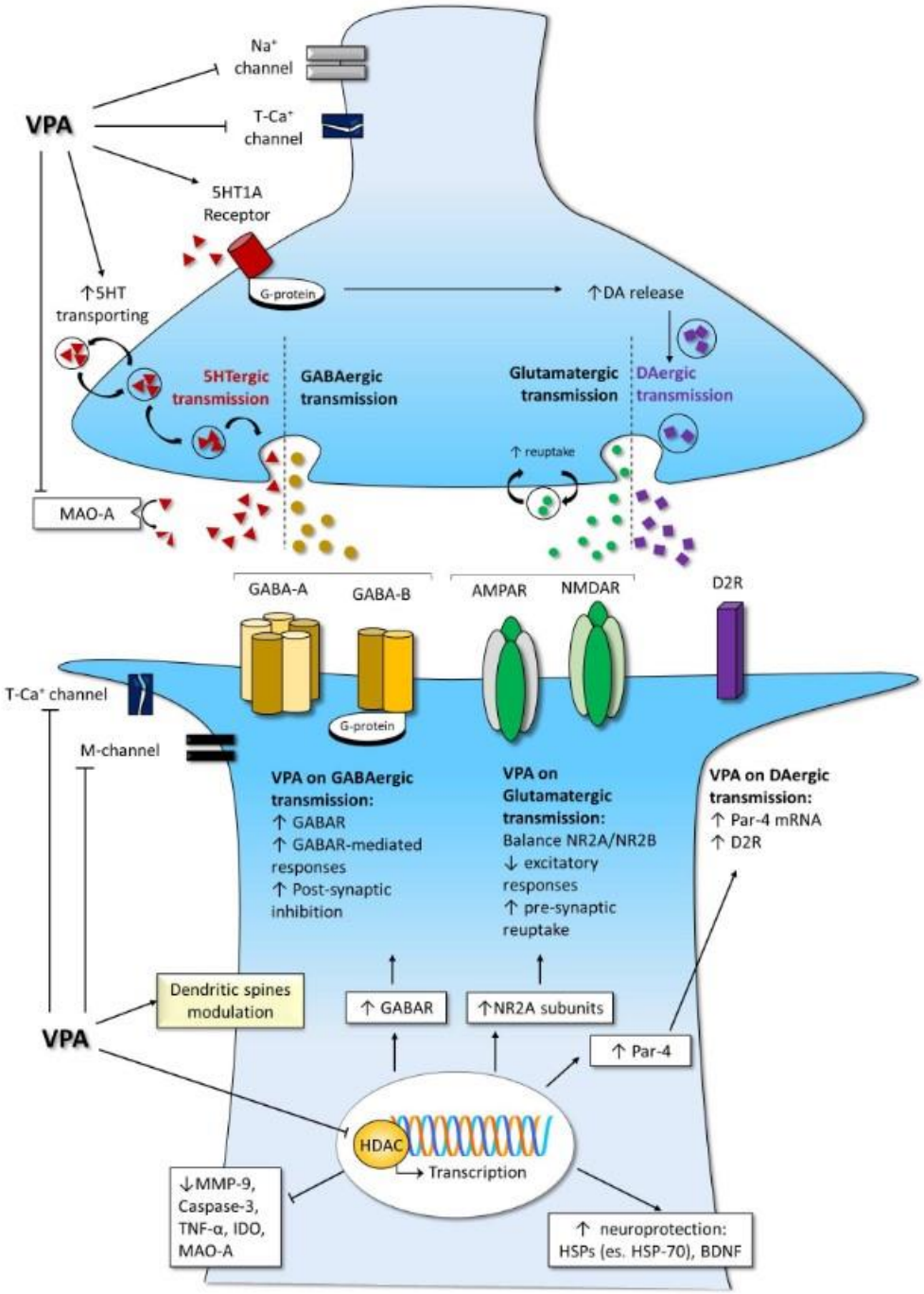

Figure 2: VPA effects on synaptic and intracellular pathways: *The increase in GABAergic transmission coincides with modulation of other aminergic systems; excitatory ionic channels, such as calcium and sodium channels are inhibited, while potassium currents are positively modulated. Furthermore, epigenetic mechanisms influence receptor expression and neuroprotective pathways.* ***Legend:*** *AMPAR: α-amino-3hydroxy-5-methyl-4-isoxazolepropionic acid –AMPA- receptor; BDNF: brain derived neurotrophic factor; DA: dopamine; D2R: dopamine D2 receptor; GABA: gaba-amino-butirric acid; GABAR: GABA receptors; GABA-A: GABA receptor type A; GABA-B: GABA receptor type B; HSPs: heat shock proteins; HSP-70: heat shock protein 70; K+: potassium; IDO: indoleamine 2,3 dioxygenase; MAO-A: mono-amines oxidase type A; M-channel: low-threshold noninactivating voltage-gated potassium current; MMP-9: metalloproteinases-9; Na+ channel: sodium channel; NMDAR: N-metyl-D-aspartate -NMDA- receptor; NR2A: 2A subunit of NMDAR; NR2B: 2B subunit of NMDAR; Par-4: prostate apoptosis response-4; T-Ca+ channel: low-threshold T-calcium channel; TNF-α: tumor necrosis factor α; VPA: valproate; 5HT: serotonin (adapted from Romoli et al., 2019).*

1.6. *In utero* exposure to VPA - animal studies

1.6.1. Epilepsy

The mechanisms linking ASD-like features in children exposed to VPA during pregnancy are not completely understood. Research efforts have utilized both *in vivo* and *in vitro* models to gain a better understanding and in the context of *in vivo* studies, VPA administration has demonstrated various effects at the molecular, structural, and behavioral levels.

VPA is considered to have antiepileptic effects also in the long-term mainly through the inhibitory interaction with the HDAC. This interaction modulates the 5HT and DAergic pathways further increasing the spectrum of antiepileptic targets, even though the interaction exerts also an effect on the glutamatergic and GABAergic balance, as shown by an *in vivo* experiment on rats treated with 800 mg/kg of valproate where an increase of dopamine presence was found after the VPA exposure (Nakasato et al., 2008). At similar concentration, VPA-treated rats at early stages of pregnancy (E9) showed an increase of dopamine levels in the frontal cortex (Narita et al., 2002). However, the results on 5-HT levels are divergent when compared to other studies. While the one of Narita and colleagues an increase in 5-HT level in the hippocampus are reported, in a more recent study a decrease in 5-HT in the same region has been observed by Dufour-Rainfray and colleagues (Dufour-Rainfray et al., 2010; Narita et al., 2002). Both independent studies used high performance liquid chromatography (HPLC) on brain tissues of 50 days postnatal male rats exposed to 600 mg/kg of valproate. The different rat strain and the different modality of exposure may be the reasons why different results were observed. ASD human patients and ASD animal models were examined to validate hyperserotonaemia as a marker for autism (Schain & Freedman, 1961; Veenstra-VanderWeele et al., 2012). More precisely, serotonin transporter (SERT) binding appears to be lower, and the dopamine transporter binding is higher in patients with autism (Nakamura et al., 2010), so a specific SERT variant has been identified as a risk factor for the disease (Veenstra-VanderWeele et al., 2012). A possible treatment for self-injurious behaviour and irritability in patients with autism has been found in the use of risperidone, a dopamine and serotonin receptor antagonist (Scott & Dhillon, 2007). Other studies are also focused on the identification of the targets that VPA regulates, in order to examine the neurobiological mechanisms underlying the aetiology of ASD. The examination of cluster differentiation 1 (CD1) genes of mouse embryos treated with 800 mg/kg of VPA or non-teratogenic analogues, such as valnoctamide or valpromide, led to the finding of 11 gene sets with increased and 20 with decreased level of expressions after VPA exposition. The role of the functionally known set of genes was attributed to regulate the cell-cycle and apoptosis processes (Okada et al., 2005). However, further studies are required both to discover the

currently unknown role of the remaining set of genes, but also to identify the mechanisms that bring to the neurodevelopmental alteration characteristic in autism.

Beyond the modulation of monoamines and molecular pathways, the administration of VPA can also alter the brain structure at the cellular and network level. At the structural level, it has been demonstrated that exposure to around 800 mg/kg of VPA induced a decrease in the transcription of BDNF in the somatosensory cortex and a reduction in the expression of neuroligin 3 (NLGN3), a gene associated with ASD, in both the cortical and hippocampal regions (Kolozsi et al., 2009; Roullet et al., 2010). In addition to that, a low expression NLGN3 was also reported in a study which assessed the possibility to use auditory evoked-responses as a biomarker to diagnose ASD in VPA-treated animal models (600 mg/kg) and human patients. This study also clarifies the role of NLGN3 in the GABAergic system response to VPA exposure (Gandal et al., 2010). *In vivo* experiments on rat pups exposed to 350 mg/kg of VPA at E12.5 have shown to increase the complexity of dendritic arborizations in pyramidal cells localized in the motor cortex (Snow et al., 2008). At the circuit level, experiments with multiple whole-cell clamping recordings in VPA rat brain slices in level 5 pyramidal cells of the somatosensory cortex and medial prefrontal cortex (mPFC) have reported a preference in local connectivity in a radius of less than 50 µm after exposure to 500 mg/kg at E11.5 (Rinaldi, Silberberg, et al., 2008). The increased connectivity between neighbouring neurons was inversely proportional to the strength of those connections and it is suggested to sustain a hyperactivity of the network (Rinaldi, Silberberg, et al., 2008). In the same region but in layers 2/3 of mPFC, rats exposed to 500 mg/kg of VPA reported an increase of the ratio of NMDA over AMPA receptors (Walcott et al., 2011). The alterations reported on the NMDA presence and the decrease in the intrinsic excitability can lead to a compensation during the development of the network. To observe these effects, they recorded miniature postsynaptic currents (mEPSCs) from all inputs to the neuron rather than specific neighbouring cells from the same layer (Rinaldi, Silberberg, et al., 2008; Walcott et al., 2011). Another investigation on the same region has examined the mPFC as a whole using field excitatory postsynaptic potential (fEPSP) recordings and contralateral stimulation. After administration of 600 mg/kg in E12, an increase in long-term potentiation (LTP) after high frequency stimulation and higher paired pulse facilitation was reported (Sui & Chen, 2012). As suggested by the authors, the increase of LTP and higher paired pulse facilitation may be linked to an enhanced retention of fear trace memories which relies on mPFC (Sui & Chen, 2012). A few studies administered VPA to rodents orally in order to resemble the regimen of administration for pregnant women with epilepsy. The main findings included elevated number of neurons in the superficial layers of neocortices on P4, increased thickness of superficial neocortical layers and higher number of non-GABAergic projection neurons in the superficial layers of P21 neocortices, and enhanced proliferation of neural progenitor cells

(NPCs) by reducing the probability of cell cycle exit (Fujimura et al., 2016). These findings are consistent with previous studies reporting that *in utero* VPA exposure increases neocortical thickness in both humans (Wood et al., 2014) and rats exposed prenatally to VPA (Sabers et al., 2014), as well as with research showing that VPA exposure to cultured mice embryonic stem cells enhances the production of superficial neocortical neurons (Juliandi et al., 2012).

1.6.2. ASD

ASD is a highly heterogenous disorder, diagnosed solely through behavioural assessment. In research, tools from behavioural neurosciences are available to monitor aspects of ASD-like behaviours, such as repetitive stereotypies and social communication, in animal models (Crawley, 2004; Roullet & Crawley, 2011; Wöhr et al., 2011). Numerous investigations performed with the administration of VPA *in utero* have been performed in order to analyse the impact of this exposure on neurodevelopment, social behaviour and stereotypic behaviours of rodents (Markram et al., 2008; Roullet et al., 2010; Schneider & Przewłocki, 2005). One of the first studies to analyse behavioural alterations post VPA exposure (800 mg/kg) was published by Schneider and Przewlocki in 2005. In this study, several tests were performed in order to validate this new VPA model and examine if the typical altered behaviours observed in ASD patients were also present in a rat model. Subsequently, this study was replicated several times using both rats (Harden et al., 2009) and mice and was shown to be robust since it performed under a variety of different protocols (Kataoka et al., 2013; Roullet et al., 2010; Wagner et al., 2006). Frequent repetitive or stereotyped behaviours, lower social interaction, neurodevelopmental delay and eye-opening delays, as well as abnormal responses to painful and non-painful stimuli are the main features that characterize rats exposed *in utero* to 800mg/kg of valproate (Kataoka et al., 2013; Schneider & Przewłocki, 2005). Additionally, a similar result was observed in a different paradigm with rats exposed to 500 mg/kg of VPA in a Y maze test (Markram et al., 2008). Interestingly, the effects of prenatal VPA exposure appear also to have significantly greater impact, both at the molecular and behavioural levels, on males when compared to female rats (Schneider et al., 2008). Beyond deficits in social interactions, a few studies were able to monitor ultrasonic vocalizations (USVs) to maternal separation or olfactory behaviour in pups. In two of these works, one in rats (Schneider & Przewłocki, 2005) and one in mice (Roullet et al., 2010), higher latency to find back the home bedding during the nest seeking response was shown after prenatal exposure of the pups to 800 mg/kg of valproate. Another study in VPA-exposed mice reported a decrease in the number of USVs after separation from the dam, and an abnormal spectral frequency pattern in response to an unfamiliar adult female. These experiments were performed in adult male mice previously

exposed to 600 mg/kg of VPA (Gandal et al., 2010). These behavioural studies validate the prenatal administration of VPA in rodents as a model that replicates the behavioural features in line with the ethology of rodents but functionally comparable to the behavioural features shown by patients affected by ASD. One particular study showed that *in utero* exposition to VPA led to an increase of ASD-like features including impaired sociability and marble burying (Choi et al., 2016). Interestingly, the same features persisted through the two subsequent generations when the VPA treated animals and the affected mice were mated with naive females (Choi et al., 2016). This kind of effect has been linked to the transgenerational inheritance of epigenetic alterations.

Strain/species	VPA dose/administration	Time of exposure	Outcome	Reference
Wistar rats	500 mg/kg; single i.p. injection	E11.5	↑ protein levels of NMDA receptor subunits (NR2A, NR2B) and CaMKII, ↑ NMDA receptor-mediated synaptic currents, ↑ postsynaptic LTP in somatosensory cortex	Rinaldi et al., 2007
Wistar rats	600 mg/kg; single i.p. injection	E12.5	↓ proenkephalin mRNA expression in the dorsal striatum and nucleus accumbens	Schneider et al., 2007
Long-Evans rats	350 mg/kg; single i.p. injection	E12.5	↑ dendritic arborization complexity of apical dendrites in motor cortex layer II pyramidal cells	Snow et al., 2008
Wistar rats	500 mg/kg; single i.p. injection	E11.5	↑ number of direct connections between close neighboring layer 5 pyramidal cells, weaker excitatory synaptic responses, ↓ cell excitability, ↑ network reactivity in somatosensory and medial prefrontal cortices	Rinaldi, Perrodin, et al., 2008; Rinaldi, Silberberg, et al., 2008
Wistar rats	500 mg/kg; single i.p. injection	E12.5	↑ reactivity to stimulation, ↑ LTP, ↓ inhibition in the basolateral amygdala	Markram et al., 2008
Hybrid of C57BL/6, CF-1, Swiss Webster and DBA-2 mouse strains	800 mg/kg; 1.5 g of peanut butter mixed with VPA	E11	↓ neuroligin 3 mRNA in hippocampal subregions (CA1, CA3, DG) and in the somatosensory cortex; ↓ BDNF mRNA in the somatosensory cortex	Kolozsi et al., 2009; Roullet et al., 2010
C57BL/6 mice	500 mg/kg; single i.p. injection	E10.5	↓ parvalbumin-positive inhibitory neurons in parietal and occipital cortices	Gogolla et al., 2009
C57BL/6Hsd mice	600 mg/kg; single s.c. injection	E13	↓ gamma-phase locking and evoked gamma-power	Gandal et al., 2010
ICR (CD-1) mice	500 mg/kg; single i.p. injection	E12.5	↓ Nissl-positive neurons in layers II-III and V of the prefrontal cortex of female mice; ↓ Nissl-positive neurons in layers II-III and V of the prefrontal cortex and layers IV-V of the somatosensory cortex of male mice	Hara et al., 2012; Kataoka et al., 2013
Sprague-Dawley rats	500 mg/kg; single i.p. injection	E12.5	↓ dendritic spine number in the prefrontal cortex, ↑ dendritic spine number in the ventral hippocampus	Bringas et al., 2013
Wistar rats	500 mg/kg; single i.p. injection	E12.5	↓ total and phosphorylated Akt, mTOR and 4E-BP1, ↓ phosphorylated rpS6	Nicolini et al., 2015

↑***Table 1: Cellular and molecular alterations induced by maternal challenge with valproic acid:*** *i.p. = intraperitoneal; s.c. = subcutaneous; E = embryonic day; LTP = long-term potentiation; rpS6 = ribosomal protein S6 (adapted from (Nicolini & Fahnestock, 2018) (see previous page for the table).*

1.6.3. *In utero* exposure to VPA - primary cultures studies

In vitro research provides several advantages over *in vivo* studies, including precise control over the experimental environment, cost-effectiveness, higher throughput capabilities, and reduced reliance on animals. These benefits make it a valuable approach for investigating biological processes and drug effects. In the context of VPA neurodevelopmental effects, it becomes apparent that the main consequence of its epigenetic effect are promotion of NPC proliferation, neuronal differentiation and imbalance between excitation and inhibition (E/I imbalance), which are associated with ASD-like behaviour, as described below.

One of the first studies on primary cultures showed that VPA promotes neural differentiation and inhibits proliferation (Jung et al., 2008). Even though the promotion of neuronal differentiation was also observed by other three studies of primary cultures isolated from mice and rat (Go et al., 2012; Juliandi et al., 2012; Kao et al., 2013), all these studies observed also an increase in the pool of NPCs. This VPA-induced increase in the NPC pool is suspected to be induced by VPA inhibition of the glycogen synthase kinase 3 (GSK3) activity (Go et al., 2012; Kao et al., 2013). Interestingly, through the use of mouse embryonic stem cells (mESCs) cultures, Juliandi and colleagues observed an enhancement of the superficial-layer neurons over the deep-layer neurons under VPA exposure (Juliandi et al., 2012). Beside GSK3 and its related pathway, also AKT/mTOR/p70S6K pathway was implicated in VPA-induced neuronal differentiation which was described to be also dose-dependent in neural stem cells (NSCs) (X. Zhang et al., 2017).

Another recent study observed that the treatment of agmatine, an endogenous NMDA receptor antagonist, led to a recovery of the ASD-like behaviour in a model of VPA. Due to this, agmatine and NMDA receptor agonists have been suggested as possible targets to restore ERK1/2 activation and resolve ASD-like behaviour (J.-W. Kim et al., 2017). Beside the NMDA receptor, also the mRNA levels of all subtypes of T-type calcium channels were increased by VPA exposure in NSCs of rats, as well as calcium influx in response to potassium chloride-induced depolarization after NSC differentiation into neurons (J.-W. Kim et al., 2020).

Further studies on primary cultures instead explored the E/I imbalance phenotype found in ASD, confirmed that the impact of the drug is dose-dependent, dependent on the time-point in which the drug is administered, and dependent on the duration of exposition. Indeed, Iijima and colleagues demonstrated that prenatal exposition to VPA alters the E/I balance through long-term epigenetic effects by HDAC inhibition (Iijima et al., 2016). More precisely, they observed that VPA *in utero* exposure differentially affected both the GABAergic and glutamatergic systems. The former was mainly affected in adolescence with a loss of function of inhibitory

transmission, while the latter was observed in primary culture of adult mice with a gain in the glutamatergic function (Iijima et al., 2016). These findings are consistent with a study conducted in rats, which observed impaired GABAergic synaptic transmission, and another study using primary cultures from rats that showed impaired formation of GABAergic synapses due to VPA exposure (Banerjee et al., 2013; Kumamaru et al., 2014). Notably, Takeda et al. demonstrated that VPA-exposed astrocytes may also play a role in the impairment of GABAergic synapse formation and synaptic transmission (Takeda et al., 2021).

When looking into the neurological field, the *in utero* administration of VPA in mice and animal primary cultures have been considered potent models to study the aetiology of autism. However, animal models have some limitations since the animal model cannot always address all the molecular pathways, structural and cellular alterations in human physiology. The possibility to perform experiments is a suitable VPA human models would give us more information on the real weight of the VPA effects on the different stages of human brain development and would help us to find alternative therapies to avoid the rise of this neurodevelopmental disorder.

In summary, administration of VPA can alter the neuronal network at several levels: the presence of monoamines (Dufour-Rainfray et al., 2010; Narita et al., 2002), local connectivity and complexity (Snow et al., 2008), cell distribution between NPCs and neuron differentiation (Fujimura et al., 2016; Go et al., 2012; Juliandi et al., 2012; Kao et al., 2013), intrinsic neuronal excitability (Iijima et al., 2016), both pre- and post-synaptic regions (Iijima et al., 2016; J.-W. Kim et al., 2017; Takeda et al., 2021), the homeostatic balance within the same network (Iijima et al., 2016), the role of glial cells (Takeda et al., 2021). These are only some of the most recent findings found so far from *in vivo* and *in vitro* animal models. However, it remains challenging to determine whether the results found so far in animals may remain applicable and similar in human models and more importantly, what are the precise pathological effects of VPA during neurodevelopment *in utero* that lead to ASD in adulthood.

1.7. The use of human stem cells for modelling the effects of VPA

The discovery of cell reprogramming techniques using the "Yamanaka factors" has revolutionized the study of neurodevelopmental disorders (Kelava & Lancaster, 2016; Marchetto et al., 2010; McDevitt, 2013; K. Takahashi et al., 2007; K. Takahashi & Yamanaka, 2006). By introducing transcription factors such as OCT3/4, SOX2, KLF4, and c-MYC to human somatic cells, it is now possible to reprogram them into human induced pluripotent stem cells (hiPSCs) (Buganim et al., 2013; Dolmetsch & Geschwind, 2011; McDevitt, 2013; Paşca et al., 2015; K.

Takahashi et al., 2007; K. Takahashi & Yamanaka, 2006). Researchers can generate various human cell types, including neurons, from hiPSCs, enabling the study of VPA's impact without the need for directly obtaining cells from vital human tissue (Buganim et al., 2013; Dolmetsch & Geschwind, 2011; McDevitt, 2013; Paşca et al., 2015; K. Takahashi et al., 2007; K. Takahashi & Yamanaka, 2006).This breakthrough has created an additional platform, alongside animal models, for investigating the VPA neurodevelopmental effects.

By utilizing hiPSCs and hESCs, it is possible to address several key limitations of VPA animal models. The administration protocols used in rodents do not accurately replicate human fetal exposure to VPA, the critical differences in neurodevelopment between humans and rodents. Moreover, animal models may not fully capture all the molecular pathways, structural alterations, and cellular changes observed in human ASD (Kelava & Lancaster, 2016; McDevitt, 2013). The hiPSC platform provides a valuable tool to overcome these limitations and gain a more comprehensive understanding of the neurodevelopmental effects of VPA exposure during human brain development.

1.7.1. Two-dimensional modelling of VPA exposure

VPA exposure in two-dimensional (2D) human stem cell cultures has been widely employed to investigate the molecular underpinnings of the teratogenicity effect of VPA providing valuable insights into the effects of VPA on neurodevelopment.

For example, VPA has been shown to affect the expression of genes involved in neural tube formation, cellular adhesion and migration, consistently between two mESCs lines (Colleoni et al., 2014). Apart from the modulation of gene sets involved in embryonic morphogenesis, this and other studies confirmed the modulation of genes related to neurodevelopment especially after long-term exposure (until 7 days of exposure between 0.1-1mM of VPA) (Colleoni et al., 2014; Schulpen et al., 2015). On the other hand, one study on using human stem cells differentiated into neurons and tested with different AEDs, including VPA, showed that transient exposure to the drug can lead to delayed cell cycle progression, but also impaired neurogenesis (Cao et al., 2015) (3 days at similar concentration as in (Colleoni et al., 2014; Schulpen et al., 2015)).

More recent studies using VPA on hiPSC-derived neurons showed acceleration in neural differentiation both at the molecular and physiological levels (Fernandes et al., 2019) confirming most of the primary culture results (Fujimura et al., 2016; Go et al., 2012; Juliandi et al., 2012; Kao et al., 2013). An interesting study using directly reprogrammed human neurons focusing more on the effects of long term VPA exposure on the physiology and morphology at different developmental stages (Chanda et al., 2019). Notably, VPA was shown to reduce the complexity

of neurite arborization (Chanda et al., 2019), confirming previous results found in mice (Snow et al., 2008), and a delay in functional maturation (Chanda et al., 2019). In addition to that, the morphological and functional impairments were limited early/mid stages of neurodevelopment or more precisely between day 1 and 21 of the differentiation protocol (Chanda et al., 2019). Despite providing valuable insights into the effects of VPA on neurodevelopment, 2D stem cell cultures, whether derived from animals or humans, have certain limitations. Firstly, they are unable to replicate the intricate three-dimensional architecture of the human brain, which hinders our understanding of the full complexity of VPA's effects. Secondly, 2D cultures can replicate only early stages of brain development, thereby providing limited information on the long-term effects of VPA during much later stages.

1.7.2. Three-dimensional modelling of VPA exposure

To overcome the aforementioned limitations of 2D hiPSC-derived neural cultures, new ways of culturing hiPSCs have been developed like three-dimensional (3D) cultures. These cultures are formed by aggregates of self-organizing hiPSCs that differentiate in a free-floating environment. By now, the most known methods of 3D cultures are mainly two: the regionalized neural organoids, developed by Paşca et colleagues, which replicate specific regions of the human brain and have the advantage to be assembled into assembloids in order to study the interaction between different systems (Paşca et al., 2015, 2019); and unguided neural organoids, developed by Lancaster et colleagues, which instead resemble the development of the cerebrum without guidance toward a particular region (Lancaster & Knoblich, 2014; Pașca et al., 2022).

These techniques have been extensively employed in studying the aetiology of various neurodevelopmental disorders. Notably, unguided neural organoids have been utilized to investigate microcephaly (Lancaster et al., 2013) as well as the impact of Zika virus infection on human brain development (Qian et al., 2016). Furthermore, 3D culture models have provided insights into the effects of environmental exposures on brain development. For instance, alcohol exposure has been modelled using unguided neural organoids (Zhu et al., 2017), cadmium exposure (Yin et al., 2018), prenatal nicotine exposure (Wang et al., 2018), and the effects of a hypoxic environment on regionalized organoids have also been investigated (Paşca et al., 2019). Nefiracetam and PHA 543613 have been used to provide insights on the effects of methyl-CpG binding protein 2 gene (MECP2) modulation in Rett syndrome (RTT) (Amir et al., 1999; Mellios et al., 2018).

In the realm of ASD modelling research, Mariani et al. undertook a study employing telencephalic regionalized organoids derived from individuals with ASD. Their investigation

revealed a significant association between a developmental precursor of ASD and a shift towards GABAergic neuron fate influenced by forkhead box protein G1 (FOXG1), a forebrain-specific marker. The study proposes FOXG1 as a potential biomarker for severe ASD, shedding light on the underlying mechanisms of the disorder. (Mariani et al., 2015). Another study investigated the effects of haploinsufficiency in ASD risk genes, including SUV420H1, ARID1B, CHD8, on cortically regionalized organoids (Paulsen et al., 2022). The study revealed that those CRISPR/Cas9-induced mutations led to asynchronous development of GABAergic neurons and deep-layer excitatory projection neurons acting on distinct molecular pathways. This study supported the theory of E/I imbalance in ASD also observed in the aforementioned study (Mariani et al., 2015; Paulsen et al., 2022). The role of CHD8 in ASD was also elucidated by another study where unguided neural organoids were produced from CHD8 mutant and control hESCs. The aim was to examine CHD8 mutation impact on the expression of other genes implicated in brain development and ASD, including AUTS2 and TCF4. Analysis of the organoids at different time points (days 20, 60, and 120) revealed differentially expressed genes (DEGs) involved in the regulation of the Wnt/β-catenin signalling pathway, which has been a focus of pharmacological studies. Additionally, alterations were observed in different populations of GABAergic neurons, indicating an imbalance between excitatory and inhibitory neurons (Weissberg & Elliott, 2021). In another investigation of CHD8 haploinsufficiency in human unguided neural organoids, it was found that this condition disrupts neurodevelopmental trajectories. Notably, the generation of inhibitory neurons was accelerated, while the generation of excitatory neurons was delayed. These findings align with the observed enlargement of cerebral organoids, which serves as an *in vitro* correlate of macrocephaly in ASD patients (Villa et al., 2022).

Another gene associated with ASD is CNTNAP, which codes for a member of the neurexin family. The CNTNAP family comprises five members, namely CNTNAP1 to CNTNAP5, and they play crucial roles in myelin formation, the current of K+ channels in the cell membrane, as well as neurite and synapse development (Tong et al., 2019). In a study involving forebrain organoids cultivated for 26 weeks, derived from ASD patients carrying the homozygous c.3709DelG mutation in CNTNAP2, it was observed that this gene exhibits high expression in early-born deep layers/subplate excitatory neurons. Additionally, an increase in various cortical cells was noted, leading to an overall enlargement of the patient-derived organoids due to enhanced proliferation of neural progenitor cells and other proliferating cells (de Jong et al., 2021). By utilizing mouse cortical organoids (mCOs) derived from induced pluripotent stem cells (miPSCs) of Cntnap2 knockout mice, researchers demonstrated that the absence of CNTNAP2 results in GABAergic neuron defects and downregulation of ventral telencephalic progenitor-related transcription factors in the ventricular zone, leading to GABAergic neuron abnormalities.

Interestingly, drug tests indicated that the antiepileptic drug retigabine increased the number of GABAergic neurons (Hali et al., 2020).

The SHANK family proteins play a crucial role as postsynaptic scaffolding proteins in regulating the development and function of excitatory synapses. Among them, SHANK3 is an abundant member of this protein family and has been implicated in various neurodevelopmental disorders (Yoo et al., 2022). SHANK3 is a recognized gene associated with ASD, and its impact was investigated by generating telencephalic organoids from isolated self-organized single neural rosettes derived from cells carrying variants in this gene. These organoids were cultured for up to 5 months, and analyses were conducted at different time points for specific experiments. Notably, neurons in organoids with a hemizygous deletion of SHANK3 exhibited intrinsic and excitatory synaptic deficits, along with impaired expression of several clustered protocadherins (Wang et al., 2022).

A recent study focused on the role of Rab39b deletion in brain development and its association with ASD and ID. Rab39b is primarily localized to Golgi vesicles and recycling endosomes and is involved in the maturation of glutamatergic receptors and the regulation of alpha-Synuclein (aSyn) homeostasis, preventing its aggregation. The study revealed that the mutation leads to the activation of the PI3K–AKT–mTOR signalling pathway. Interestingly, inhibiting this pathway rescued the enlarged size of organoids and the increased proliferation of NPCs caused by RAB39b mutations (Koss et al., 2021). To investigate the functions of RAB39b in human brain development, Zhang et al. utilized hiPSCs and unguided neural organoids. They generated mutant iPSC lines by employing the CRISPR/Cas9 approach to delete the RAB39b gene. The findings of this study align with other research presented here, highlighting alterations in organoid morphologies associated with gene mutations linked to ASD development, as well as changes in neuronal populations compared to control groups (W. Zhang et al., 2020).

When considering the use of 3D cultures in investigating the impact of VPA on neurodevelopment, there are a limited number of studies available. A recent study found that VPA exposure at the early stage (day 18) of cortical organoids derived from one male hiPSC line impairs neurodevelopment (Cui et al., 2020). In a different study, forebrain organoids (hFOs) were utilized to investigate the impact of valproic acid VPA on ASD risk in humans. The hiPSCs derived from healthy individuals were used to generate hFOs, which were then exposed to VPA at a concentration of 1 mM for 3 days, mimicking clinically relevant conditions. By employing proteomics, genomics, and electrophysiology analyses, researchers identified several genes, including *AMK4, CLCN4, DPP10, GABRB3, KCNB1, PRKCB, SCN1A,* and *SLC24A2*, that were affected by VPA exposure. Notably, these findings showed significant overlap with dysregulated pathways observed in the brains or organoids derived from ASD patients (Mariani et al., 2015; Meng et al., 2022). Single-cell RNA sequencing analysis revealed that VPA exposure altered

gene expression in specific cell types within the hFOs, such as the choroid plexus, excitatory neurons, immature neurons, and medial ganglionic eminence cells. Additionally, microelectrode array experiments demonstrated that VPA exposure disrupted synaptic transmission in the hFOs (Meng et al., 2022).

While previous studies have investigated the effects of VPA during the initial stages of organoid development using clinically relevant concentrations, there remains a considerable gap in our understanding of the long-term consequences of chronic VPA exposure on human brain development. Recognizing this limitation, our study aims to bridge this gap by administering the drug chronically in control unguided neural organoids, starting from day 15 and continuing until 6 months of development, encompassing crucial early and later stages of unguided neural organoid maturation.

Objectives and Thesis Outline

The primary objective of this project is to investigate the long-term effects of chronic administration of VPA on control neural organoids at both molecular and functional levels.

For the molecular analysis, we employed immunohistochemistry (IHC) at 1, 4, and 6 months of development, as well as bulk RNA sequencing at 1 and 6 months. Through IHC, we examined the impact of VPA on the neural organoids' capacity to generate and replenish the NPCs pool, their capability to generate neurons, and specific subpopulations such as early- and late-born neurons, and glial cells. Furthermore, we assessed the shift in the balance between excitatory and inhibitory synapses formed in the VPA-administered organoids during development. Using bulk RNA sequencing at different developmental stages, we investigated the effects of VPA on neural organoid differentiation and maturation. Our focus is to examine the expression profiles of genes associated with neurodevelopmental disorders, particularly ASD.

In terms of functional experiments, we primarily conducted electrophysiology on 6-month-old unguided neural organoids and calcium imaging on 4 and 6-month-old organoids. By performing electrophysiology at the time point when our model demonstrated the peak of maturation (around 6 months), we aimed to reveal how prolonged exposure to VPA influenced both intrinsic and extrinsic properties of the neurons generated in our model. We then employed calcium imaging to confirm these observations and explore the possibility of their occurrence at earlier stages of development.

In conclusion, our multimodal approach enables us to elucidate the effects of VPA on the development of a human *in vitro* model at various levels. By simulating VPA exposure in the developing brain of an unborn child, our objective is to gain insights into the mechanisms

affected by VPA and how these alterations may contribute to the development of neurodevelopmental disorders.

CHAPTER 2 | MATERIALS AND METHODS

2.1. Maintenance of human induced stem cells

The 31f-r1 hiPSCs (induced pluripotent stem cells) used in this study were generously provided by Prof. Dr. Oliver Brüstle from the University of Bonn. These cells were reprogrammed from human dermal fibroblasts using lentiviral infection of Yamanaka factors, including Oct3/4, Sox2, c-Myc, and Klf4. The hiPSCs were cultured in Matrigel-coated plates (Thermo Scientific) with 2 ml RT mTeSR Plus (Stem Cell Technologies) per well, supplemented with 1% Penicillin/Streptomycin (Gibco), at 37°C and 5% CO_2. The cells were passaged using ReLeSR (Stem Cell Technologies) for gentle colonies dissociation every 3-5 days depending on the cell line.

2.1.1. Maintenance, passaging and freezing of stem cells colonies

Maintenance. The hiPSCs were cultured in Matrigel-coated plates (Thermo Scientific) with 2 ml room temperature (RT) mTeSR Plus (Stem Cell Technologies) per well, supplemented with 1% Penicillin/Streptomycin (Gibco), at 37°C and 5% CO2. The cell lines were refreshed every other day with mTeSR Plus. Colonies were left for one day without cleaning, after passaging or thawing. Every other time, the colonies were cleaned every other day by scraping using a pipette tip to remove differentiated cells. After cleaning, the old medium was removed, and the wells were washed once with PBS and then refreshed with mTeSR Plus.

Passaging. The cells were passaged using ReLeSR (Stem Cell Technologies) for gentle colonies dissociation every 3-5 days depending on the cell line. When the stem cell colonies were occupying 70% of a 6-well-plate, they were passaged in new Matrigel coated wells. Before passaging, the differentiated regions of the colonies were cleaned, washed with 1 ml of PBS per well of a 6-well plate. After washing, 1 ml of RT ReLeSR (Stem Cell Technologies, Vancouver, Canada) was added for about 1 min and then, the ReLeSR was removed, and the cells were incubated for 3-4 mins depending on the cell line. After incubation, 1 ml of mTeSR Plus was added and cells that detached from the plate were subsequently collected in a 15 ml tube for centrifugation. The settings for the centrifuge were 300 g for 3 mins. After centrifugation, the supernatant was removed using a vacuum suction and cells were resuspended in 1 ml of mTeSR Plus. The colonies were pipetted 3 to 5 times with 1 ml tips depending on the size of the colonies and then the colonies were plated in the wells with new Matrigel after removing DMEM/F12 (Corning). The plate was incubated at 37°C with 5% CO2.

Freezing. After expansion of the stem cell colonies, some cells were frozen down and stored in liquid nitrogen to replenish the stock of stem cell lines. The freezing step started, as for the passaging one, with the colony with the cleaning by differentiated regions. After a wash with 1 ml of PBS per well of 6-well plate, the colonies were kept with 1 ml of RT ReLeSR per well for

about 1 min. After, ReLeSR was removed, and cells were incubated for 3-4 mins depending on the cell line. Subsequently, 1 ml of RT mTeSR Plus is added to detach the undifferentiated cells. Detached cells were then collected in a 15ml tube for centrifugation at 300g for 3 mins. In the meantime, the freezing solution of 10% of Dimethyl sulfoxide (DMSO) and 90% of FBS was prepared and the vials needed were labelled. When the centrifugation ended, the supernatant was removed the freezing solution in a 1:1 ratio was added. Finally, the stem cell colonies were rapidly collected in pre-labelled vials and placed in an isopropanol container and stored in a -80°C freezer for a day. Subsequently, the vials were stored in the liquid nitrogen.

2.2. Generation of human unguided neural organoids

Unguided neural organoids were produced following the protocol shared by Lancaster & Knoblich, 2014, starting from hiPSCs, following the instructions present in the STEMdiff Cerebral Organoid Kit (Stem Cell Technologies). The hiPSCs colonies were dissociated with Accutase (Stem Cell Technologies) and 9000 cells per well were plated on a 96-well cell suspension plate (Greiner Bio-One) in embryoid bodies (EBs) Formation Medium with 10 µM of the Y-27632 ROCK inhibitor (Stem Cell Technologies). EBs were refreshed on day 2 and day 4 with EB Formation Medium. On day 5, EBs were transferred to 24-well cell suspension plates (Greiner Bio-One) with Induction Medium. EBs were embedded on droplets of cold Matrigel (Corning) on a sterilized sheet of Parafilm, on day 7. The droplets were allowed to polymerize in the incubator at 37ºC, 5% CO2 for 30 min. Then, the droplets were gently pipetted from the Parafilm and refreshed with Expansion Medium for 3 days in ultra-low-attachment 6-well plates (Corning). The EBs droplets were kept in suspension in Maturation Medium and placed on an orbital shaker at around 65 rpm.

Treatment with VPA. Unguided neural organoids were kept in Maturation Medium for up to 6 months with exposure to VPA at low and high concentrations from day 15 of the differentiation protocol, respectively 0.5 mM (VPA_{LD}) and 1.5 mM (VPA_{HD}) **(see Figure 4)**. The former being the concentration of VPA found in the blood of women who took the drug for treatment, while the latter being a higher to highlight possible features found in the low dose. The media was changed every 3-4 days with addition of VPA. Neural organoids were then collected at 1, 4 and 6 months for further analysis.

2.3. Immunohistochemistry

Unguided neural organoids were collected at 1, 4 and 6 months of differentiation for all conditions (CTR, VPA_{LD} and VPA_{HD}). Upon collection, they were fixed in 4% paraformaldehyde (PFA) for 1 hour at 4ºC and then transferred to a solution of 30% sucrose in PBS 1x for

cryoprotection for about 2-3 days at 4ºC. Subsequently, they were transferred into optimal cutting temperature (OCT) embedding matrix (VWR), kept on ice for about 20 mins, snap-frozen on dry ice and stored at -80°C until further use for IHC experiments. Before the start of cryosection, samples were kept at -20ºC for 20 mins. Using a cryostat, 20 µm thick sections were obtained and collected directly into adhesive Superfrost Plus slides (Thermo Scientific Menzel). Slides were stored at -80ºC before the start of the immunostaining protocol. Cryosections were washed three times with PBS 1x and permeabilized with 0.5% Triton X-100 in phosphate-buffered saline (PBS) 1x for 15 min at RT. Sections were then blocked in 3% bovine serum albumin (BSA) in PBS 1x for 1 h at RT and incubated with primary antibodies diluted in 3% BSA in PBS 1x for 1 h at RT (or overnight at 4ºC). Next, sections were washed three times with PBS 1x and incubated in the dark for 2 h, at RT, (or overnight at 4ºC) with the secondary antibodies anti-rabbit Alexa Fluor-488 conjugate (Invitrogen A-11008), anti-mouse Alexa Fluor-568 conjugate (Invitrogen A-11031) and anti-guinea pig Alexa Fluor-647 conjugate (Invitrogen A-21450) diluted 1:200 in 3% BSA in PBS 1x. Nuclei were stained with Hoechst 33342 (1 µg/mL) for 5 min in the dark. Sections were washed three times in PBS 1x and mounted for microscopy using Dako Fluorescent Mounting Medium (Dako). Images were acquired using a Zeiss Confocal LSM 710 microscope with a 20× air or 40× oil objective and processed using Zen Software (Zeiss). The following primary antibodies were used: anti-NEUN (1:100, Merck Millipore MAB377), anti-MAP2 (1:1000, Synaptic Systems #188004), anti-VGLUT1 (1:5000, Merck Millipore AB5905), anti-GAD67 (1:100, Merck Millipore MAB5406B), anti-TBR1 (1:300, Abcam ab31940) and anti-SATB2 (1:200, Abcam ab51502). Entire slices were captured using z-stack, 10 stacks in total. On ImageJ, we performed orthogonal projections of the stacks and we proceeded to perform the threshold for each marker, keeping it constant throughout the experiment. After, we performed watershed only for nuclear analysis, in order to keep the nuclei as separate as possible. We proceeded to analyze the positive area occupied by each marker relative to Hoechst, keeping the options constant for all markers.

2.4. RNA extraction and Bulk RNA sequencing

Preparation of RNA samples. The human neural organoids used for this experiment were 3 per condition (CTR, VPA_{LD} and VPA_{HD}), 1- and 6-month-old, coming from one batch. Organoids collected were flash-frozen in dry ice and stored at -80°C. Total RNA was purified using the AllPrep DNA/RNA/miRNA Universal Kit (Qiagen), and according to the manufacturer's protocol. Final concentrations were measured with a Nanodrop 2000 spectrometer (Thermo Scientific) and RNA samples were stored at -80°C.

RNA sequencing and transcriptomic analysis. Before RNA sequencing, the concentration and quality of total RNA samples were determined using the Experion RNA StdSens Analysis Kit (BioRad). Illumina Stranded Total RNA – ligation was the method used on 18 RNA samples (three CTRs, three VPA_{LD} and three VPA_{HD} at both 1 and 6 months from the same batch). RNA libraries and sequencing were performed by the Edinburgh Genomics facility in association with the University of Edinburgh (United Kingdom, Edinburgh). Briefly, NovaSeq technology was used to yield approximately 21 million reads from 50bp paired end sequenced samples. In addition, quality control and trimming were also performed by the facility that provided with the final sequences in FASTQ file format ready to be further processed. Reads were aligned to the Homo sapiens primary assembly (Ensembl release v109.38) using STAR STAR/2.7.1a (Dobin et al.,2019). Reads that were uniquely aligned to annotated genes were counted with featureCounts 2.0.1 (Liao et al., 2014). Differential expression analyses were performed using DESeq2 1.30.1 on RStudio using 'normal' for log2FoldChange (LFC) shrinkage, the Normal prior from Love et al (2014).

Gene set Enrichment analysis. Gene Ontology (GO) terms associated with each gene were first obtained using BioMart. Then, Piano package version 2.6.0 (Bioconductor) in RStudio was used for Gene Set Enrichment Analysis (GSEA). More in detail, gene-level statistics are calculated for each gene set in the ranked list of genes, returning the gene set statistics and p-values of different directionality classes.

2.5. Slice preparation for whole-cell patch clamp and Ca^{2+} imaging

Unguided neural organoid slices were obtained as previously described by (Paşca et al., 2015) with some modifications. Neural organoids were collected from 6-well-plate at around 4 and 6 months (for Ca^{2+} imaging at 4 and 6 months while for electrophysiology at 6 months exclusively). The organoid was then placed into a mold with warm 3% low-melting agarose solution prepared in PBS 1x and placed on ice. After jellification, the agarose containing the organoid was quickly removed from the mold and glued to a vibratome support, fixed in the vibratome platform and ice-cold oxygenated (95%:5% O_2:CO_2 mix) N-Methyl-D-Glucamine-enriched artificial cerebrospinal fluid (NMDG-aCSF) was poured in the on the sample. NMDG-aCSF was prepared as follows: 99.69 mM NMDG, 2.55 mM KCl, 30 mM $NaHCO_3$, 1.23 mM $NaH_2PO_4.H_2O$, 20 mM HEPES, 25 mM glucose, 1.97 mM thiourea, 4.99 mM Na-ascorbate, 2.99 mM Na-pyruvate, 10 mM $MgSO_4$ and 0.5 mM $CaCl_2$ with a pH of 7.3-7.4 and osmolarity of 300-310 mOsm. Slices of 250-300 µm were obtained using a vibratome (Leica VT1200s, Leica Microsystems, USA) and immediately recovered in a baker placed in the bath at 32°C for 8 min in oxygenated NMDG-aCSF. Slices were then transferred to a baker that contained oxygenated aCSF at RT (127.48

mM NaCl, 2.55 mM KCl, 24.04 mM $NaHCO_3$, 1.23 mM $NaH_2PO_4.2H_2O$, 12.49 mM glucose, 2 mM $MgSO_4$ and 2 mM $CaCl_2$ with a pH of 7.3-7.4 and osmolarity of 300-310 mOsm). Slices were kept in aCSF for at least 1 h before recording for habituation. The osmolarity of NMDG-aCSF and aCSF was kept at 300-310 mOsm and the pH was adjusted to 7.3-7.4 using exclusively HCl.

2.6. Whole-cell patch clamp recordings

Whole-cell patch clamp recordings were registered in a recording chamber perfused with aCSF (2–3 mL/min) at 25°C at around 6 months **(See Figure 15a)**. The cells were visualized with an Axio Examiner.D1 microscope (Carl Zeiss) equipped with a Q-capture Pro7 camera (Teledyne) and putative pyramidal-shaped neurons, near the surface of organoids, were identified under infrared-differential interference contrast visualization with a 40× objective. Cells were patched with borosilicate glass recording electrodes (3–7 MΩ; Science Products) filled with an internal solution of potassium-gluconate (K-int) containing: 145 mM K-gluconate, 10 mM HEPES, 1 mM EGTA, 2 mM ATP-magnesium salt, 0.3 mM GTP-sodium salt and 2 mM $MgCl_2.6H_20$, pH adjusted to 7.36 with NaOH (298-300 mOsm). The recorded neurons were voltage-clamped at -70 mV to record sEPSCs and the recording was performed for 3 minutes. The resting membrane potential (RMP) and action potentials (APs) parameters were estimated under current-clamp mode. The RMP and the neuronal excitability was obtained by stepped current injection (1000 ms duration, 20 pA stepwise from -80 pA to +170 pA). The kinetics of the APs was acquired by stepped current injection (10 ms duration, 20 pA stepwise from -80 pA to +300 pA). Criteria for acceptance of cells was determined as stable access resistance under 25 MΩ, which did not increase or decrease more than 30% during the recording, RMP below -40 mV and cells firing activity upon current injection. Recordings were digitized at 20 kHz and filtered at 2 kHz. All electrophysiology data was acquired with a Multiclamp 700B amplifier and Digidata 1550A (Molecular Devices). Voltage clamp data was analysed using Clampfit software (v10.7, Molecular Devices) and current clamp data was analysed using Easy Electrophysiology Software (v2.4.0). All electrophysiological experiments were performed between weeks 24 and 28 of *in vitro* differentiation.

2.7. Ca^{2+} imaging recordings

Slices were incubated with 4.5 µM Fluo-4 AM (acetoxymethyl ester) (Invitrogen) in aCSF solution for 30 min in an incubator at 37°C, 5% CO_2 **(Figure 14a)**. After 45 mins, slices were washed with PBS 1x and mounted on an inverted fluorescence microscope (Zeiss Cell Observer Spinning Disk). Imaging was performed at 37°C and 5% CO2 and the emission fluorescence

was recorded at 506 nm by a highly sensitive electron multiplying camera (EM-CCD Evolve Delta). The time course of the experiments consisted of 200 ms of exposure for a total of 750 frames. Imaging post processing included 8-bit conversion, background subtraction, frame alignment and bleach correction, and were performed using ImageJ (Fiji). ROIs and their related activity were selected using the semi-automated calcium imaging analyser (CALIMA). Traces were extracted as $\Delta F/F_0$, F_0 being the baseline and ΔF the moment-to-moment deviation from the baseline. Frequency of firing per ROI was calculated using Clampfit software (v10.7, Molecular Devices) (Radstake et al., 2019). Each point in graph is average frequency of one video.

2.8. Statistical analysis

Data is represented as mean values ± SEM (standard error of the mean). Statistical analysis was calculated using unpaired two-tailed Student t-test, two-tailed Mann-Whitney test, two-way ANOVA or Kolmogorov-Smirnov test. Sample normality was tested using D'Agostino-Pearson normality test. Analysis was performed using the standard statistical software GraphPad Prism 8 or RStudio for bulk RNA sequencing results. Differences were considered statistically significant for P values < 0.05 (*p < 0.05, **p < 0.01, ****p < 0.0001).

CHAPTER 3 | VPA'S EFFECT ON NEURAL ORGANOID DEVELOPMENT AND PHYSIOLOGY

3.1. VPA chronic exposure affects neurodifferentiation of human unguided neural organoids.

The hiPSC-derived unguided neural organoids have been widely characterized as an *in vitro* model to model brain developmental (Lancaster & Knoblich, 2014). They have been shown to produce NPCs capable of forming ventricular-like zones (VZs) from which neurons differentiate. In addition to that, neurons in this model organize into deep- and superficial layer neurons resembling the formation of a primitive cortical plate. Human unguided neural organoids can also generate glial cells that are fundamental for the maturation of functional synapses (Lancaster & Knoblich, 2014) **(Figure 3).**

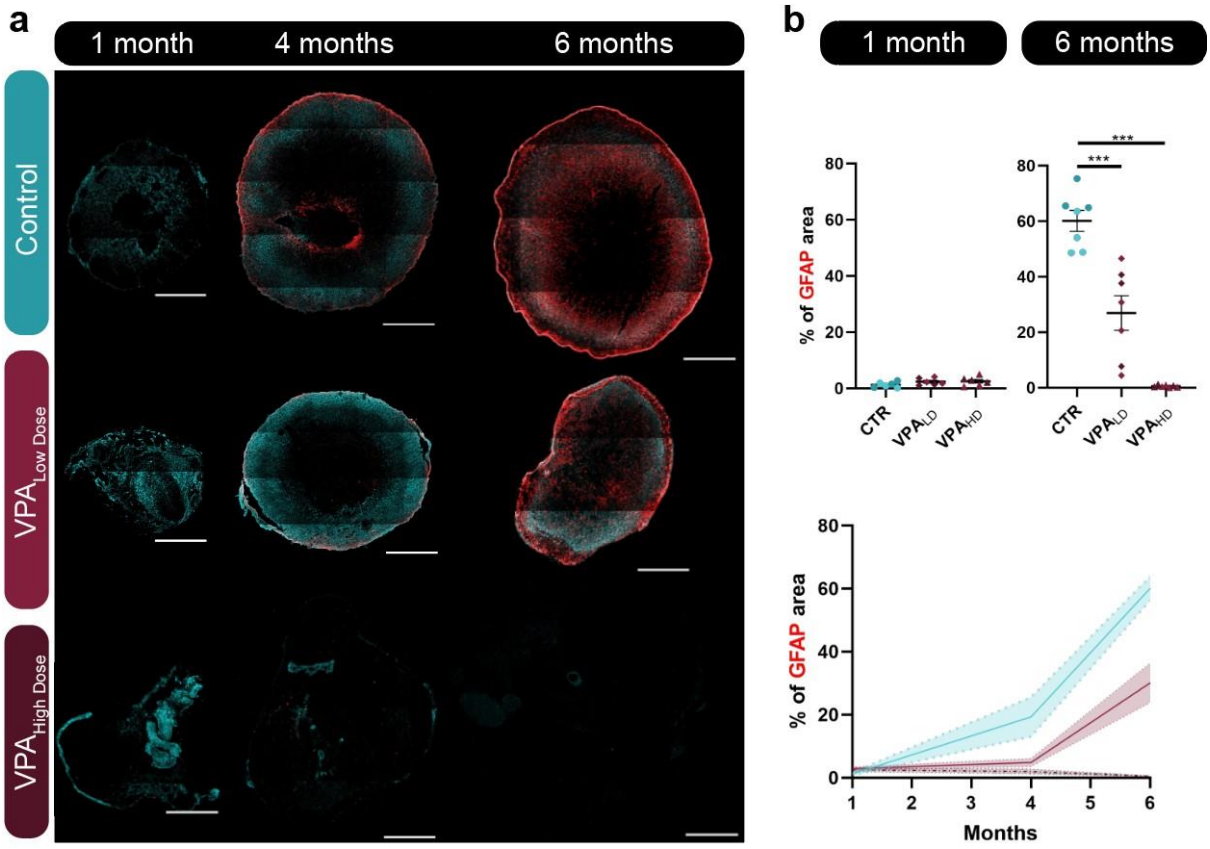

Figure 3: VPA effects on glial cells development in unguided neural organoids: a) *Representative pictures of organoid slice regions at 1, 4 and 6 months from CTR, VPA_{LD} and VPA_{HD}. Slices were stained with MAP2 (dendritic marker) and GFAP (Glial fibrillary acidic protein, marker for astrocytes). Scale bars of 200µm.* ***b)*** *Quantifications of the presence of GFAP at all timepoints (N=6-7/4/2 for CTR, N=6-7/4/2 for VPA_{LD} and N=6/4/2 for VPA_{HD}). Graphs with analysis Mann-Whitney test illustrates p<0.05 = *, p<0.01 = **, p<0.001 = ***.*

In-utero exposure to VPA, particularly during the first trimester of pregnancy, is associated with an increased risk of the unborn child to develop ASD. However, the treatment is administered chronically to the mother since the day of conception. To mimic the effects of VPA intake during the development of the child brain, we chronically treated our unguided neural organoids with 0.5 mM (VPA_{LD}) and 1.5 mM (VPA_{HD}) of VPA starting as early as 15 days of differentiation **(See**

figure 4). The first trimester of pregnancy in humans comprises neural tube closure (≈ gestational day 28), the beginning of cortical neurogenesis (≈ gestational week 5) and the beginning of synapse formation (≈ gestational week 9 to 10) (de Graaf-Peters & Hadders-Algra, 2006; Meyer et al., 2000; Rabinowicz et al., 1996). The latter two of these developmental events can be recapitulated in 3D cultures especially by taking advantage of their longevity. Considering therapeutic serum concentrations, the blood-placental barrier permeability and the substantially increased serum half-life of VPA in foetuses compared to adults, 0.3 and 1 mM seems to be a realistic representation of the actual concentration in the developing nervous system of in-utero exposed foetuses (Jäger-Roman et al., 1986; S. I. Johannessen, 1992).

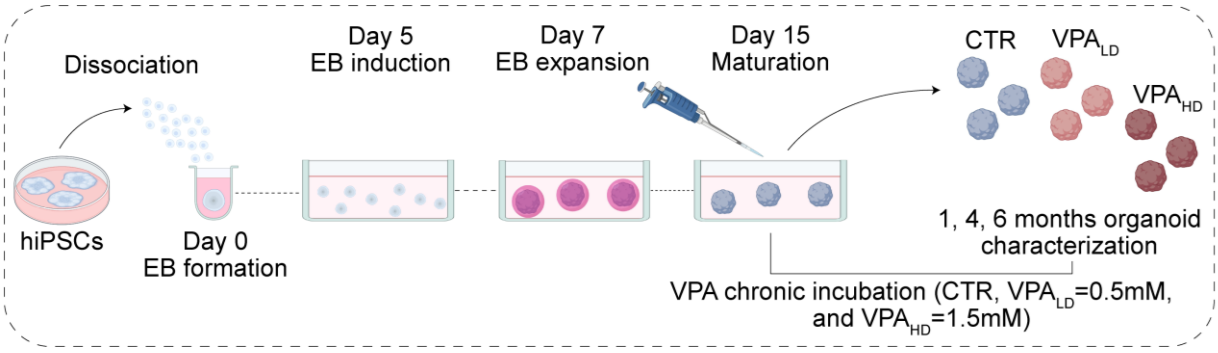

Figure 4: Schematic of the experiment design: *after human unguided neural organoid generation (see Methods 3.2.), organoids were exposed to 2 different concentrations of VPA (VPA$_{LD}$ and VPA$_{HD}$) while the control condition (CTR) received vehicle around the start of the maturation period (15 days). The conditions were characterized for IHC at 1, 4 and 6 months, for bulk RNA sequencing at 1 and 6 months, for electrophysiology at 6 months, and for calcium imaging at 4 and 6 months. VPA$_{HD}$ was excluded from the functional experiments due to the results of IHC and bulk RNA sequencing.*

As shown in **figure 5**, the development of VPA$_{HD}$ appeared distinct from the other conditions (**Figure 5a, bottom)**. At 4 and 6 months, the NEUN staining showed unspecific localization, as it was not observed in the nucleus as expected, and it lacked expected colocalization with MAP2, indicating that neuronal differentiation was heavily impaired. During the first month of development, VPA$_{HD}$ showed some SOX2-positive areas (**Figure 5a, bottom)**, nevertheless, our data suggests that the high dose of VPA has a clear detrimental effect in early developing organoids.

Interestingly, when looking at the cellular distribution of the remaining conditions, we observed that the SOX2-positive areas between the CTR and VPA$_{LD}$ conditions were similar. This is contrary to other studies that have reported an increase in the NPC pool after VPA exposure both in animal models (Fujimura et al., 2016; Go et al., 2012; Juliandi et al., 2012; Kao et al., 2013) and in human 3D *in vitro* models (Cui et al., 2020)**.** Nevertheless, this result suggests that both conditions started with a similar population of NPCs but only the CTR showed a renewal of NPCs at later stages, presenting a significantly higher presence of SOX2-positive areas compared to VPA$_{LD}$ **(Figure 6b)**. This result may also be connected to the fact that NEUN

presence in VPA_{LD} was significantly higher when compared to CTR at 6 months while MAP2 was higher only at earlier stages of development **(Figure 5b),** suggesting that neuronal differentiation in VPA_{LD} is enhanced. In line with these results, similar observations have been made both in animal models (Go et al., 2012; Juliandi et al., 2012; Kao et al., 2013; X. Zhang et al., 2017) and in human 2D *in vitro* models (Fernandes et al., 2019).

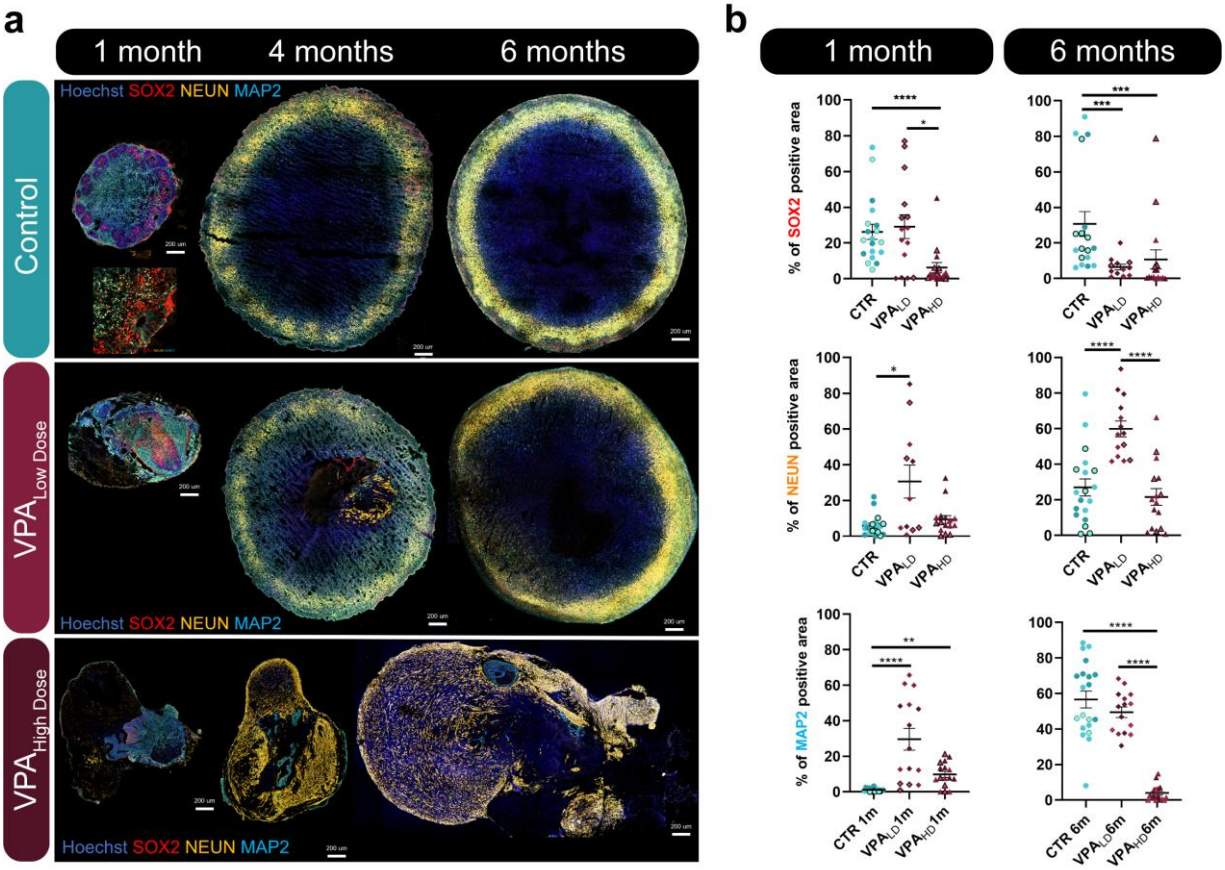

Figure 5 VPA chronic exposure affects neuronal differentiation in unguided neural organoids: a) *Representative pictures of entire slices of human neural organoids from all conditions at 1, 4 and 6 months of development. Panel of antibodies used are SOX2 for neural progenitor cells (NPCs) and NEUN together with MAP2 for neurons.* ***b)*** *Quantification of the area occupied by SOX2 and NEUN relative to Hoechst, and area occupied by MAP2 at 1 and 6 months (N=18-19/6/3 for CTR, N=11-15/5-6/3 for VPA_{LD} and N= 16/6/3 for VPA_{HD}, slices/organoids/batch). All scale bars in the representative pictures are 200 µm. Graphs with analysis Mann-Whitney test illustrates p<0.05 = *, p<0.01 = **, p<0.001 = ***.*

Figure 6a depicts 4- and 6-months-old organoid slices stained for TBR1, a marker of early-born neurons, and SATB2, a marker for late-born neurons, which we used to observe subpopulations of the NEUN positive cells. The analysis was performed in parallel with MAP2 and Hoechst in order to confirm the cellular identity of these cells, more specifically if they were MAP2-positive neurons and that TBR1 and SATB2 were nuclear staining, as expected. VPA_{HD} did not present positive staining for all neuronal markers confirming an impaired neuronal differentiation (**Figure 5b)**. TBR1 was found to be present in at all time-points in CTR and VPA_{LD}, however, it was

significantly higher in VPA_{LD} at 4 months and significantly lower at 6 months when compared to CTR (**Figure 6b)**. When looking at SATB2, VPA_{LD} shows a higher expression compared to CTR at 4 months, and it is consistent at 6 months of development. In general, our observations differ from what has been previously reported in the literature, both in animal (Juliandi et al., 2012) and human models (Cui et al., 2020), when focusing on deep-layer neuron distribution. In addition to that, previous studies have not investigated the distribution of superficial-layer neurons in 6-month-old organoids exposed to VPA.

In summary, we show that chronic VPA exposure at low dose is enhancing the neuronal differentiation and maturation into superficial-layer neurons while affecting the renewal of the NPC pool.

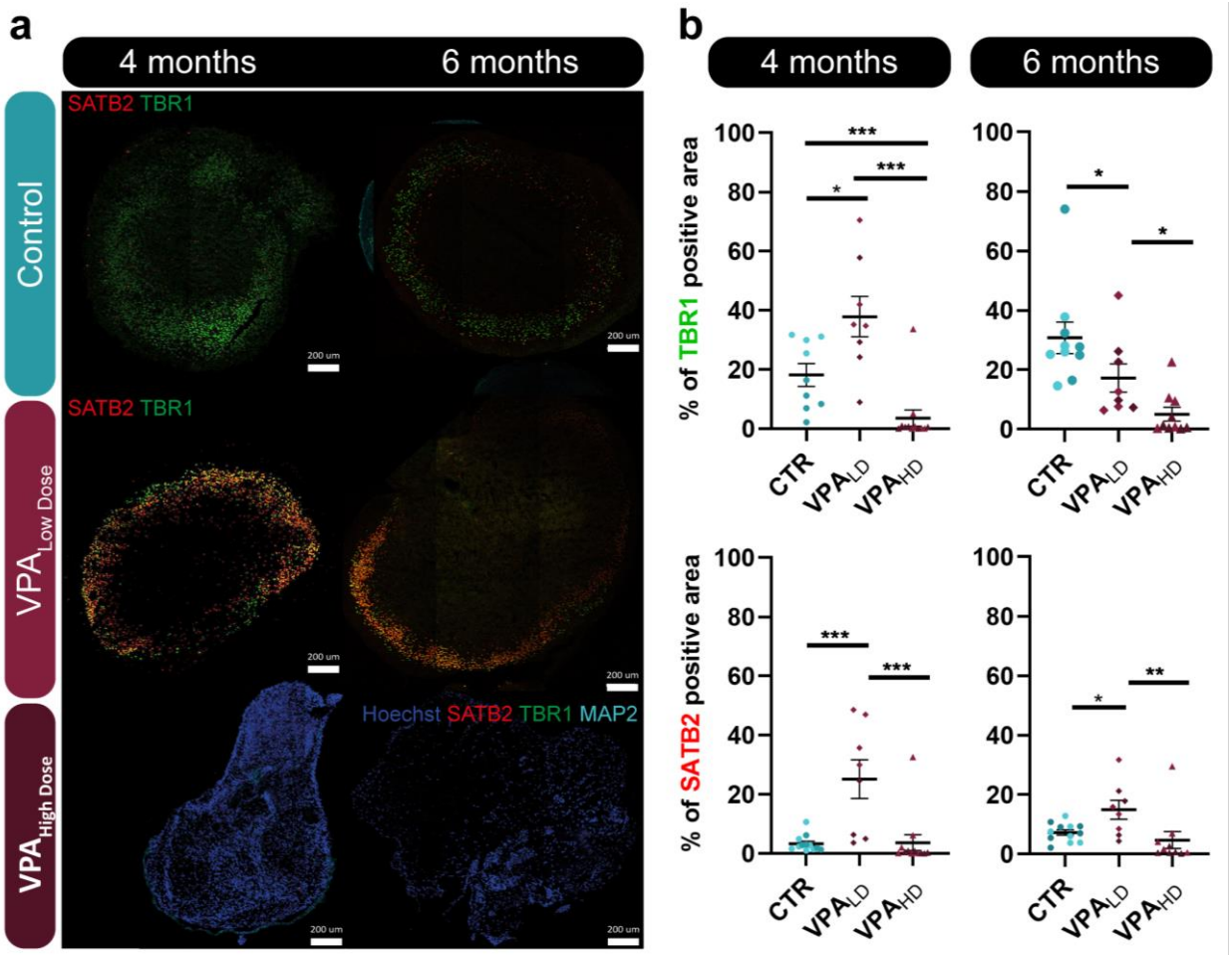

Figure 6: VPA chronic exposure affects also neuronal specification into early- and later-born neurons in unguided neural organoids: a) *Representative pictures of entire slices of human neural organoids from all conditions at 1, 4 and 6 months of development. Panel of antibodies used are TBR1 for early-born neurons and SATB2 for later-born neurons.* ***b)*** *Quantification of the area occupied by TBR1 and SATB2 at 4 and 6 months (9-12/4/2 for CTR, 8/4/2 for VPA_{LD} and N=10-12/4/2 for VPA_{HD} slices/organoids/batch). All scale bars in the representative pictures are 200 µm. Graphs with analysis Mann-Whitney test illustrates p<0.05 = *, p<0.01 = **, p<0.001 = ***.*

After observing the cellular distribution and neuronal subpopulations, we performed vGLUT1 staining to study the excitatory synapse formation in our organoids (**Figure 7a)**. We performed

vGLUT1 area analysis by calculating the area of overlap between MAP2 and vGLUT1 in order to exclude unspecific staining of the marker. We observed a higher presence of vGLUT1 both at 4 and 6 months in VPA_{LD} compared to CTR. In VPA_{HD}, instead, we found little to no presence of vGLUT1 overlap with MAP2.

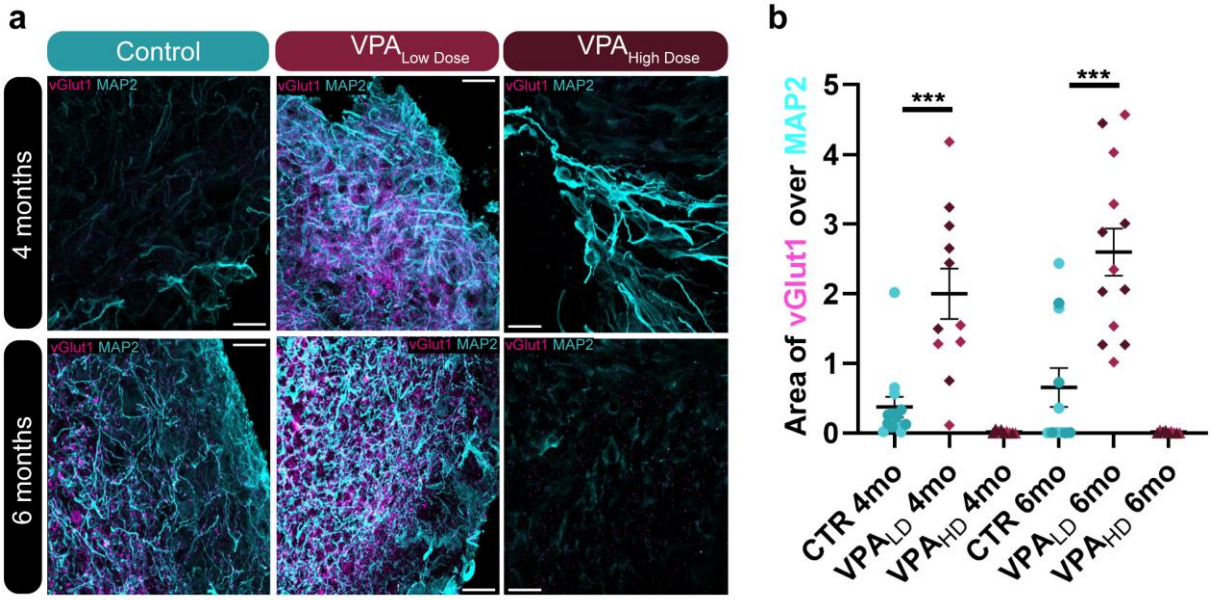

Figure 7: VPA effects on excitatory synapses in unguided neural organoid: a) *Representative pictures of organoid slice regions at 4 and 6 months from CTR, VPA_{LD} and VPA_{HD}. Slices were stained with MAP2 (dendritic marker) and vGLUT1 (excitatory synaptic marker). Scale bars of 20µm.* ***b)*** *Area quantification of overlap between MAP2 and vGLUT1. On the graph, represented as points, the average of 4 regions selected randomly within the slice of the organoid (N=11-13/4/2 for CTR, N=11-13/4/2 for VPA_{LD} and N=9/4/2 for VPA_{HD} at all time-points, average of 4 random regions/organoids/batches).*

As an additional experiment, we explored the effects of VPA on the presence of GAD67, glutamate decarboxylase, an inhibitory synaptic marker. The presence of this marker significantly increased in early maturation (at 4 months), while in later stages (around 6 months) chronic exposure to VPA reduced the presence of GAD67 thereby leading to an increase of vGLUT1 **(Figure 7b)** and a reduction of GAD67 **(Figure 8b)**.

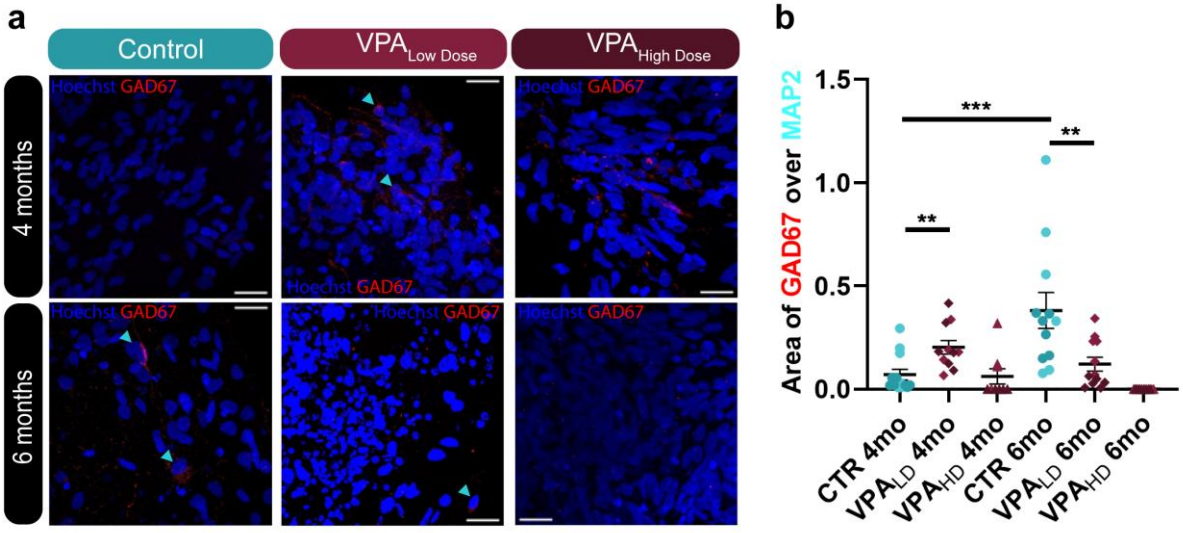

Figure 8: VPA effects on inhibitory synapses on unguided neural organoid: a) *Representative pictures of organoid slice regions at 4 and 6 months from CTR, VPA_{LD} and VPA_{HD}. Slices were stained with MAP2 (dendritic marker) and GAD67 (glutamate decarboxylase and inhibitory synaptic marker). Scale bars of 20µm.* ***b)*** *Quantification of the area of overlap between MAP2 and GAD67. On the graph, represented as points, the average of 4 regions selected randomly within the slice of the organoid (N=11-13/4/2 for CTR, N=11-13/4/2 for VPA_{LD} and N=9/4/2 for VPA_{HD} at all time-points, average of 4 random regions/organoids/batches). Graphs with analysis Mann-Whitney test illustrates p<0.05 = *, p<0.01 = **, p<0.001 = *** (for the Figure see previous page).*

Difference in the balance between these two markers, vGLUT1 and GAD67, has been previouslty demonstrated in animal models of *in utero* exposure to VPA (Banerjee et al., 2013; Iijima et al., 2016; Kumamaru et al., 2014). However, in Cui et al, observed an increase in GAD67 presence, in line with our observations. The sudden change in the presence of GAD67 between early and later stages of development may hint the possible role of glial cells in GABA synaptic transmission impairment under VPA exposure (Takeda et al., 2021). Indeed, glial cells are known to appear only at later stages of neural organoids maturation **(Figure 3b)**.

In conclusion, the findings indicate that low doses of VPA in our organoids did not have a notable impact on the initial pool of NPCs. However, it significantly enhanced the differentiation of neurons and had an impact in the density of SOX2-positive cells in later stages. Neurodevelopment in VPA_{LD} appeared to progress at a faster rate compared to the development observed in the CTR. This accelerated development is evident in the transition from increased presence of TBR1-positive areas at 4 months to SATB2-positive areas at 6 months of maturation and may explain the accelerated exhaustion of $SOX2^{+}$ progenitors. On the other hand, chronic exposure to high doses of VPA (similar to those used in animal models of ASD an acute *in utero* exposure), severely impeded typical neurodevelopment of the organoids.

3.2. Bulk RNA sequencing on VPA exposed unguided neural organoids

To assess the biological pathways affected by VPA at the beginning and the end of the experiment, we performed bulk RNA sequencing on 3 organoids from each condition at 1 and 6 months of development. Raw data from this analysis was obtained and quality control was carried out through the GSEA of the most significant differentially expressed genes (DEGs) [false discovery rate (FDR) < 0.05] **(Figure 9)**. Gene ontology (GO) terms associated with neuronal differentiation were identified, indicating that the CTR group underwent appropriate differentiation **(Figure 9a)**. Similar analyses were performed on VPA_{LD} and VPA_{HD} (**Figure 9b-c**). The former showed terms related to muscle formation, ion channel activity, and downregulation of genes related to negative regulation of neuronal differentiation and neural tube development. The latter showed terms related to muscle formation, and downregulation of several genes related to cerebral cortex development and synaptic formation. These results

may suggest that chronic exposure to high doses of VPA are detrimental for the development of neural organoids.

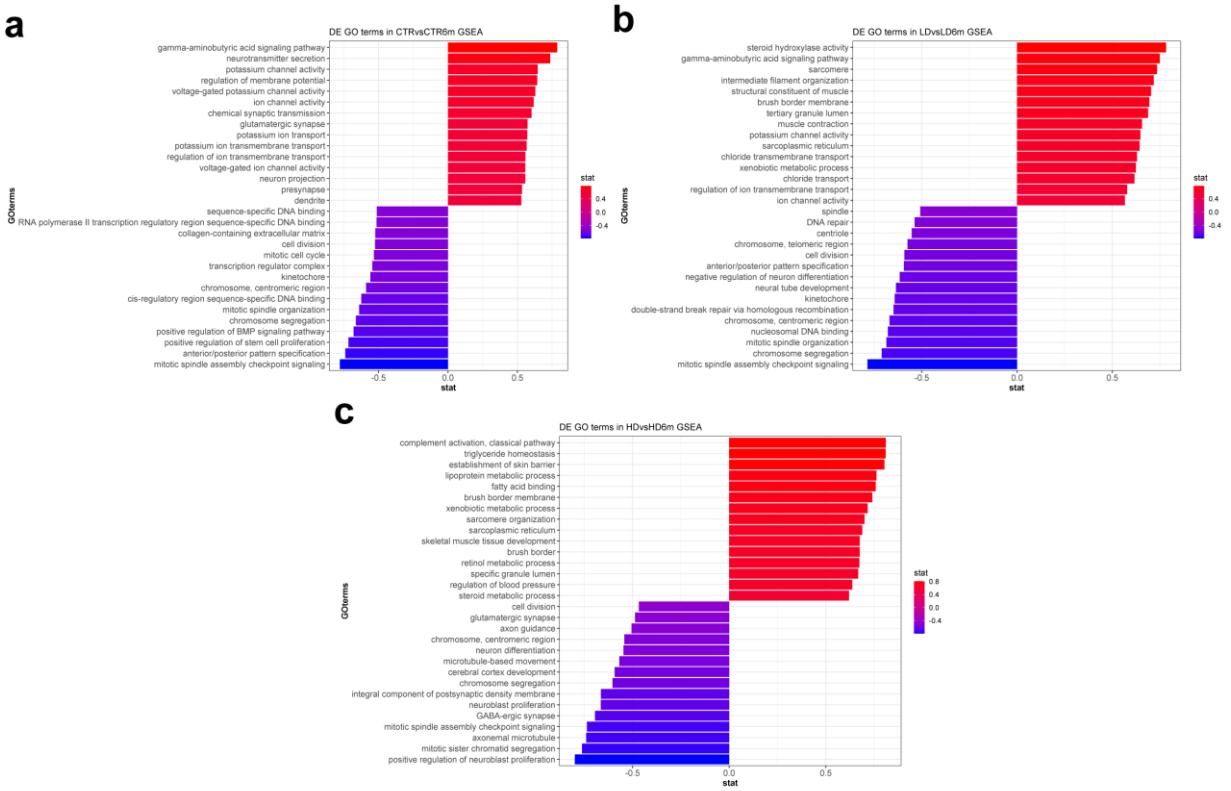

Figure 9: GSEA of developing unguided neural organoids: a) *GSEA of developing CTR condition reveals upregulated genes related to neuronal differentiation and synaptic specification* ***b)*** *GSEA of developing VPA_{LD} reveals upregulated genes related to muscle formation but also ion channel activity. Downregulated genes are related to negative regulation of neuronal differentiation and neural tube development.* ***c)*** *GSEA of developing VPA_{HD} reveals increase in the number of terms related to muscle formation, and down regulation of several genes related to cerebral cortex development and synaptic formation suggesting that chronic exposure to high doses of VPA are detrimental for the development of neural organoids (for the Figure see previous page).*

3.2.1. VPA effects on expression profiles

Principal component analysis (PCA) revealed distinct clusters between VPA-exposed and CTR organoids **(Figure 10b).** Interestingly, clusters were distinct only in samples from the 6 months' time-point highlighting the effects of prolonged exposure to the drug. DEG analysis between the VPA-exposed and CTR organoids identified 332 and 10966 DEGs (FDR <0.05) at respectively 1 and 6 months-old VPA_{LD} organoids, and 4523 and 15120 DEGs (FDR <0.05) at respectively 1 and 6 months-old VPA_{HD} organoids **(Figure 10b)**. From this observation alone we can speculate that the number of DEGs were proportional to the concentration used and the length of administration time. When observing the direction of the DEGs, we can also observe that the

majority of the genes are upregulated: with VPA_{LD} at 1 month there are 259 upregulated DEGs over 73 downregulated; VPA_{LD} at 6 months presented 6236 upregulated DEGs over 4730 downregulated; VPA_{HD} at 1 month presented 2462 upregulated DEGs over 2061 downregulated; and VPA_{HD} at 6 months presented 7844 upregulated DEGs over 7276 downregulated. The fact that the majority of the genes were upregulated may be due to the fact that VPA is an HDAC inhibitor and facilitates the access to DNA for increased gene expression. However, little is known regarding all the interactions of VPA with HDACs and the downstream effects of it.

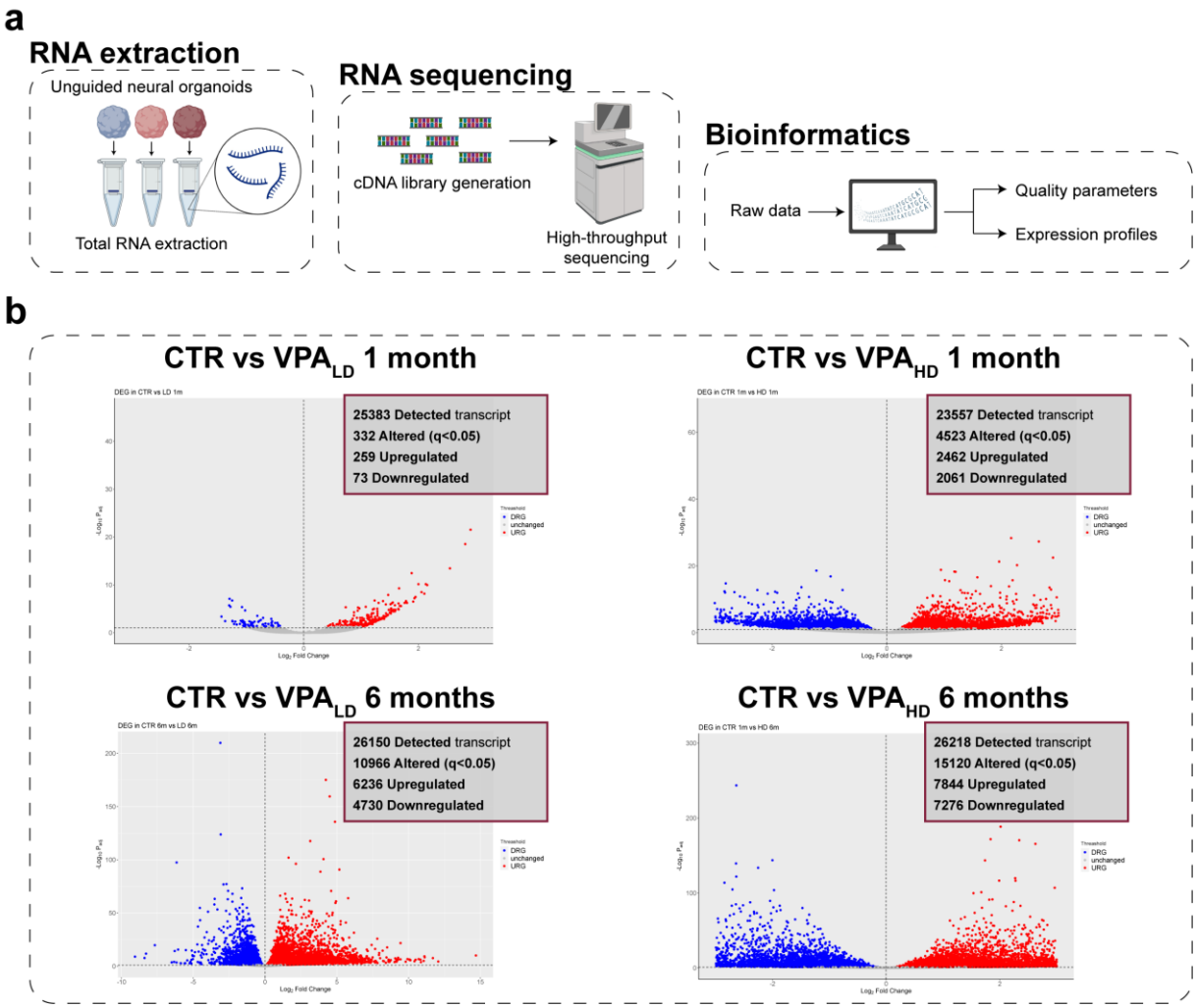

Figure 10: Expression profiles of bulk RNA sequencing of unguided neural organoids exposed to VPA at 1 and 6 months of development: a) *Schematics of RNA sequencing analysis.* ***b)*** *Differentially expressed genes in VPA_{LD} and VPA_{HD} at 1 and 6 months compared to CTR.*

3.2.2. Gene set enrichment analysis and VPA effects on organoid development

GO terms associated with each gene were obtained using BioMart. Then, Piano package version 2.6.0 (Bioconductor) in RStudio was used for GSEA **(Figure 11)**. In detail, gene-level

statistics were calculated for each gene set in the ranked list of genes (FDR<0.05), returning the gene set statistics and p-values of different directionality classes **(Figure 11)**.

In **Figure 11**, GSEA revealed distinct GO terms affected by low and high doses of VPA in VPA_{LD} and VPA_{HD} organoids at 1 and 6 months of development (FDR<0.05). For VPA_{LD} at 1 month, the upregulated GO terms were related to immune responses and GABAergic synaptic transmission, while the downregulated terms primarily involved histone acetylation and the histone acetyltransferase complex **(Figure 11a, top).** At 6 months, the upregulated terms in VPA_{LD} were mainly associated with embryonic skeletal and forelimb morphogenesis, response to fatty acids, and anterior/posterior pattern specification. On the other hand, cilia-related terms and excitatory synaptic transmission were found to be downregulated **(Figure 11a, bottom).**

In the case of VPA_{HD} at 1 month, the upregulated terms included stress-related terms and neuromuscular processes, while downregulated terms involved the histone acetyltransferase complex, excitatory synapse regulation of dendritic morphogenesis, and telencephalon development **(Figure 11b, top)**. In later stages of VPA_{HD}, the upregulated terms comprised cardiac muscle tissue morphogenesis, embryonic skeletal and forelimb morphogenesis, and muscle-related terms, while GABA, AMPA, and other synaptic terms were significantly downregulated **(Figure 11b, bottom).** Due to these gross abnormalities found both in neurodevelopment and gene expression data, we excluded VPA_{HD} from functional experiments.

The observed findings provide valuable insights into the distinct processes influenced by VPA during different developmental stages in VPA_{LD} and VPA_{HD} organoids. Remarkably, our IHC experiments targeting GAD67 presence already hinted at the upregulation of GABAergic synaptic transmission **(Figure 8)**, which aligns with the findings from the GSEA in VPA_{LD} at 1 month **(Figure 11b, top)**. Consistent with our results, previous studies that conducted GO analysis also reported similar enriched terms, including embryonic morphogenesis (Colleoni et al., 2014; Schulpen et al., 2015). Furthermore, VPA_{HD} organoids displayed terms associated with dendritic complexity, and previous findings on animal models demonstrated similar morphological results (Snow et al., 2008). While there is existing evidence indicating alterations in the inhibitory system in other ASD models (de Jong et al., 2021; Hali et al., 2020; Villa et al., 2022), there is still much to be uncovered regarding the specific role of these alterations in the development of ASD.

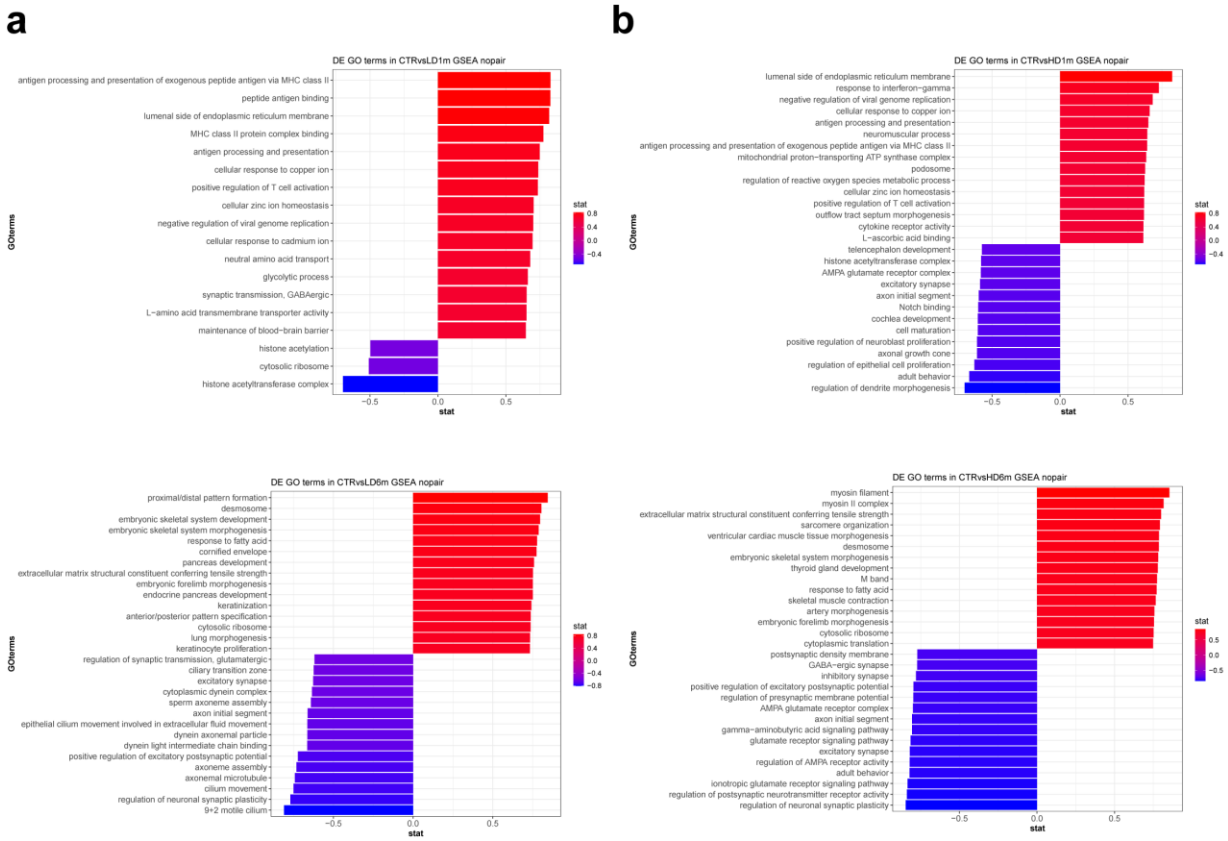

Figure 11: Gene set enrichment analysis of VPA_{LD} and VPA_{HD} at both 1 and 6 months of development: a-b) *All gene sets were elaborated from a list of DEGs below the FDR<0.05.*

3.2.3. Gene association analysis with ASD and FMRP related genes

To investigate the connection between VPA exposure and risk for ASD or FMRP, we evaluated the enrichment of VPA_{LD}- and VPA_{HD}-induced DEGs with two gene sets of ASD risk-associated genes and 1 set of FMRP risk associated genes. The first ASD gene set included 2203 DEGs between organoids (day 31) derived from four ASD patients and their respective unaffected fathers from the Mariani et al. study (Mariani et al., 2015). The second ASD gene set included 1095 ASD risk genes from the SFARI database (https://gene.sfari.org/). The FMRP risk gene set was curated by us based on information from the literature. We found that VPA-induced DEGs were significantly overlapped with genes dysregulated in ASD patient-derived organoids (overlapped genes for VPA_{LD} = 1223, P = 2.2E-16 and for VPA_{HD}= 1331, P=5.47E-06) **(Figure 12a)**. The VPA-induced DEGs were also enriched with ASD risk genes from the SFARI database (Overlapped genes for VPA_{LD}= 581, P = 2.2E-16 and for VPA_{HD}= 707, P=1.12E-07) **(Figure 12a).** Regarding the gene set for FMRP risk genes we also found a significant overlap both in VPA_{LD} and VPA_{HD} (Overlapped genes for VPA_{LD}= 1302, P = 2.2E-16 and for VPA_{HD}= 1630, P=7.18E-15). Through GO terms related to molecular functions, we found that the 61 genes in common between VPA_{LD} and VPA_{HD} were involved in amyloid-beta binding, voltage-gated channel activity (calcium, sodium, potassium, chloride) and postsynaptic membrane

potential. These results may suggest that VPA may impair signalling pathways that might lead to neurodevelopmental impairment. Notably, 61 DEGs between VPA_{LD} and VPA_{HD} including previously found genes, such as *GABRB3, KCNB1, PRKCB, SCN1A* and *SLC24A2* (Meng et al., 2022), which are known to be associated with several ion (calcium, sodium, potassium, chloride) channels and synaptic structures, were shared in all the three ASD gene sets **(Figure 12b).** Even though we found correspondence with some genes already found in the literature, it is important to highlight that the direction of the expression result to be different and that we lack validation experiments for the genes that were found. However, said differences in the fold change may be explained by the difference between the methods and models used for VPA administration (time and concentration of exposure to VPA) and for the time point taken into consideration (42 days against 6 months of development) (Meng et al., 2022).

a

CTR vs VPA_{LD} 6 months

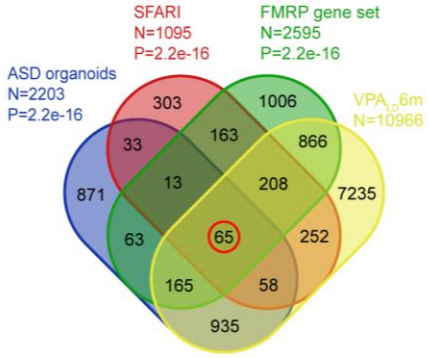

CTR vs VPA_{HD} 6 months

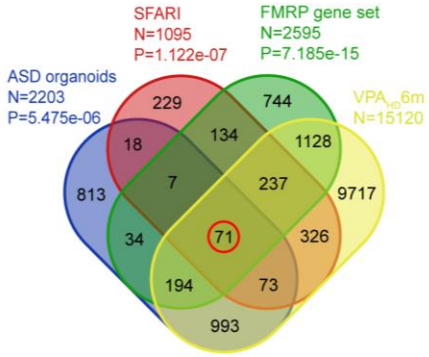

b

GSEA of VPA_{LD} and VPA_{HD} affected genes

GO terms	P-value	Q-value
Amyloid-Beta Binding (GO:0001540)	4.20E-09	3.14E-07
Voltage-Gated Calcium Channel Activity (GO:0005245)	6.09E-09	3.14E-07
High Voltage-Gated Calcium Channel Activity (GO:0008331)	7.20E-09	3.14E-07
Voltage-Gated Monoatomic Cation Channel Activity (GO:0022843)	1.16E-07	3.79E-06
Transmitter-Gated Monoatomic Ion Channel Activity (GO:0022824)	6.59E-06	0.000172695
Neurotransmitter Receptor Activity Involved In Regulation Of Postsynaptic Membrane Potential (GO:0099529)	3.45E-05	0.000753788
Voltage-Gated Monoatomic Ion Channel Activity (GO:0005244)	7.49E-05	0.001402548
Transmitter-Gated Monoatomic Ion Channel Activity Involved In Regulation Of Postsynaptic Membrane Potential (GO:1904315)	0.000151012	0.002472822
Calcium Channel Activity (GO:0005262)	0.00017165	0.002498461
Ligand-Gated Monoatomic Ion Channel Activity Involved In Regulation Of Presynaptic Membrane Potential (GO:0099507)	0.000405329	0.005309804
PDZ Domain Binding (GO:0030165)	0.000898241	0.009857989
Protein Kinase Binding (GO:0019901)	0.000903022	0.009857989
Glutamate Receptor Activity (GO:0008066)	0.001068218	0.01076435
Glutamate Receptor Binding (GO:0035254)	0.001356644	0.012389961
Voltage-Gated Sodium Channel Activity (GO:0005248)	0.001513278	0.012389961
Postsynaptic Neurotransmitter Receptor Activity (GO:0098960)	0.001513278	0.012389961
Voltage-Gated Potassium Channel Activity (GO:0005249)	0.001876873	0.014462959
Calmodulin-Dependent Protein Kinase Activity (GO:0004683)	0.002221453	0.015316335
Ligand-Gated Monoatomic Ion Channel Activity (GO:0015276)	0.002221453	0.015316335
Delayed Rectifier Potassium Channel Activity (GO:0005251)	0.003286661	0.021527627
pre-mRNA Binding (GO:0036002)	0.00376749	0.023501961
Inorganic Cation Transmembrane Transporter Activity (GO:0022890)	0.00510308	0.03038652
Calcium Channel Regulator Activity (GO:0005246)	0.005689733	0.031056458
Sodium Channel Activity (GO:0005272)	0.005689733	0.031056458

Figure 12: Enrichment of 61 shared VPA-induced DEGs with ASD and FMRP risk-associated gene sets: a) *Veen Diagram shows the overlap among VPA-exposed DEGs and two sets of ASD-associated genes and 1 set of FMRP-associated genes. The hypergeometric test was used to assess the enrichment between VPA-induced DEGs and gene sets. P values of the hypergeometric tests are indicated.* ***b)*** *Table with GO terms related to the molecular functions of the 61 genes shared between VPA_{LD} and VPA_{HD} that were sig*nificantly associated with the gene sets. P- and q-values of GO terms associated are reported on the table.

3.3. VPA_{LD} neural organoids show hyperactive networks in calcium imaging recordings

From the results of our molecular analysis, we have discovered that low doses of VPA affected the neuronal differentiation and relatively increased the presence of excitatory synapses. In particular with bulk RNA sequencing, we speculated that the exposure to VPA may affect the expression of genes that are associated to ASD and FMRP, especially in later stages (Figure RNA association). Due to this, we explored network physiology at around 4 to 6 months when calcium transient activity is firstly recorded in our model.

3.3.1. Calcium imaging recordings

Calcium imaging recording on neural organoid slices were performed with the use of Fluo4-AM without the presence of VPA in ACSF in order to measure differences in the network activity between VPA_{LD} and CTR. Firstly we tested the slices reactivity to a few compounds, such as potassium chloride (KCl), tetrodotoxin (TTX) and cyanquixaline (CNQX) **(Figure 13).**

KCl is a compound that elicits depolarization when dissolved in ACSF **(Figure 13b)**, whereas TTX and CNQX act as inhibitors of sodium voltage channels and AMPA receptors, respectively **(Figure 13c-d).**

From these experiments we observed that, indeed, most of the cells were reacting to the presence of KCl through depolarization both in VPA_{LD} and CTR. Most of the activity also stopped when exposure to TTX was performed in both conditions, suggesting that most of the activity was driven by the activity of Na^+ voltage channels. On the other hand, under the presence of CNQX not all cells stopped their activity and some even changed the pattern of their activity. These results may suggest that even though some of the activity was also driven by AMPA receptor activity, some of the cells may have also developed NMDA receptors related activity due to the change in pattern of calcium transients **(Figure 13d)**.

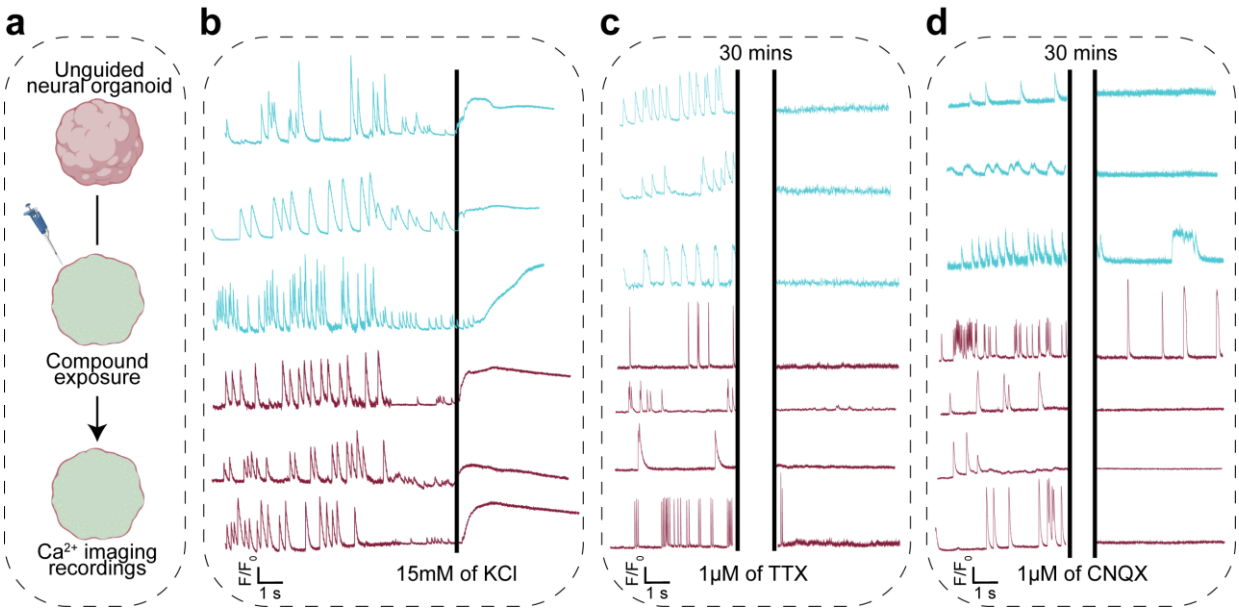

Figure 13: Reactivity Experiments Using Calcium Imaging in Unguided Neural Organoid Slices: a) *Experiment design depicting the organoid sliced labelled with Fluo4-AM exposed to the following compounds KCl, TTX and CNQX after spontaneous activity recordings. Slices were then recorded right after, for KCl, and after 30 minutes, for TTX and CNQX, in order to assess the effects.* ***b)*** *Representative traces of KCl exposure both in CTR and* VPA_{LD}*. Depolarization effect was visible right after exposure.* ***c)*** *Representative traces of TTX exposure. After 30 minutes the majority of spontaneous activity ceased suggesting that the majority of activity is driven by Na voltage channels both in CTR and* VPA_{LD}*.* ***d)*** *Representative traces of CNQX exposure both in CTR and* VPA_{LD}*. The spontaneous activity did not stop for all cells and some of them also changed pattern of activity suggesting that not all the activity is driven by AMPA receptors.*

Another observation that we made is that the cells from both conditions were spontaneously active throughout these experiments **(Figure 14b and d)**. When looking into this spontaneous calcium activity we noticed that VPA_{LD} was showing a higher frequency in the activity. These observations were replicated at both 4 and 6 months, showing consistent results with no significant alteration in the overall frequency **(Figure 14c and e)**. This initial evidence suggests that VPA_{LD} may have developed a hyperactive network because of chronic exposure to VPA.

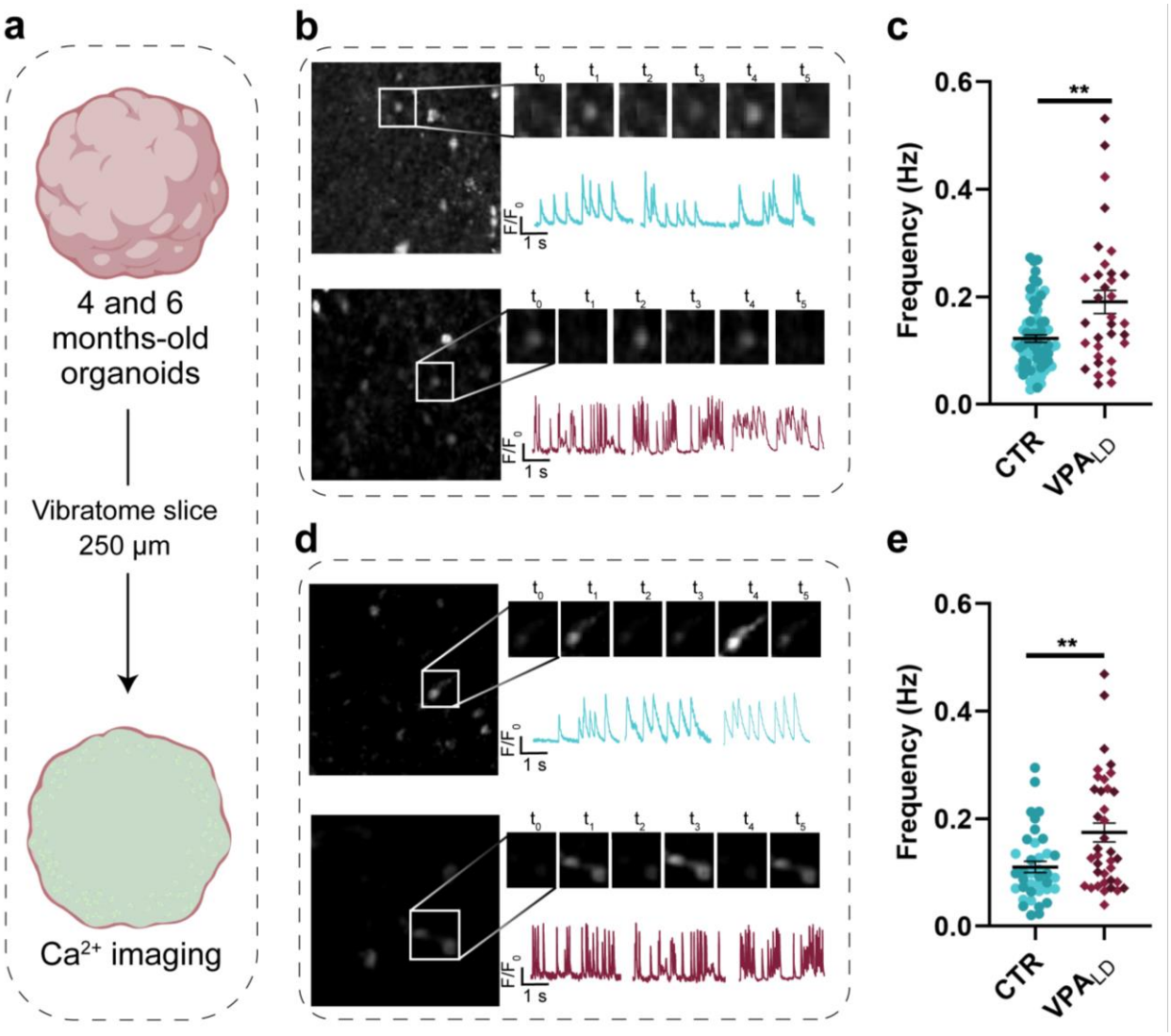

Figure 14: Calcium imaging of spontaneous activity shows that VPA-exposed unguided neural organoids generate hyperactive networks: a) *Schematic of calcium imaging experiments at 4 and 6 months.* ***b)*** *Representative pictures of video recordings and representative traces of 3 different ROIs of CTR and VPA_{LD} at 4 months.* ***c)*** *Average frequency of each video is represented as a point on the graphs which show a significant higher frequency in CTR and VPA_{LD} both at 4 months (N=74/6/2 for CTR and N=33/6/2 for VPA_{LD}, average per region/organoids/batches).* ***d)*** *Representative pictures of video recordings and representative traces of 3 different ROIs of CTR and VPA_{LD} at 6 months.* ***e)*** *Average frequency of each video is represented as a point on the graphs which show a significant higher frequency in CTR and VPA_{LD} at 6 months (N=38/6/2 for CTR and 37/6/2 for VPA_{LD}, average per region/organoids/batches). Graphs with analysis Mann-Whitney test illustrates p<0.05 = *, p<0.01 = **, p<0.001 = ***.*

3.4. Neurons generated in VPA-exposed neural organoids are easily excitable in a hyperactive network

Electrophysiological assessments were conducted to evaluate the effects of VPA on the functional maturation of the neurons generated by our model. This was done solely on 6-months-old unguided neural organoids slices near this time-point we could reliably record action potentials from neurons generated by our model.

Neuronal network dynamics showed a tendency of increased amplitude in spontaneous excitatory postsynaptic current (sEPSCs) in VPA-exposed organoids **(Figure 15a-b)** together with increased frequency **(Figure 15c)**. Importantly, in calcium imaging experiments, we observed an increased calcium transients in VPA-exposed organoids at both 4 and 6 months of development, further corroborating the observation of increased excitation. Similar sEPSCs frequency increase were recorded also in primary 2D cultures of animal models of ASD (Iijima et al., 2016).

The observed increase in the frequency of sPSCs and calcium transient activity in VPA-treated organoids may be explained by an alteration in the excitability of neurons. While neuronal intrinsic properties such as capacitance and membrane resistance did not show significant differences between VPA_{LD} and CTR **(Figure 15d-e)**, analysis of action potential kinetics revealed several noteworthy distinctions **(Figure 16)**.

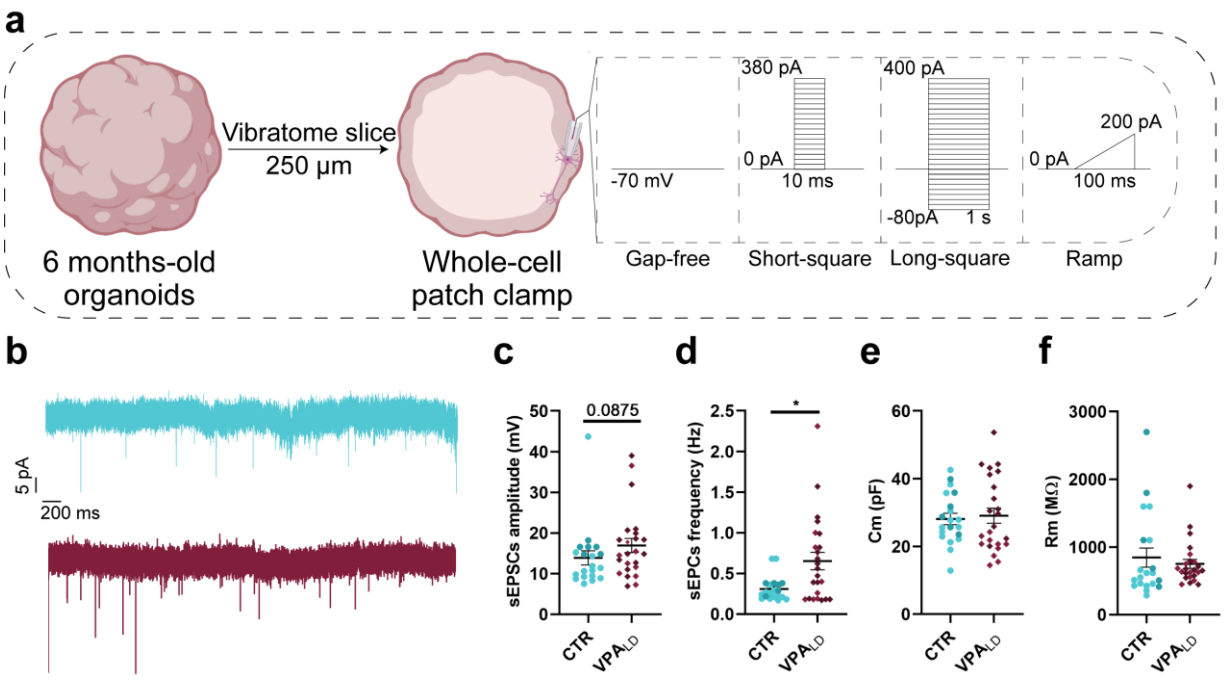

Figure 15: Increased network activity in human neurons following incubation with low doses of VPA: a) *Schematics of electrophysiology experiments performed in ACSF without VPA: Gap free experiment aims in assessing the spontaneous post synaptic activity in a neuron, short-square aims to assess the properties of an action potential, long-square aims to assess the parameters of bursts of action potentials, and the ramp aims to assess the amount of current needed to elicit an action potential (rehobase). Representative traces of CTR and VPA_{LD} of sEPSCs.* ***b-c)*** *The amplitude of sPSECs tended to be higher in VPA_{LD} compared to CTR (p=0.088) while the frequency was significantly higher in VPA_{LD} compared to CTR (N=20/6/2 for CTR and for 24/6/2 for VPA_{LD}, cells/organoids/batches).* ***d-e)*** *No changes were observed in the capacitance and membrane resistance of both CTR and VPA_{LD}. Graphs with analysis Mann-Whitney test illustrates p<0.05 = *, p<0.01 = **, p<0.001 = *** (for the Figure see previous page).*

Specifically, action potentials in VPA_{LD} took longer to reach their peak compared to CTR, while the decay time remained similar between the two conditions **(Figure 16c-d)**. Interestingly, VPA_{LD} exhibited a lower threshold potential and rheobase compared to CTR, indicating a higher excitability following prolonged exposure to low doses of VPA **(Figs. 16e-f)**. Supporting this, the resting membrane potential was significantly depolarized in VPA_{LD} **(Figure 16g)**.

In voltage clamp experiments **(Figure 18h)**, we observed an increased burst of action potentials in VPA_{LD} compared to CTR at a current step of approximately 20 pA. Conversely, at higher current steps, a lower frequency of action potentials was recorded in VPA_{LD}, suggesting a reduced ability to handle excessive currents, when compared to CTR **(Figure 16i)**. Taken together, these findings indicate that organoids chronically exposed to low doses of VPA generated hyperexcitable neurons compared to CTR. When considered alongside the results from gap-free assessment and calcium imaging, it suggests that the networks in VPA_{LD} may consist of hyperexcitable neurons, resulting in the formation of a hyperactive network.

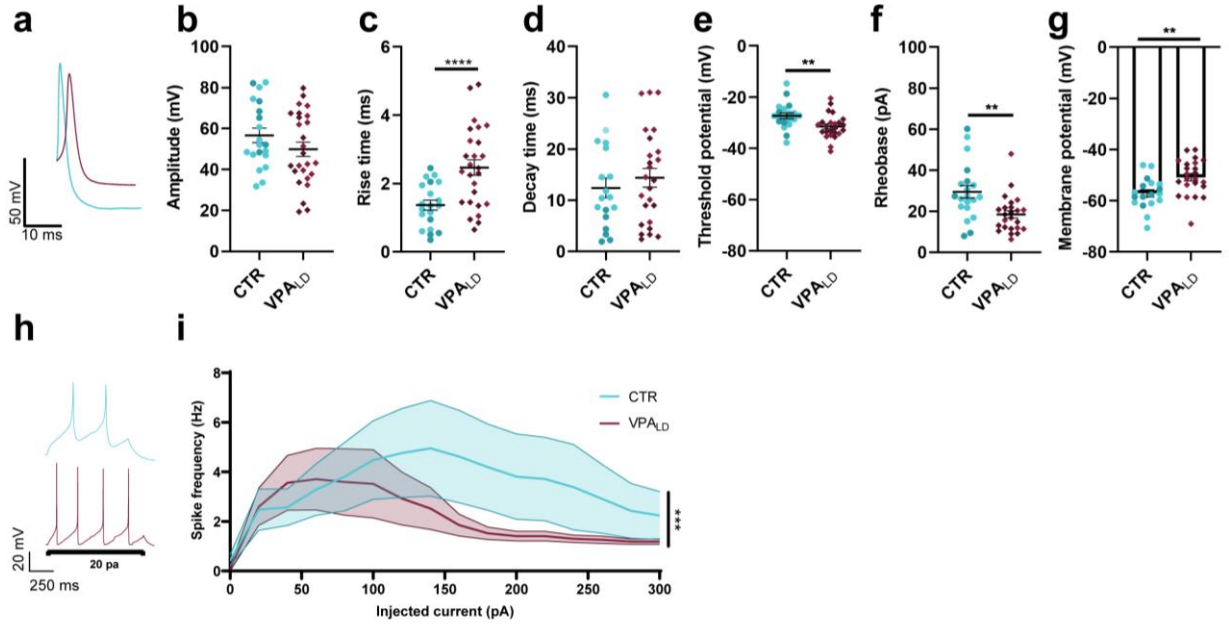

Figure 16: Action potential kinetics and intrinsic properties of neurons in VPA-exposed neural organoids: a) *Representative traces of action potentials of both CTR and VPA_{LD}.* ***b-d)*** *and rise time is shown to be significantly different in VPA_{LD} compared to CTR (N=20/6/2 for CTR and N=26/6/2 for VPA_{LD}).* ***e-f)*** *The threshold potential and rheobase are shown to be significantly lower in VPA_{LD} compared to CTR (N=20/6/2 for CTR and N=24/6/2 for VPA_{LD}, cells/organoids/batches),* ***g)*** *Membrane potential is shown to be lower in VPA_{LD} compared to CTR (N=20/6/2 for CTR and N=24/6/2 for VPA_{LD}, cells/organoids/batches).* ***h-i)*** *Representative traces of bursts of action potentials of both CTR and VPA_{LD} on step 20pA of current injection. Upon current injection, VPA_{LD} showed a higher frequency only around 20pA. At later steps, VPA_{LD} frequency drops showing a lower frequency compared to CTR (N=21/6/2 for CTR and N=27/6/2 for VPA_{LD}, cells/organoids/batches). Graphs with analysis Mann-Whitney test illustrates p<0.05 = *, p<0.01 = **, p<0.001 = *** (for the Figure see previous page).*

CHAPTER 4 | GENERAL DISCUSSION

4.1. Discussion

For the aim of this project, we showed that human unguided neural organoids are suitable for drug testing and to model *in vitro* VPA effects on neurodevelopment. By taking advantage of the longevity of our 3D human cultures, we replicated the chronic exposure to VPA in a developing human brain and its long-term effects. Our model included NPCs that rapidly differentiated into synaptically connected neuronal networks specified early- and later-born neurons, both glutamatergic and GABAergic neurons, and, in later stages, populated by astrocytes.

Using molecular analysis, we demonstrated that the presence of VPA in low doses accelerates the neuronal differentiation with an increase of the late-born neurons both at 4 and 6 months. This acceleration in the differentiation came in parallel with a lower renewal of the NPC pool and an increase in the presence of excitatory synapses. We also observed a switch in the inhibitory marker from an increased presence at an early stage of development to a decrease at a later stage, compared to CTR. Notably, this shift was also observed through RNA sequencing in GABAergic transmission-related genes in VPA_{LD} organoid samples.

In addition to that, the transcriptome profile of VPA_{LD} and VPA_{HD} revealed that the number of DEGs was dose- and time-dependent. GSEA confirmed the inhibitory effect of VPA on HDAC processes, especially in the early stages of exposure. In VPA_{LD} at later stages, there was an upregulation of terms associated with the development of embryonic skeletal systems, as well as the specification of anterior/posterior patterns. Conversely, terms related to cilia function and excitatory synaptic transmission were downregulated. Similar findings were observed in VPA_{HD}, with a greater number of upregulated terms related to embryonic skeletal and forelimb development and a downregulation of various synaptic transmission-related genes (glutamate, calcium and chloride). The molecular changes in embryonic skeletal and forelimb structures may be associated with the MCA observed in children exposed to VPA during pregnancy. The downregulation of cilia-related terms and excitatory synaptic transmission may also contribute to the higher prevalence of cognitive impairments, including ASD, observed in these children.

It is crucial, however, to consider that the effects of VPA may extend beyond genes directly associated with ASD or FMRP. The presence of off-target effects should not be overlooked, particularly when attempting to replicate neurodevelopmental disorders using this drug. Also, VPA´s effects are not exclusive to the nervous system but also to kidney and mitochondria. These systems were not replicated by our neural organoids.

Using electrophysiology, we assessed the maturation of important functional parameters in the network generated by our neural organoids – such as electrical input resistance, electrical

capacitance, membrane time constant and the ability to fire APs – and how they would change under the effect of VPA. Interestingly, we observed an increased frequency of sPSCs which demonstrates a hyperactive network. These observations were also confirmed to happen already at 4 months when we recorded increased spontaneous calcium activity in VPA_{LD}. The difference in GAD67 presence found specifically at 6 months in VPA_{LD} may explain the hyperactive network.

In addition to that, we found in VPA_{LD} an increase in the excitability of the neurons exposed to the drug. Indeed, the membrane and threshold potentials and the rheobase were found to be altered during the electrophysiology recording in VPA_{LD} without the presence of VPA.

4.1.1. VPA affects unguided neural organoid maturation

The effect of VPA exposure on the viability and differentiation of NPCs has been subject of many studies in both rodent and human model systems. Many of these studies reported a positive effect of VPA on neuronal differentiation via different mechanisms including the suppression of progenitor cell proliferation (Jung et al., 2008) and progenitor cell death (Go et al., 2011), decrease of the distribution of the deep-layer neuron distribution, but an increase in superficial layer neurons (Juliandi et al., 2012), the suppression of glial differentiation (Chu et al., 2015) and the epigenetically mediated induction of glutamatergic differentiation (Hsieh et al., 2004; K. C. Kim et al., 2014). Individual studies also report a pro-apoptotic effect on progenitors of glutamatergic neurons (Fujiki et al., 2013) and enhanced gliogenesis during rodent cortical development (Lee et al., 2016) upon VPA exposure.

In previous studies conducted on *in vitro* human 3D cultures, Cui and colleagues observed in human cortical organoids an initial increase in the NPC pool and a decrease in neuronal differentiation after 5 to 10 days of exposure at 16 days of differentiation. However, they reported a subsequent increase in neuronal differentiation, along with elevated levels of vGLUT1 and GAD67, around 30 days of development, but only after discontinuing VPA administration for 10 days (Cui et al., 2020). In contrast, another study focused on RNA sequencing analysis and discovered enhanced neuronal development at approximately 42 days of development (Meng et al., 2022). Although the VPA concentration used in our project may be similar to those previous studies, there were differences in the time points analysed and the methods employed. These discrepancies could potentially account for the variation observed between previous findings and our results.

Our IHC results did fall in line with some of the aforementioned effects of VPA (Meng et al., 2022). The treatment with the drug impaired the renewal of the NPC pool and an enhanced

differentiation of neurons during the development of our organoids **(Figures 7b)**. More specifically, we have observed a switch from an increase of both early- **(Figures 8b top)** and later-born neurons **(Figures 8b bottom)** in VPA_{LD} to an increase of exclusively SATB2 positive neurons at later stages of development **(Figures 8b bottom)**. Beside the neuronal markers, we also observed impaired glial differentiation in VPA_{LD}, further proving the enhanced neuronal differentiation under VPA influence (**Figures 6b bottom)**. The specification of neuronal subpopulations and the presence of astrocytes under the chronic presence of VPA has not been previously investigated in 3D cultures. Previous studies have primarily focused on broader aspects of neuronal differentiation and developmental processes.

4.1.2. VPA affects unguided neural organoid synapse formation

Enhanced glutamatergic synapse formation **(Figure 9b)** could be explained by an induction of glutamatergic neuronal differentiation as it was shown for primary cultures of mouse neuronal precursors. Via its HDAC inhibition function, VPA led to an upregulation of Pax6-dependent gene expression that resulted in increased levels of glutamatergic synaptic proteins including synaptophysin, VGLUT1 and PSD95 (K. C. Kim et al., 2014). In line with this observation, Iijima and colleagues have provided functional evidence for enhanced glutamatergic synapse formation in VPA-exposed mouse primary cortical cultures which exhibited an increased mEPSC frequency as well as an upregulation of VGLUT1 expression (Iijima et al., 2016). An enhanced density of glutamatergic synapses was also shown in acute slices of the lateral amygdala, which assumed to contribute to anxiety and fear memory in ASD, of in-utero VPA-exposed rats (Lin et al., 2013).

An increased E/I ratio in certain key neural systems is one of the most widely accepted concepts of ASD pathogenesis (Rubenstein & Merzenich, 2003). At the synaptic level, this can result from an increased function of excitatory synapses, a decreased function of inhibitory synapses or the combination of both. Several studies reporting VPA-mediated upregulation of glutamatergic RNA/protein expression or glutamatergic synapse function have shown concomitant effects on inhibitory synaptic RNA/protein expression or GABAergic synapse function (Fukuchi et al., 2009; Iijima et al., 2016; K. C. Kim et al., 2014). In VPA rodent models, decreased levels of GABAergic marker proteins such as GAD67 (Hou et al., 2018) and GAD65 (K. C. Kim et al., 2014) have been detected in different cortical areas. At the functional level, the frequency of GABAergic miniature inhibitory postsynaptic currents (mIPSCs) was shown to be substantially decreased in layer 2/3 pyramidal neurons in the temporal cortex of adolescent in-utero VPA exposed rats (Banerjee et al., 2013). Primary cultures of cortical neurons from neonatal rats that were treated with 1 mM VPA for 4 days showed significantly reduced VGAT expression und

less VGAT-positive puncta whereas VGLUT1 expression was increased (Kumamaru et al., 2014). In our work, we have observed an increase in the presence of glutamatergic synapses, using vGLUT1 **(Figures 9b)** both at early and later stages of development. However, glutamatergic regulation of synaptic transmission was found to be significantly down regulated in GSEA at 6 months of development **(Figure 13a bottom)**.

In our additional IHC experiments and RNA sequencing, we observed that exposure to VPA brought a shift in the presence of GAD67 **(Figure 10b)** and GABAergic transmission **(Figure 13a)**. Alterations in the expression of GABAergic markers or GABAergic transmission were described in either adolescent or adult i*n-utero* VPA-exposed animals or in primary cell cultures that had undergone prolonged *in vitro* differentiation and probably reached a level of maturation that is comparable to postnatal neurons. In the abovementioned study the differences in GABAergic synaptic transmission between the VPA-treated and the untreated group were mainly attributed to a disturbed maturation of progenitors of parvalbumin-positive interneurons (Iijima et al., 2016). *In vivo*, fast-spiking interneurons are generated around embryonic day 13.5 (in rodents), migrate tangentially and integrate into the cortical circuitry while the cortical layers are still being formed. Their fully mature state is not reached until after birth (Butt et al., 2005; Miyamae et al., 2017). While we did not specifically perform molecular and functional experiments targeting the inhibitory system, our observations concerning the distribution of GAD67, and the expression of genes related to GABAergic transmission offer insights into the E/I balance within the network of our VPA-exposed organoids. Furthermore, the observed changes in GABAergic transmission throughout the development of our 3D organoids highlight the advantages of employing long-term *in vitro* models like neural organoids for detecting such shifts.

Notably, the issue of E/I imbalance in ASD models has recently regained attention, as evidenced by a study that compared four distinct mouse models of ASD (Antoine et al., 2019). In adult animals, a decrease in excitation-inhibition was observed in layer 2/3 pyramidal neurons that receive thalamic inputs. However, this decrease in the E/I ratio stemmed from an initial deficiency in inhibitory input, which was compensated by increased excitation to ensure adequate neuronal depolarization near the spiking threshold. Thus, the authors propose that the elevated E/I ratio in mature neuronal networks reflects the homeostatic stabilization of hypoconnected networks, rather than generating network hyperexcitability (Antoine et al., 2019). This underscores the adaptive capacity of brain circuitry and suggests that early changes in network activity may not persist into later developmental stages, emphasizing the importance of studying neuronal activity during early development.

The increased density of glutamatergic synapses, coupled with the decrease in GABAergic synapses, can result in an overall increase in the number of synaptic connections, aligning with the concept of (local) hyperconnectivity observed in ASD (H. Markram et al., 2007; K. Markram & Markram, 2010). Studies in VPA-exposed rats have shown hyperconnectivity of glutamatergic synapses in various neocortical regions, including layer 2/3 and layer 5 pyramidal cell hyperconnectivity in the somatosensory cortex and medial prefrontal cortex (Codagnone et al., 2015; Rinaldi, Perrodin, et al., 2008; Rinaldi, Silberberg, et al., 2008; Silva et al., 2009). The "intense world theory" of ASD suggests that hyperconnected cortical areas, which are more sensitive to stimulation and exhibit greater autonomy, may underlie some core symptoms of ASD, such as intense perceptions and hypersensitivity to external stimuli. These findings are aligned with our observations on the hyperactive networks developed by our mature unguided neural organoids.

4.1.3. Network hyperactivity in VPA-treated neurons

In a previous study, Ijima and colleagues conducted whole-cell voltage-clamp recordings on mouse primary cortical neurons treated with 2 mM VPA for 6 days after isolation on embryonic day 15. They observed large synaptic burst discharges in the VPA-treated neurons, which were absent in the untreated control neurons (Iijima et al., 2016). In other studies, higher rates of postsynaptic currents and spontaneous action potentials were observed in the amygdala and hippocampal CA1 pyramidal neurons of rats exposed to VPA *in utero* (Hajisoltani et al., 2019; Lin et al., 2013).

The effect of VPA on spontaneous neuronal activity in hPSC-derived neurons was first investigated in a drug screening study focused on *SHANK3* haploinsufficiency syndrome. Treatment with 2 mM VPA for 5 days resulted in enhanced spontaneous calcium oscillations in control hPSC-derived neurons aged 5 to 6 weeks. In hPSC-derived neurons from patients with SHANK3 haploinsufficiency, VPA treatment increased the presence of SHANK3-PSD95 double-positive puncta and restored calcium oscillations. Additionally, VPA treatment led to significant changes in the mRNA expression levels of synaptic genes, including an upregulation of VGLUT1, synaptopodin, and mGluR1 mRNA (Darville et al., 2016), indicating an involvement of altered synapse formation in the enhanced spontaneous activity observed after VPA treatment. However, contrasting findings were reported in human forebrain organoids exposed to VPA, where neuronal activity recorded using microelectrode arrays (MEA) showed impairment in synaptic transmission. This discrepancy in findings may be attributed to differences in experimental methods and the time point at which the recordings were performed (Meng et al., 2022).

In our study, we observed a prominent synaptic phenotype characterized by an enhanced frequency of sEPSCs in VPA-treated neurons **(Figure 13a-c)**. These changes in neuronal activity may be linked to the impact of chronic VPA exposure on neuronal differentiation and the formation of glutamatergic and GABAergic synapses **(Figure 10b and 13a, top)**. Additionally, we found evidence of altered excitability in VPA-treated neural organoids, where at 6 months of development, the membrane potentials were significantly higher, while the threshold potential and rheobase were significantly lower **(Figure 18e-g).**

Taken together, these findings reveal the suitability human unguided neural organoids for drug testing and modelling the effects of VPA on neurodevelopment. We were able to replicate the effects of chronic exposure to VPA and observe its lasting effects on neuronal distribution and synaptic connectivity. Molecular analysis revealed an acceleration in neuronal differentiation, with an increase in the presence of superficial layer neurons, an increase in excitatory synapses, and a shift in inhibitory markers and gene expression. Furthermore, electrophysiological recordings confirmed our molecular observations indicating a hyperactive network and increased excitability of neurons under low doses of VPA, providing insights into the functional alterations induced by VPA. In addition to the wide-ranging effects of VPA on gene expression, it is noteworthy that a subset of DEGs identified in our study is associated with the neurodevelopmental disorder ASD. These findings underscore the relevance of VPA-induced molecular changes in the context of ASD pathogenesis. However, it is now clear that the effects of VPA in the adult brain and in the developing brain are significantly different, whereas it undoubtedly controls seizures in mature neuronal networks, its effects seem to induce neuronal hyperexcitability and accelerated neuronal differentiation in early brain development. This change in excitation may be sufficient to impinge on proper circuit function and provide a common landscape linking early hyperexcitability to ASD-linked insults.

CHAPTER 5 | BIBLIOGRAPHY

Amir, R. E., Van den Veyver, I. B., Wan, M., Tran, C. Q., Francke, U., & Zoghbi, H. Y. (1999). Rett syndrome is caused by mutations in X-linked MECP2, encoding methyl-CpG-binding protein 2. *Nature Genetics*, *23*(2), Article 2. https://doi.org/10.1038/13810

Antoine, M. W., Langberg, T., Schnepel, P., & Feldman, D. E. (2019). Increased Excitation-Inhibition Ratio Stabilizes Synapse and Circuit Excitability in Four Autism Mouse Models. *Neuron*, *101*(4), 648-661.e4. https://doi.org/10.1016/j.neuron.2018.12.026

Baker, G. A., Bromley, R. L., Briggs, M., Cheyne, C. P., Cohen, M. J., García-Fiñana, M., Gummery, A., Kneen, R., Loring, D. W., Mawer, G., Meador, K. J., Shallcross, R., & Clayton-Smith, J. (2015). IQ at 6 years after in utero exposure to antiepileptic drugs. *Neurology*, *84*(4), 382–390. https://doi.org/10.1212/WNL.0000000000001182

Banerjee, A., García-Oscos, F., Roychowdhury, S., Galindo, L. C., Hall, S., Kilgard, M. P., & Atzori, M. (2013). Impairment of cortical GABAergic synaptic transmission in an environmental rat model of autism. *International Journal of Neuropsychopharmacology*, *16*(6), 1309–1318. https://doi.org/10.1017/S1461145712001216

Baquet, Z. C., Gorski, J. A., & Jones, K. R. (2004). Early Striatal Dendrite Deficits followed by Neuron Loss with Advanced Age in the Absence of Anterograde Cortical Brain-Derived Neurotrophic Factor. *The Journal of Neuroscience*, *24*(17), 4250–4258. https://doi.org/10.1523/JNEUROSCI.3920-03.2004

Bath, K. G., & Pimentel, T. (2017). Effect of Early Postnatal Exposure to Valproate on Neurobehavioral Development and Regional BDNF Expression in Two Strains of Mice. *Epilepsy & Behavior : E&B*, *70*(Pt A), 110–117. https://doi.org/10.1016/j.yebeh.2017.02.026

Biggs, C. S., Pearce, B. R., Fowler, L. J., & Whitton, P. S. (1992). Regional Effects of Sodium Valproate on Extracellular Concentrations of 5-Hydroxytryptamine, Dopamine, and Their Metabolites in the Rat Brain: An In Vivo Microdialysis Study. *Journal of Neurochemistry*, *59*(5), 1702–1708. https://doi.org/10.1111/j.1471-4159.1992.tb11001.x

Bittigau, P., Sifringer, M., & Ikonomidou, C. (2003). Antiepileptic drugs and apoptosis in the developing brain. *Annals of the New York Academy of Sciences*, *993*, 103–114; discussion 123-124. https://doi.org/10.1111/j.1749-6632.2003.tb07517.x

Bringas, M. E., Carvajal-Flores, F. N., López-Ramírez, T. A., Atzori, M., & Flores, G. (2013). Rearrangement of the dendritic morphology in limbic regions and altered exploratory behavior in a rat model of autism spectrum disorder. *Neuroscience*, *241*, 170–187. https://doi.org/10.1016/j.neuroscience.2013.03.030

Bromley, R. L., Mawer, G., Clayton-Smith, J., Baker, G. A., & Liverpool and Manchester Neurodevelopment Group. (2008). Autism spectrum disorders following in utero exposure to antiepileptic drugs. *Neurology*, *71*(23), 1923–1924. https://doi.org/10.1212/01.wnl.0000339399.64213.1a

Buganim, Y., Faddah, D. A., & Jaenisch, R. (2013). Mechanisms and models of somatic cell reprogramming. *Nature Reviews. Genetics*, *14*(6), 427–439. https://doi.org/10.1038/nrg3473

Butt, S. J. B., Fuccillo, M., Nery, S., Noctor, S., Kriegstein, A., Corbin, J. G., & Fishell, G. (2005). The temporal and spatial origins of cortical interneurons predict their physiological subtype. *Neuron*, *48*(4), 591–604. https://doi.org/10.1016/j.neuron.2005.09.034

Cao, W. S., Livesey, J. C., & Halliwell, R. F. (2015). An evaluation of a human stem cell line to identify risk of developmental neurotoxicity with antiepileptic drugs. *Toxicology in Vitro*, *29*(3), 592–599. https://doi.org/10.1016/j.tiv.2015.01.010

Cerrizuela, S., Vega-Lopez, G. A., & Aybar, M. J. (2020). The role of teratogens in neural crest development. *Birth Defects Research*, *112*(8), 584–632. https://doi.org/10.1002/bdr2.1644

Cervoni, N., Detich, N., Seo, S., Chakravarti, D., & Szyf, M. (2002). The Oncoprotein Set/TAF-1β, an Inhibitor of Histone Acetyltransferase, Inhibits Active Demethylation of DNA, Integrating DNA Methylation and Transcriptional Silencing *. *Journal of Biological Chemistry*, *277*(28), 25026–25031. https://doi.org/10.1074/jbc.M202256200

Cervoni, N., & Szyf, M. (2001). Demethylase Activity Is Directed by Histone Acetylation *. *Journal of Biological Chemistry*, *276*(44), 40778–40787. https://doi.org/10.1074/jbc.M103921200

Chanda, S., Ang, C. E., Lee, Q. Y., Ghebrial, M., Haag, D., Shibuya, Y., Wernig, M., & Südhof, T. C. (2019). Direct Reprogramming of Human Neurons Identifies MARCKSL1 as a Pathogenic Mediator of Valproic Acid-Induced Teratogenicity. *Cell Stem Cell*, *25*(1), 103-119.e6. https://doi.org/10.1016/j.stem.2019.04.021

Chao, M. V. (2003). Neurotrophins and their receptors: A convergence point for many signalling pathways. *Nature Reviews Neuroscience*, *4*(4), Article 4. https://doi.org/10.1038/nrn1078

Chateauvieux, S., Morceau, F., Dicato, M., & Diederich, M. (2010). Molecular and Therapeutic Potential and Toxicity of Valproic Acid. *Journal of Biomedicine and Biotechnology*, *2010*, 479364. https://doi.org/10.1155/2010/479364

Chen, G., Yuan, P., Hawver, D. B., Potter, W. Z., & Manji, H. K. (1997). Increase in AP-1 Transcription Factor DNA Binding Activity by Valproic Acid. *Neuropsychopharmacology*, *16*(3), Article 3. https://doi.org/10.1016/S0893-133X(96)00239-4

Chen, G., Yuan, P.-X., Jiang, Y.-M., Huang, L.-D., & Manji, H. K. (1999). Valproate robustly enhances AP-1 mediated gene expression. *Molecular Brain Research*, *64*(1), 52–58. https://doi.org/10.1016/S0169-328X(98)00303-9

Choi, C. S., Gonzales, E. L., Kim, K. C., Yang, S. M., Kim, J.-W., Mabunga, D. F., Cheong, J. H., Han, S.-H., Bahn, G. H., & Shin, C. Y. (2016). The transgenerational inheritance of autism-like phenotypes in mice exposed to valproic acid during pregnancy. *Scientific Reports*, *6*(1), Article 1. https://doi.org/10.1038/srep36250

Christianson, A. L., Chester, N., & Kromberg, J. G. R. (1994). Fetal Valproate Syndrome: Clinical and Neuro-developmental Features in Two Sibling Pairs. *Developmental Medicine & Child Neurology*, *36*(4), 361–369. https://doi.org/10.1111/j.1469-8749.1994.tb11858.x

Chu, T., Zhou, H., Wang, T., Lu, L., Li, F., Liu, B., Kong, X., & Feng, S. (2015). In vitro characteristics of valproic acid and all-trans-retinoic acid and their combined use in promoting

neuronal differentiation while suppressing astrocytic differentiation in neural stem cells. *Brain Research*, *1596*, 31–47. https://doi.org/10.1016/j.brainres.2014.11.029

Codagnone, M. G., Podestá, M. F., Uccelli, N. A., & Reinés, A. (2015). Differential Local Connectivity and Neuroinflammation Profiles in the Medial Prefrontal Cortex and Hippocampus in the Valproic Acid Rat Model of Autism. *Developmental Neuroscience*, *37*(3), 215–231. https://doi.org/10.1159/000375489

Colleoni, S., Galli, C., Gaspar, J. A., Meganathan, K., Jagtap, S., Hescheler, J., Zagoura, D., Bremer, S., Sachinidis, A., & Lazzari, G. (2014). A comparative transcriptomic study on the effects of valproic acid on two different hESCs lines in a neural teratogenicity test system. *Toxicology Letters*, *231*(1), 38–44. https://doi.org/10.1016/j.toxlet.2014.08.023

Costa, C., Martella, G., Picconi, B., Prosperetti, C., Pisani, A., Di Filippo, M., Pisani, F., Bernardi, G., & Calabresi, P. (2006). Multiple Mechanisms Underlying the Neuroprotective Effects of Antiepileptic Drugs Against In Vitro Ischemia. *Stroke*, *37*(5), 1319–1326. https://doi.org/10.1161/01.STR.0000217303.22856.38

Crawley, J. N. (2004). Designing mouse behavioral tasks relevant to autistic-like behaviors. *Mental Retardation and Developmental Disabilities Research Reviews*, *10*(4), 248–258. https://doi.org/10.1002/mrdd.20039

Cui, K., Wang, Y., Zhu, Y., Tao, T., Yin, F., Guo, Y., Liu, H., Li, F., Wang, P., Chen, Y., & Qin, J. (2020). Neurodevelopmental impairment induced by prenatal valproic acid exposure shown with the human cortical organoid-on-a-chip model. *Microsystems & Nanoengineering*, *6*(1), Article 1. https://doi.org/10.1038/s41378-020-0165-z

Cunningham, M. O., Woodhall, G. L., & Jones, R. S. G. (2003). Valproate modifies spontaneous excitation and inhibition at cortical synapses in vitro. *Neuropharmacology*, *45*(7), 907–917. https://doi.org/10.1016/S0028-3908(03)00270-3

Darville, H., Poulet, A., Rodet-Amsellem, F., Chatrousse, L., Pernelle, J., Boissart, C., Héron, D., Nava, C., Perrier, A., Jarrige, M., Cogé, F., Millan, M. J., Bourgeron, T., Peschanski, M., Delorme, R., & Benchoua, A. (2016). Human Pluripotent Stem Cell-derived Cortical Neurons for High Throughput Medication Screening in Autism: A Proof of Concept Study in SHANK3 Haploinsufficiency Syndrome. *EBioMedicine*, *9*, 293–305. https://doi.org/10.1016/j.ebiom.2016.05.032

de Graaf-Peters, V. B., & Hadders-Algra, M. (2006). Ontogeny of the human central nervous system: What is happening when? *Early Human Development*, *82*(4), 257–266. https://doi.org/10.1016/j.earlhumdev.2005.10.013

de Jong, J. O., Llapashtica, C., Genestine, M., Strauss, K., Provenzano, F., Sun, Y., Zhu, H., Cortese, G. P., Brundu, F., Brigatti, K. W., Corneo, B., Migliori, B., Tomer, R., Kushner, S. A., Kellendonk, C., Javitch, J. A., Xu, B., & Markx, S. (2021). Cortical overgrowth in a preclinical forebrain organoid model of CNTNAP2-associated autism spectrum disorder. *Nature Communications*, *12*(1), Article 1. https://doi.org/10.1038/s41467-021-24358-4

Dolmetsch, R., & Geschwind, D. H. (2011). The human brain in a dish: The promise of iPSC-derived neurons. *Cell*, *145*(6), 831–834. https://doi.org/10.1016/j.cell.2011.05.034

Du, J., Creson, T. K., Wu, L.-J., Ren, M., Gray, N. A., Falke, C., Wei, Y., Wang, Y., Blumenthal, R., Machado-Vieira, R., Yuan, P., Chen, G., Zhuo, M., & Manji, H. K. (2008). The Role of Hippocampal GluR1 and GluR2 Receptors in Manic-Like Behavior. *The Journal of Neuroscience*, *28*(1), 68–79. https://doi.org/10.1523/JNEUROSCI.3080-07.2008

Dufour-Rainfray, D., Vourc'h, P., Le Guisquet, A.-M., Garreau, L., Ternant, D., Bodard, S., Jaumain, E., Gulhan, Z., Belzung, C., Andres, C. R., Chalon, S., & Guilloteau, D. (2010). Behavior and serotonergic disorders in rats exposed prenatally to valproate: A model for autism. *Neuroscience Letters*, *470*(1), 55–59. https://doi.org/10.1016/j.neulet.2009.12.054

Feinberg, A. P. (2007). Phenotypic plasticity and the epigenetics of human disease. *Nature*, *447*(7143), Article 7143. https://doi.org/10.1038/nature05919

Fernandes, S., Vinnakota, R., Kumar, J., Kale, V., & Limaye, L. (2019). Improved neural differentiation of normal and abnormal induced pluripotent stem cell lines in the presence of valproic acid. *Journal of Tissue Engineering and Regenerative Medicine*, *13*(8), 1482–1496. https://doi.org/10.1002/term.2904

Fombonne, E. (2003). Epidemiological surveys of autism and other pervasive developmental disorders: An update. *Journal of Autism and Developmental Disorders*, *33*(4), 365–382. https://doi.org/10.1023/a:1025054610557

Fujiki, R., Sato, A., Fujitani, M., & Yamashita, T. (2013). A proapoptotic effect of valproic acid on progenitors of embryonic stem cell-derived glutamatergic neurons. *Cell Death & Disease*, *4*(6), e677. https://doi.org/10.1038/cddis.2013.205

Fujimura, K., Mitsuhashi, T., Shibata, S., Shimozato, S., & Takahashi, T. (2016). In Utero Exposure to Valproic Acid Induces Neocortical Dysgenesis via Dysregulation of Neural Progenitor Cell Proliferation/Differentiation. *The Journal of Neuroscience*, *36*(42), 10908–10919. https://doi.org/10.1523/JNEUROSCI.0229-16.2016

Fukuchi, M., Nii, T., Ishimaru, N., Minamino, A., Hara, D., Takasaki, I., Tabuchi, A., & Tsuda, M. (2009). Valproic acid induces up- or down-regulation of gene expression responsible for the neuronal excitation and inhibition in rat cortical neurons through its epigenetic actions. *Neuroscience Research*, *65*(1), 35–43. https://doi.org/10.1016/j.neures.2009.05.002

Gandal, M. J., Edgar, J. C., Ehrlichman, R. S., Mehta, M., Roberts, T. P. L., & Siegel, S. J. (2010). Validating gamma oscillations and delayed auditory responses as translational biomarkers of autism. *Biological Psychiatry*, *68*(12), 1100–1106. https://doi.org/10.1016/j.biopsych.2010.09.031

Genton, P., Semah, F., & Trinka, E. (2006). Valproic Acid in Epilepsy. *Drug Safety*, *29*(1), 1–21. https://doi.org/10.2165/00002018-200629010-00001

Ghiglieri, V., Picconi, B., Sgobio, C., Bagetta, V., Barone, I., Paillè, V., Di Filippo, M., Polli, F., Gardoni, F., Altrock, W., Gundelfinger, E. D., De Sarro, G., Bernardi, G., Ammassari-Teule, M., Di Luca, M., & Calabresi, P. (2009). Epilepsy-induced abnormal striatal plasticity in Bassoon

mutant mice. *European Journal of Neuroscience*, *29*(10), 1979–1993. https://doi.org/10.1111/j.1460-9568.2009.06733.x

Ghiglieri, V., Sgobio, C., Patassini, S., Bagetta, V., Fejtova, A., Giampà, C., Marinucci, S., Heyden, A., Gundelfinger, E. D., Fusco, F. R., Calabresi, P., & Picconi, B. (2010). TrkB/BDNF-Dependent Striatal Plasticity and Behavior in a Genetic Model of Epilepsy: Modulation by Valproic Acid. *Neuropsychopharmacology*, *35*(7), 1531–1540. https://doi.org/10.1038/npp.2010.23

Ghodke-Puranik, Y., Thorn, C. F., Lamba, J. K., Leeder, J. S., Song, W., Birnbaum, A. K., Altman, R. B., & Klein, T. E. (2013). Valproic acid pathway: Pharmacokinetics and pharmacodynamics. *Pharmacogenetics and Genomics*, *23*(4), 236–241. https://doi.org/10.1097/FPC.0b013e32835ea0b2

Go, H. S., Kim, K. C., Choi, C. S., Jeon, S. J., Kwon, K. J., Han, S.-H., Lee, J., Cheong, J. H., Ryu, J. H., Kim, C.-H., Ko, K. H., & Shin, C. Y. (2012). Prenatal exposure to valproic acid increases the neural progenitor cell pool and induces macrocephaly in rat brain via a mechanism involving the GSK-3β/β-catenin pathway. *Neuropharmacology*, *63*(6), 1028–1041. https://doi.org/10.1016/j.neuropharm.2012.07.028

Go, H. S., Seo, J. E., Kim, K. C., Han, S. M., Kim, P., Kang, Y. S., Han, S. H., Shin, C. Y., & Ko, K. H. (2011). Valproic acid inhibits neural progenitor cell death by activation of NF-κB signaling pathway and up-regulation of Bcl-XL. *Journal of Biomedical Science*, *18*(1), 48. https://doi.org/10.1186/1423-0127-18-48

Gobbi, G., & Janiri, L. (2006). Sodium- and magnesium-valproate in vivo modulate glutamatergic and GABAergic synapses in the medial prefrontal cortex. *Psychopharmacology*, *185*(2), 255–262. https://doi.org/10.1007/s00213-006-0317-3

Gogolla, N., Leblanc, J. J., Quast, K. B., Südhof, T. C., Fagiolini, M., & Hensch, T. K. (2009). Common circuit defect of excitatory-inhibitory balance in mouse models of autism. *Journal of Neurodevelopmental Disorders*, *1*(2), 172–181. https://doi.org/10.1007/s11689-009-9023-x

Goodman, J. H. (1998). Experimental Models of Status Epilepticus. In *Neuropharmacology Methods in Epilepsy Research*. CRC Press.

Guo, F., Yu, N., Cai, J.-Q., Quinn, T., Zong, Z.-H., Zeng, Y.-J., & Hao, L.-Y. (2008). Voltage-gated sodium channel Nav1.1, Nav1.3 and β1 subunit were up-regulated in the hippocampus of spontaneously epileptic rat. *Brain Research Bulletin*, *75*(1), 179–187. https://doi.org/10.1016/j.brainresbull.2007.10.005

Gurvich, N., & Klein, P. S. (2002). Lithium and valproic acid: Parallels and contrasts in diverse signaling contexts. *Pharmacology & Therapeutics*, *96*(1), 45–66. https://doi.org/10.1016/s0163-7258(02)00299-1

Hajisoltani, R., Karimi, S. A., Rahdar, M., Davoudi, S., Borjkhani, M., Hosseinmardi, N., Behzadi, G., & Janahmadi, M. (2019). Hyperexcitability of hippocampal CA1 pyramidal neurons in male offspring of a rat model of autism spectrum disorder (ASD) induced by prenatal exposure to

valproic acid: A possible involvement of Ih channel current. *Brain Research*, *1708*, 188–199. https://doi.org/10.1016/j.brainres.2018.12.011

Hali, S., Kim, J., Kwak, T. H., Lee, H., Shin, C. Y., & Han, D. W. (2020). Modelling monogenic autism spectrum disorder using mouse cortical organoids. *Biochemical and Biophysical Research Communications*, *521*(1), 164–171. https://doi.org/10.1016/j.bbrc.2019.10.097

Hara, Y., Maeda, Y., Kataoka, S., Ago, Y., Takuma, K., & Matsuda, T. (2012). Effect of Prenatal Valproic Acid Exposure on Cortical Morphology in Female Mice. *Journal of Pharmacological Sciences*, *118*(4), 543–546. https://doi.org/10.1254/jphs.12025SC

Harden, C. L., Meador, K. J., Pennell, P. B., Hauser, W. A., Gronseth, G. S., French, J. A., Wiebe, S., Thurman, D., Koppel, B. S., Kaplan, P. W., Robinson, J. N., Hopp, J., Ting, T. Y., Gidal, B., Hovinga, C. A., Wilner, A. N., Vazquez, B., Holmes, L., Krumholz, A., … American Epilepsy Society. (2009). Management issues for women with epilepsy-Focus on pregnancy (an evidence-based review): II. Teratogenesis and perinatal outcomes: Report of the Quality Standards Subcommittee and Therapeutics and Technology Subcommittee of the American Academy of Neurology and the American Epilepsy Society. *Epilepsia*, *50*(5), 1237–1246. https://doi.org/10.1111/j.1528-1167.2009.02129.x

Hou, Q., Wang, Y., Li, Y., Chen, D., Yang, F., & Wang, S. (2018). A Developmental Study of Abnormal Behaviors and Altered GABAergic Signaling in the VPA-Treated Rat Model of Autism. *Frontiers in Behavioral Neuroscience*, *12*. https://www.frontiersin.org/articles/10.3389/fnbeh.2018.00182

Hsieh, J., Nakashima, K., Kuwabara, T., Mejia, E., & Gage, F. H. (2004). Histone deacetylase inhibition-mediated neuronal differentiation of multipotent adult neural progenitor cells. *Proceedings of the National Academy of Sciences of the United States of America*, *101*(47), 16659–16664. https://doi.org/10.1073/pnas.0407643101

Ichikawa, J., & Meltzer, H. Y. (1999). Valproate and carbamazepine increase prefrontal dopamine release by 5-HT1A receptor activation. *European Journal of Pharmacology*, *380*(1), R1–R3. https://doi.org/10.1016/S0014-2999(99)00517-8

Ichiyama, T., Okada, K., Lipton, J. M., Matsubara, T., Hayashi, T., & Furukawa, S. (2000). Sodium valproate inhibits production of TNF-α and IL-6 and activation of NF-κB. *Brain Research*, *857*(1), 246–251. https://doi.org/10.1016/S0006-8993(99)02439-7

Iijima, Y., Behr, K., Iijima, T., Biemans, B., Bischofberger, J., & Scheiffele, P. (2016). Distinct Defects in Synaptic Differentiation of Neocortical Neurons in Response to Prenatal Valproate Exposure. *Scientific Reports*, *6*(1), Article 1. https://doi.org/10.1038/srep27400

Jäger-Roman, E., Deichl, A., Jakob, S., Hartmann, A. M., Koch, S., Rating, D., Steldinger, R., Nau, H., & Helge, H. (1986). Fetal growth, major malformations, and minor anomalies in infants born to women receiving valproic acid. *The Journal of Pediatrics*, *108*(6), 997–1004. https://doi.org/10.1016/s0022-3476(86)80949-0

Jankowsky, J. L., & Patterson, P. H. (2001). The role of cytokines and growth factors in seizures and their sequelae. *Progress in Neurobiology*, *63*(2), 125–149. https://doi.org/10.1016/S0301-0082(00)00022-8

Jentink, J., Loane, M. A., Dolk, H., Barisic, I., Garne, E., Morris, J. K., & de Jong-van den Berg, L. T. W. (2010). Valproic Acid Monotherapy in Pregnancy and Major Congenital Malformations. *New England Journal of Medicine*, *362*(23), 2185–2193. https://doi.org/10.1056/NEJMoa0907328

Johannessen, C. U. (2000). Mechanisms of action of valproate: A commentatory. *Neurochemistry International*, *37*(2), 103–110. https://doi.org/10.1016/S0197-0186(00)00013-9

Johannessen, C. U., & Johannessen, S. I. (2003). Valproate: Past, Present, and Future. *CNS Drug Reviews*, *9*(2), 199–216. https://doi.org/10.1111/j.1527-3458.2003.tb00249.x

Johannessen, S. I. (1992). Pharmacokinetics of valproate in pregnancy: Mother-foetus-newborn. *Pharmaceutisch Weekblad. Scientific Edition*, *14*(3A), 114–117. https://doi.org/10.1007/BF01962699

Juliandi, B., Abematsu, M., Sanosaka, T., Tsujimura, K., Smith, A., & Nakashima, K. (2012). Induction of superficial cortical layer neurons from mouse embryonic stem cells by valproic acid. *Neuroscience Research*, *72*(1), 23–31. https://doi.org/10.1016/j.neures.2011.09.012

Jung, G.-A., Yoon, J.-Y., Moon, B.-S., Yang, D.-H., Kim, H.-Y., Lee, S.-H., Bryja, V., Arenas, E., & Choi, K.-Y. (2008). Valproic acid induces differentiation and inhibition of proliferation in neural progenitor cells via the beta-catenin-Ras-ERK-p21Cip/WAF1 pathway. *BMC Cell Biology*, *9*, 66. https://doi.org/10.1186/1471-2121-9-66

Kao, C.-Y., Hsu, Y.-C., Liu, J.-W., Lee, D.-C., Chung, Y.-F., & Chiu, I.-M. (2013). The mood stabilizer valproate activates human FGF1 gene promoter through inhibiting HDAC and GSK-3 activities. *Journal of Neurochemistry*, *126*(1), 4–18. https://doi.org/10.1111/jnc.12292

Kataoka, S., Takuma, K., Hara, Y., Maeda, Y., Ago, Y., & Matsuda, T. (2013). Autism-like behaviours with transient histone hyperacetylation in mice treated prenatally with valproic acid. *International Journal of Neuropsychopharmacology*, *16*(1), 91–103. https://doi.org/10.1017/S1461145711001714

Kay, H. Y., Greene, D. L., Kang, S., Kosenko, A., & Hoshi, N. (2015). M-current preservation contributes to anticonvulsant effects of valproic acid. *The Journal of Clinical Investigation*, *125*(10), 3904–3914. https://doi.org/10.1172/JCI79727

Kelava, I., & Lancaster, M. A. (2016). Stem Cell Models of Human Brain Development. *Cell Stem Cell*, *18*(6), 736–748. https://doi.org/10.1016/j.stem.2016.05.022

Kelly, K. M., Gross, R. A., & Macdonald, R. L. (1990). Valproic acid selectively reduces the low-threshold (T) calcium current in rat nodose neurons. *Neuroscience Letters*, *116*(1), 233–238. https://doi.org/10.1016/0304-3940(90)90416-7

Kim, A. J., Shi, Y., Austin, R. C., & Werstuck, G. H. (2005). Valproate protects cells from ER stress-induced lipid accumulation and apoptosis by inhibiting glycogen synthase kinase-3. *Journal of Cell Science*, *118*(1), 89–99. https://doi.org/10.1242/jcs.01562

Kim, C.-H., & Lisman, J. E. (1999). A Role of Actin Filament in Synaptic Transmission and Long-Term Potentiation. *The Journal of Neuroscience*, *19*(11), 4314–4324. https://doi.org/10.1523/JNEUROSCI.19-11-04314.1999

Kim, J.-W., Oh, H. A., Kim, S. R., Ko, M. J., Seung, H., Lee, S. H., & Shin, C. Y. (2020). Epigenetically Upregulated T-Type Calcium Channels Contribute to Abnormal Proliferation of Embryonic Neural Progenitor Cells Exposed to Valproic Acid. *Biomolecules & Therapeutics*, *28*(5), 389–396. https://doi.org/10.4062/biomolther.2020.027

Kim, J.-W., Seung, H., Kim, K. C., Gonzales, E. L. T., Oh, H. A., Yang, S. M., Ko, M. J., Han, S.-H., Banerjee, S., & Shin, C. Y. (2017). Agmatine rescues autistic behaviors in the valproic acid-induced animal model of autism. *Neuropharmacology*, *113*, 71–81. https://doi.org/10.1016/j.neuropharm.2016.09.014

Kim, K. C., Lee, D.-K., Go, H. S., Kim, P., Choi, C. S., Kim, J.-W., Jeon, S. J., Song, M.-R., & Shin, C. Y. (2014). Pax6-dependent cortical glutamatergic neuronal differentiation regulates autism-like behavior in prenatally valproic acid-exposed rat offspring. *Molecular Neurobiology*, *49*(1), 512–528. https://doi.org/10.1007/s12035-013-8535-2

Kobow, K., & Blümcke, I. (2011). The methylation hypothesis: Do epigenetic chromatin modifications play a role in epileptogenesis? *Epilepsia*, *52*(s4), 15–19. https://doi.org/10.1111/j.1528-1167.2011.03145.x

Koch, S., Jäger-Roman, E., Lösche, G., Nau, H., Rating, D., & Helge, H. (1996). Antiepileptic drug treatment in pregnancy: Drug side effects in the neonate and neurological outcome. *Acta Paediatrica*, *85*(6), 739–746. https://doi.org/10.1111/j.1651-2227.1996.tb14137.x

Kolozsi, E., Mackenzie, R. N., Roullet, F. I., Decatanzaro, D., & Foster, J. A. (2009). Prenatal exposure to valproic acid leads to reduced expression of synaptic adhesion molecule neuroligin 3 in mice. *Neuroscience*, *163*(4), 1201–1210. https://doi.org/10.1016/j.neuroscience.2009.07.021

Koss, D. J., Bondarevaite, O., Adams, S., Leite, M., Giorgini, F., Attems, J., & Outeiro, T. F. (2021). RAB39B is redistributed in dementia with Lewy bodies and is sequestered within aβ plaques and Lewy bodies. *Brain Pathology*, *31*(1), 120–132. https://doi.org/10.1111/bpa.12890

Kulaga, S., Sheehy, O., Zargarzadeh, A. H., Moussally, K., & Bérard, A. (2011). Antiepileptic drug use during pregnancy: Perinatal outcomes. *Seizure*, *20*(9), 667–672. https://doi.org/10.1016/j.seizure.2011.06.012

Kumamaru, E., Egashira, Y., Takenaka, R., & Takamori, S. (2014). Valproic acid selectively suppresses the formation of inhibitory synapses in cultured cortical neurons. *Neuroscience Letters*, *569*, 142–147. https://doi.org/10.1016/j.neulet.2014.03.066

Laeng, P., Pitts, R. L., Lemire, A. L., Drabik, C. E., Weiner, A., Tang, H., Thyagarajan, R., Mallon, B. S., & Altar, C. A. (2004). The mood stabilizer valproic acid stimulates GABA neurogenesis from rat forebrain stem cells. *Journal of Neurochemistry*, *91*(1), 238–251. https://doi.org/10.1111/j.1471-4159.2004.02725.x

Lancaster, M. A., & Knoblich, J. A. (2014). Generation of cerebral organoids from human pluripotent stem cells. *Nature Protocols*, *9*(10), Article 10. https://doi.org/10.1038/nprot.2014.158

Lancaster, M. A., Renner, M., Martin, C.-A., Wenzel, D., Bicknell, L. S., Hurles, M. E., Homfray, T., Penninger, J. M., Jackson, A. P., & Knoblich, J. A. (2013). Cerebral organoids model human brain development and microcephaly. *Nature*, *501*(7467), 10.1038/nature12517. https://doi.org/10.1038/nature12517

Lee, H. J., Dreyfus, C., & DiCicco-Bloom, E. (2016). Valproic acid stimulates proliferation of glial precursors during cortical gliogenesis in developing rat. *Developmental Neurobiology*, *76*(7), 780–798. https://doi.org/10.1002/dneu.22359

Lin, H.-C., Gean, P.-W., Wang, C.-C., Chan, Y.-H., & Chen, P. S. (2013). The Amygdala Excitatory/Inhibitory Balance in a Valproate-Induced Rat Autism Model. *PLOS ONE*, *8*(1), e55248. https://doi.org/10.1371/journal.pone.0055248

Lonze, B. E., & Ginty, D. D. (2002). Function and Regulation of CREB Family Transcription Factors in the Nervous System. *Neuron*, *35*(4), 605–623. https://doi.org/10.1016/S0896-6273(02)00828-0

Löscher, W. (1993). Effects of the antiepileptic drug valproate on metabolism and function of inhibitory and excitatory amino acids in the brain. *Neurochemical Research*, *18*(4), 485–502. https://doi.org/10.1007/BF00967253

Löscher, W. (1999). Valproate: A reappraisal of its pharmacodynamic properties and mechanisms of action. *Progress in Neurobiology*, *58*(1), 31–59. https://doi.org/10.1016/S0301-0082(98)00075-6

Löscher, W. (2002). Basic Pharmacology of Valproate. *CNS Drugs*, *16*(10), 669–694. https://doi.org/10.2165/00023210-200216100-00003

Löscher, W. (2011). Critical review of current animal models of seizures and epilepsy used in the discovery and development of new antiepileptic drugs. *Seizure*, *20*(5), 359–368. https://doi.org/10.1016/j.seizure.2011.01.003

Löscher, W., & Schmidt, D. (1980). Increase of Human Plasma GABA by Sodium Valproate. *Epilepsia*, *21*(6), 611–615. https://doi.org/10.1111/j.1528-1157.1980.tb04314.x

Löscher, W., & Schmidt, D. (2006). Experimental and Clinical Evidence for Loss of Effect (Tolerance) during Prolonged Treatment with Antiepileptic Drugs. *Epilepsia*, *47*(8), 1253–1284. https://doi.org/10.1111/j.1528-1167.2006.00607.x

Marchetto, M. C. N., Winner, B., & Gage, F. H. (2010). Pluripotent stem cells in neurodegenerative and neurodevelopmental diseases. *Human Molecular Genetics*, *19*(R1), R71–R76. https://doi.org/10.1093/hmg/ddq159

Mariani, J., Coppola, G., Zhang, P., Abyzov, A., Provini, L., Tomasini, L., Amenduni, M., Szekely, A., Palejev, D., Wilson, M., Gerstein, M., Grigorenko, E., Chawarska, K., Pelphrey, K., Howe, J., & Vaccarino, F. M. (2015). FOXG1-dependent dysregulation of GABA/glutamate

neuron differentiation in autism spectrum disorders. *Cell*, *162*(2), 375–390. https://doi.org/10.1016/j.cell.2015.06.034

Markram, H., Rinaldi, T., & Markram, K. (2007). The Intense World Syndrome – an Alternative Hypothesis for Autism. *Frontiers in Neuroscience*, *1*(1), 77–96. https://doi.org/10.3389/neuro.01.1.1.006.2007

Markram, K., & Markram, H. (2010). The Intense World Theory – A Unifying Theory of the Neurobiology of Autism. *Frontiers in Human Neuroscience*, *4*. https://www.frontiersin.org/articles/10.3389/fnhum.2010.00224

Markram, K., Rinaldi, T., Mendola, D. L., Sandi, C., & Markram, H. (2008). Abnormal Fear Conditioning and Amygdala Processing in an Animal Model of Autism. *Neuropsychopharmacology*, *33*(4), Article 4. https://doi.org/10.1038/sj.npp.1301453

Mawhinney, E., Campbell, J., Craig, J., Russell, A., Smithson, W., Parsons, L., Robertson, I., Irwin, B., Morrison, P., Liggan, B., Delanty, N., Hunt, S., & Morrow, J. (2012). Valproate and the risk for congenital malformations: Is formulation and dosage regime important? *Seizure - European Journal of Epilepsy*, *21*(3), 215–218. https://doi.org/10.1016/j.seizure.2012.01.005

McDevitt, T. C. (2013). Scalable culture of human pluripotent stem cells in 3D. *Proceedings of the National Academy of Sciences*, *110*(52), 20852–20853. https://doi.org/10.1073/pnas.1320575111

McLean, M. J., & Macdonald, R. L. (1986). Sodium valproate, but not ethosuximide, produces use- and voltage-dependent limitation of high frequency repetitive firing of action potentials of mouse central neurons in cell culture. *Journal of Pharmacology and Experimental Therapeutics*, *237*(3), 1001–1011. https://jpet.aspetjournals.org/content/237/3/1001

Meador, K. J. (2008). Effects of In Utero Antiepileptic Drug Exposure. *Epilepsy Currents*, *8*(6), 143–147. https://doi.org/10.1111/j.1535-7511.2008.00273.x

Meador, K. J., Baker, G. A., Browning, N., Clayton-Smith, J., Combs-Cantrell, D. T., Cohen, M., Kalayjian, L. A., Kanner, A., Liporace, J. D., Pennell, P. B., Privitera, M., & Loring, D. W. (2009). Cognitive Function at 3 Years of Age after Fetal Exposure to Antiepileptic Drugs. *The New England Journal of Medicine*, *360*(16), 1597–1605. https://doi.org/10.1056/NEJMoa0803531

Meador, K. J., Baker, G. A., Browning, N., Cohen, M. J., Bromley, R. L., Clayton-Smith, J., Kalayjian, L. A., Kanner, A., Liporace, J. D., Pennell, P. B., Privitera, M., & Loring, D. W. (2013). Fetal antiepileptic drug exposure and cognitive outcomes at age 6 years (NEAD study): A prospective observational study. *Lancet Neurology*, *12*(3), 244. https://doi.org/10.1016/S1474-4422(12)70323-X

Meador, K. J., Baker, G. A., Browning, N., Cohen, M. J., Clayton-Smith, J., Kalayjian, L. A., Kanner, A., Liporace, J. D., Pennell, P. B., Privitera, M., & Loring, D. W. (2011). Foetal antiepileptic drug exposure and verbal versus non-verbal abilities at three years of age. *Brain*, *134*(2), 396–404. https://doi.org/10.1093/brain/awq352

Mellios, N., Feldman, D. A., Sheridan, S. D., Ip, J. P. K., Kwok, S., Amoah, S. K., Rosen, B., Rodriguez, B. A., Crawford, B., Swaminathan, R., Chou, S., Li, Y., Ziats, M., Ernst, C., Jaenisch,

R., Haggarty, S. J., & Sur, M. (2018). MeCP2-regulated miRNAs control early human neurogenesis through differential effects on ERK and AKT signaling. *Molecular Psychiatry*, *23*(4), Article 4. https://doi.org/10.1038/mp.2017.86

Meng, Q., Zhang, W., Wang, X., Jiao, C., Xu, S., Liu, C., Tang, B., & Chen, C. (2022). Human forebrain organoids reveal connections between valproic acid exposure and autism risk. *Translational Psychiatry*, *12*(1), Article 1. https://doi.org/10.1038/s41398-022-01898-x

Meyer, G., Schaaps, J. P., Moreau, L., & Goffinet, A. M. (2000). Embryonic and Early Fetal Development of the Human Neocortex. *The Journal of Neuroscience*, *20*(5), 1858–1868. https://doi.org/10.1523/JNEUROSCI.20-05-01858.2000

Milutinovic, S., D'Alessio, A. C., Detich, N., & Szyf, M. (2007). Valproate induces widespread epigenetic reprogramming which involves demethylation of specific genes. *Carcinogenesis*, *28*(3), 560–571. https://doi.org/10.1093/carcin/bgl167

Miyamae, T., Chen, K., Lewis, D. A., & Gonzalez-Burgos, G. (2017). Distinct Physiological Maturation of Parvalbumin-Positive Neuron Subtypes in Mouse Prefrontal Cortex. *The Journal of Neuroscience*, *37*(19), 4883–4902. https://doi.org/10.1523/JNEUROSCI.3325-16.2017

Monti, B., Polazzi, E., & Contestabile, A. (2009). Biochemical, Molecular and Epigenetic Mechanisms of Valproic Acid Neuroprotection. *Current Molecular Pharmacology*, *2*(1), 95–109. https://doi.org/10.2174/1874467210902010095

Nadebaum, C., Anderson, V. A., Vajda, F., Reutens, D. C., Barton, S., & Wood, A. G. (2011a). Language skills of school-aged children prenatally exposed to antiepileptic drugs. *Neurology*, *76*(8), 719–726. https://doi.org/10.1212/WNL.0b013e31820d62c7

Nadebaum, C., Anderson, V., Vajda, F., Reutens, D., Barton, S., & Wood, A. (2011b). The Australian Brain and Cognition and Antiepileptic Drugs Study: IQ in School-Aged Children Exposed to Sodium Valproate and Polytherapy. *Journal of the International Neuropsychological Society*, *17*(1), 133–142. https://doi.org/10.1017/S1355617710001359

Nakamura, K., Sekine, Y., Ouchi, Y., Tsujii, M., Yoshikawa, E., Futatsubashi, M., Tsuchiya, K. J., Sugihara, G., Iwata, Y., Suzuki, K., Matsuzaki, H., Suda, S., Sugiyama, T., Takei, N., & Mori, N. (2010). Brain Serotonin and Dopamine Transporter Bindings in Adults With High-Functioning Autism. *Archives of General Psychiatry*, *67*(1), 59–68. https://doi.org/10.1001/archgenpsychiatry.2009.137

Nakasato, A., Nakatani, Y., Seki, Y., Tsujino, N., Umino, M., & Arita, H. (2008). Swim stress exaggerates the hyperactive mesocortical dopamine system in a rodent model of autism. *Brain Research*, *1193*, 128–135. https://doi.org/10.1016/j.brainres.2007.11.043

Nalivaeva, N. N., Belyaev, N. D., & Turner, A. J. (2009). Sodium valproate: An old drug with new roles. *Trends in Pharmacological Sciences*, *30*(10), 509–514. https://doi.org/10.1016/j.tips.2009.07.002

Narita, N., Kato, M., Tazoe, M., Miyazaki, K., Narita, M., & Okado, N. (2002). Increased Monoamine Concentration in the Brain and Blood of Fetal Thalidomide- and Valproic Acid–

Exposed Rat: Putative Animal Models for Autism. *Pediatric Research*, *52*(4), Article 4. https://doi.org/10.1203/00006450-200210000-00018

Nicolini, C., Ahn, Y., Michalski, B., Rho, J. M., & Fahnestock, M. (2015). Decreased mTOR signaling pathway in human idiopathic autism and in rats exposed to valproic acid. *Acta Neuropathologica Communications*, *3*(1), 3. https://doi.org/10.1186/s40478-015-0184-4

Nicolini, C., & Fahnestock, M. (2018). The valproic acid-induced rodent model of autism. *Experimental Neurology*, *299*, 217–227. https://doi.org/10.1016/j.expneurol.2017.04.017

Okada, A., Kushima, K., Aoki, Y., Bialer, M., & Fujiwara, M. (2005). Identification of early-responsive genes correlated to valproic acid–induced neural tube defects in mice. *Birth Defects Research Part A: Clinical and Molecular Teratology*, *73*(4), 229–238. https://doi.org/10.1002/bdra.20131

Ornoy, A. (2009). Valproic acid in pregnancy: How much are we endangering the embryo and fetus? *Reproductive Toxicology*, *28*(1), 1–10. https://doi.org/10.1016/j.reprotox.2009.02.014

Paşca, A. M., Park, J.-Y., Shin, H.-W., Qi, Q., Revah, O., Krasnoff, R., O'Hara, R., Willsey, A. J., Palmer, T. D., & Paşca, S. P. (2019). Human 3D Cellular Model of Hypoxic Brain Injury of Prematurity. *Nature Medicine*, *25*(5), 784–791. https://doi.org/10.1038/s41591-019-0436-0

Paşca, A. M., Sloan, S. A., Clarke, L. E., Tian, Y., Makinson, C. D., Huber, N., Kim, C. H., Park, J.-Y., O'Rourke, N. A., Nguyen, K. D., Smith, S. J., Huguenard, J. R., Geschwind, D. H., Barres, B. A., & Paşca, S. P. (2015). Functional cortical neurons and astrocytes from human pluripotent stem cells in 3D culture. *Nature Methods*, *12*(7), 671–678. https://doi.org/10.1038/nmeth.3415

Pașca, S. P., Arlotta, P., Bateup, H. S., Camp, J. G., Cappello, S., Gage, F. H., Knoblich, J. A., Kriegstein, A. R., Lancaster, M. A., Ming, G.-L., Muotri, A. R., Park, I.-H., Reiner, O., Song, H., Studer, L., Temple, S., Testa, G., Treutlein, B., & Vaccarino, F. M. (2022). A nomenclature consensus for nervous system organoids and assembloids. *Nature*, *609*(7929), Article 7929. https://doi.org/10.1038/s41586-022-05219-6

Paulsen, B., Velasco, S., Kedaigle, A. J., Pigoni, M., Quadrato, G., Deo, A. J., Adiconis, X., Uzquiano, A., Sartore, R., Yang, S. M., Simmons, S. K., Symvoulidis, P., Kim, K., Tsafou, K., Podury, A., Abbate, C., Tucewicz, A., Smith, S. N., Albanese, A., … Arlotta, P. (2022). Autism genes converge on asynchronous development of shared neuron classes. *Nature*, *602*(7896), Article 7896. https://doi.org/10.1038/s41586-021-04358-6

Peckman, H. (2010). The U.S. Food and Drug Adminstration (FDA) has assigned pregnancy category D to valproate. *North Carolina Medical Journal*, *71*(4), 396–398.

Péraudeau, E., Cronier, L., Monvoisin, A., Poinot, P., Mergault, C., Guilhot, F., Tranoy-Opalinski, I., Renoux, B., Papot, S., & Clarhaut, J. (2018). Enhancing tumor response to targeted chemotherapy through up-regulation of folate receptor α expression induced by dexamethasone and valproic acid. *Journal of Controlled Release*, *269*, 36–44. https://doi.org/10.1016/j.jconrel.2017.11.011

Qian, X., Nguyen, H. N., Song, M. M., Hadiono, C., Ogden, S. C., Hammack, C., Yao, B., Hamersky, G., Jacob, F., Zhong, C., Yoon, K., Jeang, W., Lin, L., Li, Y., Thakor, J., Berg, D.,

Zhang, C., Kang, E., Chickering, M., … Ming, G. (2016). Brain Region-specific Organoids using Mini-bioreactors for Modeling ZIKV Exposure. *Cell*, *165*(5), 1238–1254. https://doi.org/10.1016/j.cell.2016.04.032

Qiu, H.-M., Yang, J.-X., Liu, D., Fei, H.-Z., Hu, X.-Y., & Zhou, Q.-X. (2014). Antidepressive effect of sodium valproate involving suppression of corticotropin-releasing factor expression and elevation of BDNF expression in rats exposed to chronic unpredicted stress. *NeuroReport*, *25*(4), 205. https://doi.org/10.1097/WNR.0000000000000054

Rabinowicz, T., de Courten-Myers, G. M., Petetot, J. M., Xi, G., & de los Reyes, E. (1996). Human cortex development: Estimates of neuronal numbers indicate major loss late during gestation. *Journal of Neuropathology and Experimental Neurology*, *55*(3), 320–328.

Radstake, F. D. W., Raaijmakers, E. A. L., Luttge, R., Zinger, S., & Frimat, J. P. (2019). CALIMA: The semi-automated open-source calcium imaging analyzer. *Computer Methods and Programs in Biomedicine*, *179*, 104991. https://doi.org/10.1016/j.cmpb.2019.104991

Rasalam, A., Hailey, H., Williams, J. H. G., Moore, S. J., Turnpenny, P. D., Lloyd, D. J., & Dean, J. C. S. (2005). Characteristics of fetal anticonvulsant syndrome associated autistic disorder. *Developmental Medicine & Child Neurology*, *47*(8), 551–555. https://doi.org/10.1111/j.1469-8749.2005.tb01190.x

Rinaldi, T., Kulangara, K., Antoniello, K., & Markram, H. (2007). Elevated NMDA receptor levels and enhanced postsynaptic long-term potentiation induced by prenatal exposure to valproic acid. *Proceedings of the National Academy of Sciences*, *104*(33), 13501–13506. https://doi.org/10.1073/pnas.0704391104

Rinaldi, T., Perrodin, C., & Markram, H. (2008). Hyper-connectivity and hyper-plasticity in the medial prefrontal cortex in the valproic Acid animal model of autism. *Frontiers in Neural Circuits*, *2*, 4. https://doi.org/10.3389/neuro.04.004.2008

Rinaldi, T., Silberberg, G., & Markram, H. (2008). Hyperconnectivity of Local Neocortical Microcircuitry Induced by Prenatal Exposure to Valproic Acid. *Cerebral Cortex*, *18*(4), 763–770. https://doi.org/10.1093/cercor/bhm117

Rogawski, M. A., & Löscher, W. (2004). The neurobiology of antiepileptic drugs for the treatment of nonepileptic conditions. *Nature Medicine*, *10*(7), Article 7. https://doi.org/10.1038/nm1074

Romoli, M., Mazzocchetti, P., D'Alonzo, R., Siliquini, S., Rinaldi, V. E., Verrotti, A., Calabresi, P., & Costa, C. (2019). Valproic Acid and Epilepsy: From Molecular Mechanisms to Clinical Evidences. *Current Neuropharmacology*, *17*(10), 926–946. https://doi.org/10.2174/1570159X17666181227165722

Roullet, F. I., & Crawley, J. N. (2011). Mouse Models of Autism: Testing Hypotheses About Molecular Mechanisms. In J. J. Hagan (Ed.), *Molecular and Functional Models in Neuropsychiatry* (pp. 187–212). Springer. https://doi.org/10.1007/7854_2010_113

Roullet, F. I., Lai, J. K. Y., & Foster, J. A. (2013). In utero exposure to valproic acid and autism—A current review of clinical and animal studies. *Neurotoxicology and Teratology*, *36*, 47–56. https://doi.org/10.1016/j.ntt.2013.01.004

Roullet, F. I., Wollaston, L., deCatanzaro, D., & Foster, J. A. (2010). Behavioral and molecular changes in the mouse in response to prenatal exposure to the anti-epileptic drug valproic acid. *Neuroscience*, *170*(2), 514–522. https://doi.org/10.1016/j.neuroscience.2010.06.069

Rubenstein, J. L. R., & Merzenich, M. M. (2003). Model of autism: Increased ratio of excitation/inhibition in key neural systems. *Genes, Brain, and Behavior*, *2*(5), 255–267. https://doi.org/10.1034/j.1601-183x.2003.00037.x

Sabers, A., Bertelsen, F. C. B., Scheel-Krüger, J., Nyengaard, J. R., & Møller, A. (2014). Long-term valproic acid exposure increases the number of neocortical neurons in the developing rat brain. A possible new animal model of autism. *Neuroscience Letters*, *580*, 12–16. https://doi.org/10.1016/j.neulet.2014.07.036

Schain, R. J., & Freedman, D. X. (1961). Studies on 5-hydroxyindole metabolism in autistic and other mentally retarded children. *The Journal of Pediatrics*, *58*(3), 315–320. https://doi.org/10.1016/S0022-3476(61)80261-8

Schneider, T., & Przewłocki, R. (2005). Behavioral Alterations in Rats Prenatally Exposed to Valproic Acid: Animal Model of Autism. *Neuropsychopharmacology*, *30*(1), Article 1. https://doi.org/10.1038/sj.npp.1300518

Schneider, T., Roman, A., Basta-Kaim, A., Kubera, M., Budziszewska, B., Schneider, K., & Przewłocki, R. (2008). Gender-specific behavioral and immunological alterations in an animal model of autism induced by prenatal exposure to valproic acid. *Psychoneuroendocrinology*, *33*(6), 728–740. https://doi.org/10.1016/j.psyneuen.2008.02.011

Schneider, T., Ziółkowska, B., Gieryk, A., Tyminska, A., & Przewłocki, R. (2007). Prenatal exposure to valproic acid disturbs the enkephalinergic system functioning, basal hedonic tone, and emotional responses in an animal model of autism. *Psychopharmacology*, *193*(4), 547–555. https://doi.org/10.1007/s00213-007-0795-y

Schulpen, S. H. W., Pennings, J. L. A., & Piersma, A. H. (2015). Gene Expression Regulation and Pathway Analysis After Valproic Acid and Carbamazepine Exposure in a Human Embryonic Stem Cell-Based Neurodevelopmental Toxicity Assay. *Toxicological Sciences*, *146*(2), 311–320. https://doi.org/10.1093/toxsci/kfv094

Scott, L. J., & Dhillon, S. (2007). Risperidone. *Pediatric Drugs*, *9*(5), 343–354. https://doi.org/10.2165/00148581-200709050-00006

Shallcross, R., Bromley, R. L., Irwin, B., Bonnett, L. J., Morrow, J., & Baker, G. A. (2011). Child development following in utero exposure. *Neurology*, *76*(4), 383–389. https://doi.org/10.1212/WNL.0b013e3182088297

Shi, X.-Y., Wang, J.-W., Cui, H., Li, B.-M., Lei, G.-F., & Sun, R.-P. (2010). Effects of antiepileptic drugs on mRNA levels of BDNF and NT-3 and cell neogenesis in the developing rat brain. *Brain and Development*, *32*(3), 229–235. https://doi.org/10.1016/j.braindev.2009.03.012

Silva, G., Le Bé, J.-V., Riachi, I., Rinaldi, T., Markram, K., & Markram, H. (2009). Enhanced long term microcircuit plasticity in the valproic acid animal model of autism. *Frontiers in Synaptic Neuroscience*, *1*. https://www.frontiersin.org/articles/10.3389/neuro.19.001.2009

Sinn, D.-I., Kim, S.-J., Chu, K., Jung, K.-H., Lee, S.-T., Song, E.-C., Kim, J.-M., Park, D.-K., Kun Lee, S., Kim, M., & Roh, J.-K. (2007). Valproic acid-mediated neuroprotection in intracerebral hemorrhage via histone deacetylase inhibition and transcriptional activation. *Neurobiology of Disease*, *26*(2), 464–472. https://doi.org/10.1016/j.nbd.2007.02.006

Sitges, M., Chiu, L. M., & Reed, R. C. (2016). Effects of Levetiracetam, Carbamazepine, Phenytoin, Valproate, Lamotrigine, Oxcarbazepine, Topiramate, Vinpocetine and Sertraline on Presynaptic Hippocampal Na+ and Ca2+ Channels Permeability. *Neurochemical Research*, *41*(4), 758–769. https://doi.org/10.1007/s11064-015-1749-0

Snow, W. M., Hartle, K., & Ivanco, T. L. (2008). Altered morphology of motor cortex neurons in the VPA rat model of autism. *Developmental Psychobiology*, *50*(7), 633–639. https://doi.org/10.1002/dev.20337

Sui, L., & Chen, M. (2012). Prenatal exposure to valproic acid enhances synaptic plasticity in the medial prefrontal cortex and fear memories. *Brain Research Bulletin*, *87*(6), 556–563. https://doi.org/10.1016/j.brainresbull.2012.01.011

Sullivan, N. R., Burke, T., Siafaka-Kapadai, A., Javors, M., & Hensler, J. G. (2004). Effect of valproic acid on serotonin-2A receptor signaling in C6 glioma cells. *Journal of Neurochemistry*, *90*(5), 1269–1275. https://doi.org/10.1111/j.1471-4159.2004.02690.x

Takahashi, K., Tanabe, K., Ohnuki, M., Narita, M., Ichisaka, T., Tomoda, K., & Yamanaka, S. (2007). Induction of Pluripotent Stem Cells from Adult Human Fibroblasts by Defined Factors. *Cell*, *131*(5), 861–872. https://doi.org/10.1016/j.cell.2007.11.019

Takahashi, K., & Yamanaka, S. (2006). Induction of Pluripotent Stem Cells from Mouse Embryonic and Adult Fibroblast Cultures by Defined Factors. *Cell*, *126*(4), 663–676. https://doi.org/10.1016/j.cell.2006.07.024

Takahashi, M., Hayashi, S., Kakita, A., Wakabayashi, K., Fukuda, M., Kameyama, S., Tanaka, R., Takahashi, H., & Nawa, H. (1999). Patients with temporal lobe epilepsy show an increase in brain-derived neurotrophic factor protein and its correlation with neuropeptide Y. *Brain Research*, *818*(2), 579–582. https://doi.org/10.1016/S0006-8993(98)01355-9

Takeda, K., Watanabe, T., Oyabu, K., Tsukamoto, S., Oba, Y., Nakano, T., Kubota, K., Katsurabayashi, S., & Iwasaki, K. (2021). Valproic acid-exposed astrocytes impair inhibitory synapse formation and function. *Scientific Reports*, *11*(1), Article 1. https://doi.org/10.1038/s41598-020-79520-7

Tan, N.-N., Tang, H.-L., Lin, G.-W., Chen, Y.-H., Lu, P., Li, H.-J., Gao, M.-M., Zhao, Q.-H., Yi, Y.-H., Liao, W.-P., & Long, Y.-S. (2017). Epigenetic Downregulation of Scn3a Expression by Valproate: A Possible Role in Its Anticonvulsant Activity. *Molecular Neurobiology*, *54*(4), 2831–2842. https://doi.org/10.1007/s12035-016-9871-9

Taverna, S., Mantegazza, M., Franceschetti, S., & Avanzini, G. (1998). Valproate selectively reduces the persistent fraction of Na+ current in neocortical neurons. *Epilepsy Research*, *32*(1), 304–308. https://doi.org/10.1016/S0920-1211(98)00060-6

Terbach, N., & Williams, R. S. B. (2009). Structure–function studies for the panacea, valproic acid. *Biochemical Society Transactions*, *37*(5), 1126–1132. https://doi.org/10.1042/BST0371126

Thomas, S. V., Ajaykumar, B., Sindhu, K., Nair, M. K. C., George, B., & Sarma, P. S. (2008). Motor and mental development of infants exposed to antiepileptic drugs in utero. *Epilepsy & Behavior*, *13*(1), 229–236. https://doi.org/10.1016/j.yebeh.2008.01.010

Thomas, S. V., Sukumaran, S., Lukose, N., George, A., & Sarma, P. S. (2007). Intellectual and language functions in children of mothers with epilepsy. *Epilepsia*, *48*(12), 2234–2240. https://doi.org/10.1111/j.1528-1167.2007.01376.x

Tomson, T., & Battino, D. (2011). Antiepileptic Treatment in Pregnant Women: Morphological and Behavioural Effects. In H. W. Seyberth, A. Rane, & M. Schwab (Eds.), *Pediatric Clinical Pharmacology* (pp. 295–315). Springer. https://doi.org/10.1007/978-3-642-20195-0_15

Tomson, T., & Battino, D. (2012). Teratogenic effects of antiepileptic drugs. *The Lancet Neurology*, *11*(9), 803–813. https://doi.org/10.1016/S1474-4422(12)70103-5

Tomson, T., Battino, D., Bonizzoni, E., Craig, J., Lindhout, D., Perucca, E., Sabers, A., Thomas, S. V., Vajda, F., Faravelli, F., Pantaleoni, C., Robert-Gnansia, E., Cabral-Lim, L., Čebular, B., Marinis, A. D., Kälviäinen, R., Khomeriki, K., Kiteva-Trencevska, G., Kochen, S., … Zarifi-Oskoie, M. (2018). Comparative risk of major congenital malformations with eight different antiepileptic drugs: A prospective cohort study of the EURAP registry. *The Lancet Neurology*, *17*(6), 530–538. https://doi.org/10.1016/S1474-4422(18)30107-8

Tomson, T., Battino, D., Bonizzoni, E., Craig, J., Lindhout, D., Perucca, E., Sabers, A., Thomas, S. V., Vajda, F., & Group, for T. E. S. (2019). Declining malformation rates with changed antiepileptic drug prescribing: An observational study. *Neurology*, *93*(9), e831–e840. https://doi.org/10.1212/WNL.0000000000008001

Tomson, T., Battino, D., Bonizzoni, E., Craig, J., Lindhout, D., Perucca, E., Sabers, A., Thomas, S. V., Vajda, F., & Group, F. the E. S. (2015). Dose-dependent teratogenicity of valproate in mono- and polytherapy: An observational study. *Neurology*, *85*(10), 866–872. https://doi.org/10.1212/WNL.0000000000001772

Tomson, T., Battino, D., Bonizzoni, E., Craig, J., Lindhout, D., Sabers, A., Perucca, E., & Vajda, F. (2011). Dose-dependent risk of malformations with antiepileptic drugs: An analysis of data from the EURAP epilepsy and pregnancy registry. *The Lancet Neurology*, *10*(7), 609–617. https://doi.org/10.1016/S1474-4422(11)70107-7

Tomson, T., Battino, D., & Perucca, E. (2016). Valproic acid after five decades of use in epilepsy: Time to reconsider the indications of a time-honoured drug. *The Lancet Neurology*, *15*(2), 210–218. https://doi.org/10.1016/S1474-4422(15)00314-2

Tomson, T., Marson, A., Boon, P., Canevini, M. P., Covanis, A., Gaily, E., Kälviäinen, R., & Trinka, E. (2015). Valproate in the treatment of epilepsy in girls and women of childbearing potential. *Epilepsia*, *56*(7), 1006–1019. https://doi.org/10.1111/epi.13021

Tong, D., Chen, R., Lu, Y., Li, W., Zhang, Y., Lin, J., He, L., Dang, T., Shan, S., Xu, X.-H., Zhang, Y., Zhang, C., Du, Y.-S., Zhou, W.-H., Wang, X., & Qiu, Z. (2019). The critical role of ASD-related gene CNTNAP3 in regulating synaptic development and social behavior in mice. *Neurobiology of Disease*, *130*, 104486. https://doi.org/10.1016/j.nbd.2019.104486

Vajda, F. J. E., Horgan, D., Hollingworth, S., Graham, J., Hitchcock, A. A., Roten, A., O'brien, T. J., Lander, C. M., & Eadie, M. J. (2012). The prescribing of antiepileptic drugs for pregnant Australian women. *Australian and New Zealand Journal of Obstetrics and Gynaecology*, *52*(1), 49–53. https://doi.org/10.1111/j.1479-828X.2011.01359.x

Valproate-related-substances-article-31-referral-prac-assessment-report_en.pdf. (n.d.). Retrieved 21 May 2023, from https://www.ema.europa.eu/en/documents/referral/valproate-related-substances-article-31-referral-prac-assessment-report_en.pdf

Van den Berg, R. J., Kok, P., & Voskuyl, R. A. (1993). Valproate and sodium currents in cultured hippocampal neurons. *Experimental Brain Research*, *93*(2), 279–287. https://doi.org/10.1007/BF00228395

Veenstra-VanderWeele, J., Muller, C. L., Iwamoto, H., Sauer, J. E., Owens, W. A., Shah, C. R., Cohen, J., Mannangatti, P., Jessen, T., Thompson, B. J., Ye, R., Kerr, T. M., Carneiro, A. M., Crawley, J. N., Sanders-Bush, E., McMahon, D. G., Ramamoorthy, S., Daws, L. C., Sutcliffe, J. S., & Blakely, R. D. (2012). Autism gene variant causes hyperserotonemia, serotonin receptor hypersensitivity, social impairment and repetitive behavior. *Proceedings of the National Academy of Sciences of the United States of America*, *109*(14), 5469–5474. https://doi.org/10.1073/pnas.1112345109

Villa, C. E., Cheroni, C., Dotter, C. P., López-Tóbon, A., Oliveira, B., Sacco, R., Yahya, A. Ç., Morandell, J., Gabriele, M., Tavakoli, M. R., Lyudchik, J., Sommer, C., Gabitto, M., Danzl, J. G., Testa, G., & Novarino, G. (2022). CHD8 haploinsufficiency links autism to transient alterations in excitatory and inhibitory trajectories. *Cell Reports*, *39*(1), 110615. https://doi.org/10.1016/j.celrep.2022.110615

Virta, L. J., Kälviäinen, R. K., Villikka, K., & Keränen, T. (2018, March 6). *Declining trend in valproate use in Finland among females of childbearing age in 2012–2016 – a nationwide registry-based outpatient study* [A1]. Blackwell Publishing Ltd. https://www.julkari.fi/handle/10024/137407

Wagner, G. C., Reuhl, K. R., Cheh, M., McRae, P., & Halladay, A. K. (2006). A New Neurobehavioral Model of Autism in Mice: Pre- and Postnatal Exposure to Sodium Valproate. *Journal of Autism and Developmental Disorders*, *36*(6), 779–793. https://doi.org/10.1007/s10803-006-0117-y

Walcott, E. C., Higgins, E. A., & Desai, N. S. (2011). Synaptic and Intrinsic Balancing during Postnatal Development in Rat Pups Exposed to Valproic Acid in Utero. *The Journal of Neuroscience*, *31*(37), 13097–13109. https://doi.org/10.1523/JNEUROSCI.1341-11.2011

Walden, J., Altrup, U., Reith, H., & Speckmann, E.-J. (1993). Effects of valproate on early and late potassium currents of single neurons. *European Neuropsychopharmacology*, *3*(2), 137–141. https://doi.org/10.1016/0924-977X(93)90265-N

Wang, Y., Chiola, S., Yang, G., Russell, C., Armstrong, C. J., Wu, Y., Spampanato, J., Tarboton, P., Ullah, H. M. A., Edgar, N. U., Chang, A. N., Harmin, D. A., Bocchi, V. D., Vezzoli, E., Besusso, D., Cui, J., Cattaneo, E., Kubanek, J., & Shcheglovitov, A. (2022). Modeling human telencephalic development and autism-associated SHANK3 deficiency using organoids generated from single neural rosettes. *Nature Communications*, *13*(1), Article 1. https://doi.org/10.1038/s41467-022-33364-z

Wang, Y., Wang, L., Zhu, Y., & Qin, J. (2018). Human brain organoid-on-a-chip to model prenatal nicotine exposure. *Lab on a Chip*, *18*(6), 851–860. https://doi.org/10.1039/C7LC01084B

Weissberg, O., & Elliott, E. (2021). The Mechanisms of CHD8 in Neurodevelopment and Autism Spectrum Disorders. *Genes*, *12*(8), Article 8. https://doi.org/10.3390/genes12081133

Whitaker, W. R. J., Faull, R. L. M., Waldvogel, H. J., Plumpton, C. J., Emson, P. C., & Clare, J. J. (2001). Comparative distribution of voltage-gated sodium channel proteins in human brain. *Molecular Brain Research*, *88*(1), 37–53. https://doi.org/10.1016/S0169-328X(00)00289-8

Williams, G., King, J., Cunningham, M., Stephan, M., Kerr, B., & Hersh, J. H. (2001). Fetal valproate syndrome and autism: Additional evidence of an association. *Developmental Medicine and Child Neurology*, *43*(3), 202–206.

Williams, P. G., & Hersh, J. H. (1997). A male with fetal valproate syndrome and autism. *Developmental Medicine & Child Neurology*, *39*(9), 632–634. https://doi.org/10.1111/j.1469-8749.1997.tb07500.x

Wilson, S. J., Bladin, P. F., & Saling, M. M. (2007). The burden of normality: A framework for rehabilitation after epilepsy surgery. *Epilepsia*, *48*(s9), 13–16. https://doi.org/10.1111/j.1528-1167.2007.01393.x

Wöhr, M., Roullet, F. I., & Crawley, J. N. (2011). Reduced Scent Marking and Ultrasonic Vocalizations in the BTBR T+tf/J Mouse Model of Autism. *Genes, Brain, and Behavior*, *10*(1), 35–43. https://doi.org/10.1111/j.1601-183X.2010.00582.x

Wood, A. G., Chen, J., Barton, S., Nadebaum, C., Anderson, V. A., Catroppa, C., Reutens, D. C., O'Brien, T. J., & Vajda, F. (2014). Altered cortical thickness following prenatal sodium valproate exposure. *Annals of Clinical and Translational Neurology*, *1*(7), 497–501. https://doi.org/10.1002/acn3.74

Wu, X., Chen, P. S., Dallas, S., Wilson, B., Block, M. L., Wang, C.-C., Kinyamu, H., Lu, N., Gao, X., Leng, Y., Chuang, D.-M., Zhang, W., Lu, R. B., & Hong, J.-S. (2008). Histone deacetylase inhibitors up-regulate astrocyte GDNF and BDNF gene transcription and protect dopaminergic neurons. *The International Journal of Neuropsychopharmacology / Official Scientific Journal of the Collegium Internationale Neuropsychopharmacologicum (CINP)*, *11*(8), 1123–1134. https://doi.org/10.1017/S1461145708009024

Wyneken, U., Marengo, J.-J., Villanueva, S., Soto, D., Sandoval, R., Gundelfinger, E. D., & Orrego, F. (2003). Epilepsy-induced Changes in Signaling Systems of Human and Rat Postsynaptic Densities. *Epilepsia*, *44*(2), 243–246. https://doi.org/10.1046/j.1528-1157.2003.17602.x

Wyneken, U., Smalla, K.-H., Marengo, J. J., Soto, D., de la Cerda, A., Tischmeyer, W., Grimm, R., Boeckers, T. M., Wolf, G., Orrego, F., & Gundelfinger, E. D. (2001). Kainate-induced seizures alter protein composition and N-methyl-d-aspartate receptor function of rat forebrain postsynaptic densities. *Neuroscience*, *102*(1), 65–74. https://doi.org/10.1016/S0306-4522(00)00469-3

Yoo, T., Yoo, Y.-E., Kang, H., & Kim, E. (2022). Age, brain region, and gene dosage-differential transcriptomic changes in Shank3-mutant mice. *Frontiers in Molecular Neuroscience*, *15*, 1017512. https://doi.org/10.3389/fnmol.2022.1017512

Zhang, W., Ma, L., Yang, M., Shao, Q., Xu, J., Lu, Z., Zhao, Z., Chen, R., Chai, Y., & Chen, J.-F. (2020). Cerebral organoid and mouse models reveal a RAB39b–PI3K–mTOR pathway-dependent dysregulation of cortical development leading to macrocephaly/autism phenotypes. *Genes & Development*, *34*(7–8), 580–597. https://doi.org/10.1101/gad.332494.119

Zhang, X., He, X., Li, Q., Kong, X., Ou, Z., Zhang, L., Gong, Z., Long, D., Li, J., Zhang, M., Ji, W., Zhang, W., Xu, L., & Xuan, A. (2017). PI3K/AKT/mTOR Signaling Mediates Valproic Acid-Induced Neuronal Differentiation of Neural Stem Cells through Epigenetic Modifications. *Stem Cell Reports*, *8*(5), 1256–1269. https://doi.org/10.1016/j.stemcr.2017.04.006

Zhu, Y., Wang, L., Yin, F., Yu, Y., Wang, Y., Shepard, M. J., Zhuang, Z., & Qin, J. (2017). Probing impaired neurogenesis in human brain organoids exposed to alcohol. *Integrative Biology*, *9*(12), 968–978. https://doi.org/10.1039/c7ib00105c

Zuccato, C., & Cattaneo, E. (2009). Brain-derived neurotrophic factor in neurodegenerative diseases. *Nature Reviews Neurology*, *5*(6), Article 6. https://doi.org/10.1038/nrneurol.2009.54